PL-TR-95-2056

VARIABILITY OF TOTAL ELECTRON CONTENT IN THE HIGH-LATITUDE IONOSPHERE FOLLOWING SOLAR MAXIMUM

C. Charley Andreasen
Elizabeth A. Holland

Northwest Research Associates, Inc.
PO Box 3027
Bellevue, WA 98009-3027

15 March 1995

Final Report
27 August 1992 - 26 November 1994

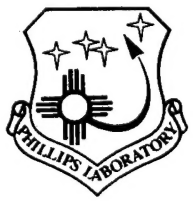

PHILLIPS LABORATORY
Directorate of Geophysics
AIR FORCE MATERIEL COMMAND
HANSCOM AFB, MA 01731-3010

"This technical report has been reviewed and is approved for publication"

GREGORY J. BISHOP
Contract Manager

EDWARD J. BERGHORN
Branch Chief

WILLIAM K. VICKERY
Division Director

This document has been reviewed by the ESC Public Affairs Office (PA) and is releasable to the National Technical Information Service (NTIS).

Qualified requestors may obtain additional copies from the Defense Technical Information Center. All others should apply to the National Technical Information Service.

If your address has changed, or if you wish to be removed from the mailing list, or if the addressee is no longer employed by your organization, please notify PL/IM, 29 Randolph Road, Hanscom AFB, MA 01731-3010. This will assist us in maintaining a current mailing list.

Do not return copies of this report unless contractual obligations or notices on a specific document requires that it be returned.

DISCLAIMER NOTICE

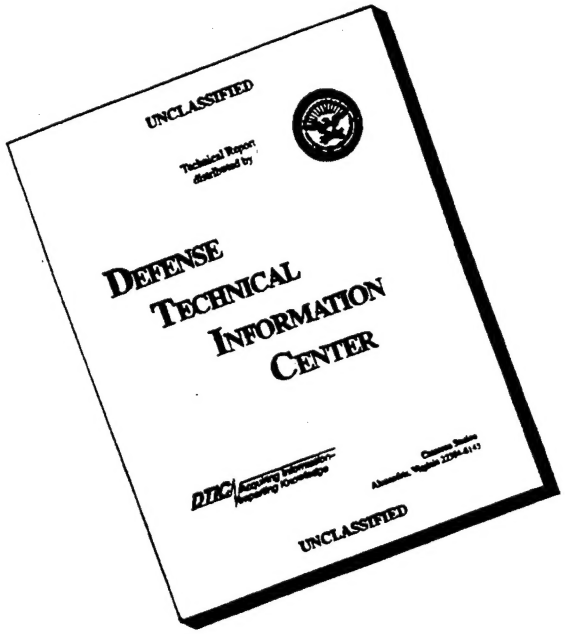

THIS DOCUMENT IS BEST QUALITY AVAILABLE. THE COPY FURNISHED TO DTIC CONTAINED A SIGNIFICANT NUMBER OF PAGES WHICH DO NOT REPRODUCE LEGIBLY.

REPORT DOCUMENTATION PAGE

Form Approved
OMB No. 0704-0188

1. AGENCY USE ONLY (Leave blank)	2. REPORT DATE	3. REPORT TYPE AND DATES COVERED
	15 March 1995	Final Report: 27 Aug 92 - 26 Nov 94

4. TITLE AND SUBTITLE
Variability of Total Electron Content in the High-Latitude Ionosphere Following Solar Maximum

5. FUNDING NUMBERS
F19628-92-C-0162
PE62101F
PRESD2 TA GH
WV AA

6. AUTHOR(S)
C. Charley Andreasen
Elizabeth A. Holland

7. PERFORMING ORGANIZATION NAME(S) AND ADDRESS(ES)
Northwest Research Associates, Inc.
300 120th Avenue, NE, Bldg 7, Ste 220
PO Box 3027
Bellevue, WA 98009-3027

8. PERFORMING ORGANIZATION REPORT NUMBER
NWRA-CR-95-R134

9. SPONSORING/MONITORING AGENCY NAME(S) AND ADDRESS(ES)
Phillips Laboratory
29 Randolph Road
Hanscom AFB, MA 01731-3010
Contract Manager: Greg Bishop/GPIA

10. SPONSORING/MONITORING AGENCY REPORT NUMBER
PL-TR-95-2056

11. SUPPLEMENTARY NOTES

12a. DISTRIBUTION/AVAILABILITY STATEMENT
approved for public release
distribution unlimited

12b. DISTRIBUTION CODE

13. ABSTRACT *(Maximum 200 words)*

Northwest Research Associates, Inc., (NWRA) has developed a data archive of Total Electron Content (TEC) data through operation and maintenance of GPS satellite receiver equipment at Shemya, AK; Hanscom AFB, MA; Thule AB, Greenland; Tucuman, Argentina; and Agua Verde, Chile. Scintillation data can be extracted from much of this database. The Shemya, AK, data provide a valuable source for characterizing TEC morphology and variability with look direction at this site. The Shemya data were also used in an initial assessment of the seasonal and directional specification accuracy of the Bent ionospheric model, specific to this site. Analysis of an existing NWRA database has produced ionospheric trough boundary signatures in the sub-auroral European sector. These signatures will support studies aimed at real-time detection of the trough boundary. Innovative software techniques were developed to improve data quality in the areas of multipath mitigation (the Multipath Template Technique) and the automated calibration of an installed receiver system for the combination of all system components' contributions to pseudorange error (SCORE: Self-Calibration Of pseudoRange Errors).

14. SUBJECT TERMS
Total electron content, Ionospheric scintillation, Bent ionospheric model, Ionospheric trough, Global Positioning Satellite system, Multipath mitigation, Pseudorange error correction

15. NUMBER OF PAGES
80

16. PRICE CODE

17. SECURITY CLASSIFICATION OF REPORT	18. SECURITY CLASSIFICATION OF THIS PAGE	19. SECURITY CLASSIFICATION OF ABSTRACT	20. LIMITATION OF ABSTRACT
Unclassified	Unclassified	Unclassified	SAR

TABLE OF CONTENTS

Tables

Illustrations

VARIABILITY OF TOTAL ELECTRON CONTENT IN THE HIGH-LATITUDE IONOSPHERE FOLLOWING SOLAR MAXIMUM

1. INTRODUCTION AND OBJECTIVES

Ionospheric total electron content (TEC) can significantly affect RF propagation. Knowledge of ionospheric structure in the region of interest allows for correction of TEC-induced errors. TEC is defined as the total integrated number of electrons contained in a column of one-meter-squared cross-section centered on the signal's ray path. It is expressed in TEC units, where 1 TEC unit = $1x10^{16}$ electrons/m^2. NorthWest Research Associates (NWRA) has recorded a database containing measurements of the differential carrier phase (DCP) and the differential group delay (DGD) between the two L-band signals transmitted by satellites of the Global Positioning System (GPS). DGD is an absolute measure of TEC, but is susceptible to multipath contamination. DCP is a relative measure of TEC and is much less affected by multipath. Multipath reduction is achieved by referencing the DCP to the DGD.

During this contract period, as solar activity descended from the 1989/1990 maximum, data were collected at Shemya, AK; Hanscom AFB, MA; Thule, Greenland; Tucuman, Argentina; and Agua Verde, Chile. Station coordinates are listed in Table 1. Software was developed to process these data and produce measurements of trans-ionospheric absolute total electron content (TEC). These data, along with existing multi-direction satellite data developed by NWRA in other high-latitude studies in the Shetland Islands, UK, may be used to quantify longitudinal characteristics of TEC morphology in the northern mid-latitude and trough regimes of the ionosphere. This database has application to validating and improving ionospheric models for the Shemya region in particular, and the higher latitudes in general.

Table 1. Station Locations

Station	Lat (deg)	Long (deg)	Corrected Geomag Lat (deg)
Shemya, AK	42.4	-71.3	54.0
Hanscom AFB, MA	52.7	-185.9	46.6
Thule, Greenland	76.6	-68.7	85.3
Tucuman, Argentina	-27.0	-65.0	-13.3
Agua Verde, Chile	-25.4	-70.0	-11.3

The first objective of this effort was the generation of a database sufficient to document variability in ionospheric total electron content and associated scintillation effects due to plasma-density structures, using measurements made at Shemya, AK, and other high-latitude locations. This database is suited to analyses aimed at correcting ionospheric errors that affect the operation of Air Force surveillance systems at high latitudes, specifying TEC morphology in these regions, and developing and validating improved ionospheric models.

The second objective was to develop an assessment of the signature(s) of the ionospheric trough region seen in diurnal TEC data from a multi-direction GPS receiver. Data from Shetland Islands, UK, were used in the assessment.

The third objective was the extension of these databases into the declining phase of the solar cycle and the comparison of the data to predictions from available ionospheric models, emphasizing the data from Shemya, AK. Such a comparison discloses the accuracy of present ionospheric specifications, permitting definition of approaches for improving models for these specific regions.

To accomplish these goals, NWRA maintained and operated, or directed the operation of, receiving equipment at Shemya, AK; Hanscom AFB, MA; Thule, Greenland; Tucuman, Argentina; and Agua Verde, Chile. The received data are stored on various magnetic media. Software to reduce and analyze the data was developed.

2. DATA COLLECTION AND PROCESSING

During this 27-month study period, NWRA maintained and operated data collection equipment at two sites: Shemya, AK, and Hanscom AFB, MA. In addition, equipment was deployed for short periods of time to Thule, Greenland; Tucuman, Argentina; and Agua Verde, Chile.

2.1. Description of Instrumentation

The government-furnished equipment (GFE) operated and serviced by NWRA includes the following: Stanford Telecommunication, Inc. (STEL) STEL-5010 single-channel GPS receivers; Texas Instruments (TI) TI-4100 four-channel GPS receivers; Magnavox MX-1502 Transit receivers; a National Institute of Standards and Technology Ionospheric Measurement System (NIMS) code-free, multi-channel GPS receiver manufactured by Atmospheric Instrumentation Research, Inc. (AIR); a Trimble Pathfinder six-channel, single-frequency GPS receiver; and a NWRA-designed and -built ITS-10S Transit coherent receiver system. An Ashtech Z-12, a modern, twelve-channel GPS receiver, was borrowed from Charles Stark Draper Laboratories, Cambridge, MA, for three months of data collection at Hanscom AFB, MA.

The STEL-5010 GPS receiver tracks a single satellite pass for up to six hours. It measures the DGD between the L1 (1575.4 MHz) and L2 (1227.6 MHz) signals, the DCP between those two signals, and the received intensities of the L1 and L2 signals from the older Block 1 GPS satellites only. It cannot receive the Block 2 satellites whose L2 signals are encoded such that the GPS selective-availability function can be invoked. Except for a two-week period in November, 1993, at Thule AFB, Greenland, the STEL-5010 receivers at Thule AB, Greenland; Shetland Islands, UK; and Hanscom AFB, MA; have not been operational during this period due to a large number of hardware failures. Because they can receive only the few remaining Block-1 GPS satellites, it is not considered cost effective to repair these systems.

The TI-4100 four-channel receivers, located at Shemya, AK, and Hanscom AFB, MA, collect data simultaneously from four different GPS satellites, both Block 1 and Block 2. DGD

and DCP are recorded at one sample every six seconds. Intensities of the L1 and L2 signals are not directly measured, and therefore scintillation indices, S4, cannot be derived from the TI-4100 data. The TI-4100 receivers cannot acquire encrypted GPS L2 signals and do not have an L1-only mode. Therefore, these receivers have been non-functional since GPS L2 encryption (Anti-Spoofing, AS) commenced on 30 Jan 94.

The MX-1502 Transit receivers, located at Shetland Islands, UK, and Hanscom AFB, MA, provide latitudinal relative TEC from north-south traveling satellites of the Navy Navigation Satellite System (NNSS). The transmitted signals from these satellites are at 150 MHz and 400 MHz. Each satellite pass lasts approximately 15 minutes. In order to determine absolute TEC levels along the satellite track, complementary absolute TEC data are required to calibrate the relative TEC measurements. Absolute TEC information from collocated GPS receivers provides such a reference.

The NIMS receiver is a code-free GPS receiver whose output consists of 15-minute averaged values of relative TEC. This receiver is located at Hanscom AFB, MA. In a letter dated 27 July 1992, Mr. David B. Call, president of AIR, Inc., reported that this receiver fails to meet the specified accuracy levels due to a design flaw in the antenna. AIR intends to correct this problem with a redesigned antenna. This redesigned antenna had not been received by NWRA as of the end of this contract, and the receiver was not used.

The ITS-10S receiver located at Hanscom AFB, MA, provides latitudinal relative TEC from the north-south traveling satellites of the NNSS. The 50-Hz sampling rate of this receiver is fast enough to yield scintillation information. Absolute TEC data, available from collocated GPS receivers, is required to calibrate the receiver's relative TEC measurements.

The Trimble Pathfinder six-channel, single-frequency GPS receiver is located at Hanscom AFB, MA. It is capable of collecting data from up to eight satellites simultaneously. The receiver sampling rate is a maximum of two samples per second. Its data output is stored in binary files containing pseudorange, doppler, signal-to-noise ratio (SNR), latitude, longitude, time of week (TOW), ephemeris data, and satellite ID. Its small size makes it suitable as an easily deployable indicator of ionospheric fading. This receiver was sent to Thule, Greenland; Tucuman, Argentina; and Agua Verde, Chile; and collected data for short periods at each site.

2.2. Instrumentation and Operation at Each Site

THULE, DK (GREENLAND)

A 14-day campaign to Thule AFB, Greenland, collected data that were used to study TEC variation in that region and to test and evaluate the operation of the NWRA ITS-10S Transit receiver and the Trimble Pathfinder GPS receiver for scintillation measurement in conjunction with TEC. Phillips Laboratory, Hanscom AFB, MA, conducted a concurrent experiment at Sondestrom, Greenland. From 4 November 1993 to 19 November 1993, Mr. C. Charley Andreasen (NWRA) operated the Trimble Pathfinder GPS receiver, the ITS-10S Transit receiver, and repaired, reprogrammed and operated the STEL-5010 GPS receiver.

The Trimble Pathfinder GPS receiver system operated without any problems during the entire period. Fourteen days of continuous data were collected and are stored on 4 mm magnetic tape. Analysis of the recorded signal-to-noise ratio showed evidence of ionospheric scintillation.

The ITS-10S Transit receiver system collected data during this period. Its operation was halted on two occasions when Arctic foxes ate the power cable from the receiver system to the antenna. The cable was replaced with a less appetizing type, and 11 days of Transit data were recorded on QIC-80 tapes.

The STEL-5010 receiver system was repaired and reprogrammed to record only the L1 amplitude signal at a sampling rate of twenty Hz. Since the L1 signal of all the GPS satellites is not encoded, this change allowed the STEL-5010 to track any GPS satellite, not just Block 1. The 20-Hz sampling rate is fast enough to allow the determination of the scintillation index S_4 (L1). This test was intended to evaluate the usefulness of retaining the STEL-5010 as a scintillation monitor.

SHEMYA, AK

At the Shemya site, NWRA maintained and directed the operation of the TI-4100 four-channel receiver. This receiver was combined with a 486 PC running specialized software written by Applied Research Laboratories of the University of Texas at Austin (ARL-UT) to form a Real Time Ionospheric Monitor (RTM). Very good quality DGD and DCP data (absolute and relative TEC, respectively) were collected. The TI-4100 system operated from August 1992 through the end of January 1994, when anti-spoofing was permanently enabled. The TI-4100 receiver can not decode the encrypted signals, and data collection terminated.

HANSCOM AFB, MA

The ITS-10S Transit receiver system was delivered to Hanscom AFB, MA, on 4 September 1993 and set up for testing. Due to apparent rough handling during shipping and the need for hardware upgrades, Phillips Laboratory (PL) decided to send the ITS-10S back to NWRA in Bellevue, WA, for warranty repair. It was repaired and returned to Hanscom AFB on 14 October 1993. The system operated satisfactorily for a two-week period prior to deployment to Thule. During that time, the ITS-10S receiver system's operation was demonstrated to a group of people from the MITRE Corporation [MITRE is on contract to support ESC (Electronic Systems Center) on the project that funded PL to purchase the ITS-10S receiver]. The ITS-10S receiver system was intended for installation at the Ballistic Missile Early Warning System (BMEWS) radar site at Fylingdales, UK, but due to lack of funding, was never deployed.

A TI-4100 four-channel receiver system operated at Hanscom AFB concurrently with the Shemya TI-4100. Both receiver systems ran the same collection software. The Hanscom receiver experienced intermittent failures, and the data from this site are not continuous. The quality of the data that was collected is good.

An Ashtech Z-12 GPS receiver was operated at Hanscom AFB from March to June, 1994. Three different antennas were tested with the receiver: a Micropulse antenna, an Allen Osborne

Associates antenna, and an Ashtech antenna. TEC data were generated from the RINEX (Receiver INdependent Exchange format) files produced by the receiver's data collection software.

The STEL-5010 receiver is not operational due to equipment failure. The redesigned antenna for the NIMS code-free receiver, required in order to meet its specified accuracy, was never supplied by the manufacturer and was not operated. The MX-1502 was not operated because there was no defined use for the data.

TUCUMAN, ARGENTINA

The Trimble Pathfinder single-frequency GPS receiver was coupled with a 486-notebook PC and collected data from 1-13 April 1994 at Tucuman, Argentina. Signal-to-noise data from this equatorial region showed widespread and prolonged occurrence of ionospheric scintillation during two periods of high geomagnetic activity. At other times, occasional occurrence of scintillation was noted during pre-midnight evening hours. This is consistent with past observations.

AGUA VERDE, CHILE

The Trimble Pathfinder single-frequency GPS receiver was deployed to another equatorial site, Agua Verde, Chile, from 26 September 1994 to 3 October 1994. Scintillation was observed during pre-midnight evening hours, often associated with large "depletion" structures observed concurrently by Phillips Laboratory (PL) using optical images. Seventeen days of data were collected.

2.3. Software Tools Developed for Data Analysis

Research software was developed to process and analyze the data collected during this study period. Programs exist that display equivalent vertical TEC as 24-hour, pass-file, and latitude-specific (north, overhead, and south of the observing station) plots. The multipath content of the data can be analyzed and minimized using other existing programs. Code that will allow analysis and plotting of RINEX-formatted data from many sources has been developed. A description of these programs is given in Appendix 1.

2.4. Data Archive

NWRA has created a data archive from measurements taken at Shemya, AK; Hanscom AFB, MA; Thule AB, Greenland; Tucuman, Argentina; and Agua Verde, Chile. A listing of these data, specifying site, dates, and type of receiver, is given in Appendix 2. In addition, NWRA has accessed a small amount of complementary data from IGS's (International GPS Service for Geodynamics) substantial RINEX database of GPS measurements from stations around the globe. These data were processed into a form that is similar to NWRA-collected data for analysis.

TEC was monitored at Shemya, AK, using a TI-4100 four-channel GPS receiver, yielding data that support study of TEC variability with look direction at this location and provide a basis for validating new global ionospheric models applied to this site. A comparison of empirical measurements to the Bent ionospheric model's predictions was performed.

Scintillation effects were seen in the Trimble Pathfinder GPS single-channel receiver data collected at Tucuman, Argentina, and Agua Verde, Chile. These data may be used to support validation and improvement of ionospheric scintillation models for the near-equatorial region.

A data archive was developed of amplitude scintillation data from both radar and Transit navigation satellite receivers observing in the vicinity of York, England. These data will support validation and improvement of ionospheric scintillation modeling in that region.

3. RESULTS

3.1. Total Electron Content Data

3.1.1. Shemya

The DCP and DGD measurement data collected by the TI-4100 four-channel GPS receiver system at Shemya, AK, are stored as RINEX files. This format was designed to facilitate the exchange of GPS data by the international geodetic user community. For compatibility with existing analysis and plotting programs, a program was written to convert the RINEX data to the single-channel file format developed by NWRA for analysis of STEL-5010 data. Since RINEX has become the standard data format, a program was also written to extract individual satellite pass files, containing satellite number, Julian date, year, time, DGD, and DCP, from the RINEX file. This pass-file format is simpler than the single-channel file format and allows greater flexibility for analysis and plotting.

Initial Shemya data, from days 153-159, 1992, were processed and plotted (see Figure 1). The TEC profiles as predicted by the Bent ionospheric model (Ref. 1) and generated by RDP, Inc., of Waltham, MA, are shown in Figure 2. Initial results indicated three areas of study for improvement of data quality. First, an assessment of satellite bias and receiver offset values (i.e., system calibration) was needed. Second, the DCP data contained discontinuities and required correction. Third, the DGD data were found to have a high degree of multipath contamination.

In order to determine TEC values accurately, the measurement contributions of satellite biases and receiver offset must be considered. (The satellite bias is referred to as the differential group delay correction term, T_{gd}, which is the difference in transmit time between the code on the two frequencies). Mr. Gregory J. Bishop of Phillips Laboratory at Hanscom AFB, MA, postulated the following method for determining the proper receiver offset and satellite bias values (Ref. 2). First, several days of data were plotted. Data collected from satellites located within one degree of latitude of the site were processed into equivalent vertical TEC and plotted on a 24-hour scale of local time at the ionospheric penetration point (IPP) of the ray path to the satellites. These data should yield a continuous curve that shows the diurnal variation of TEC. Distortion of portions of the curve is attributable to incorrect bias values for the satellites contributing those portions. The receiver offset value affects the overall level of the curve. By iteratively adjusting these quantities and evaluating the plotted results, a set of values can be determined that produces ionospheric equivalent vertical TEC curves with proper diurnal and seasonal behavior. It was shown that very little change from these empirically derived bias values

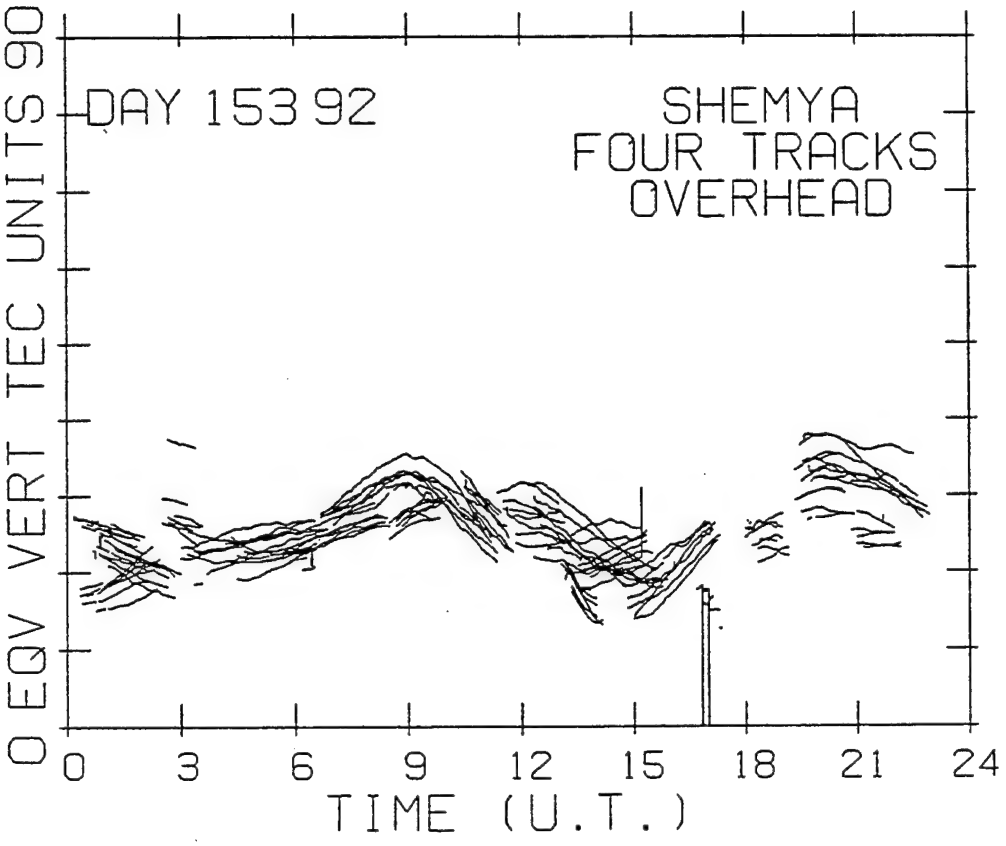

Figure 1. Overplot of Shemya TEC data from days 153 - 159, 1992.

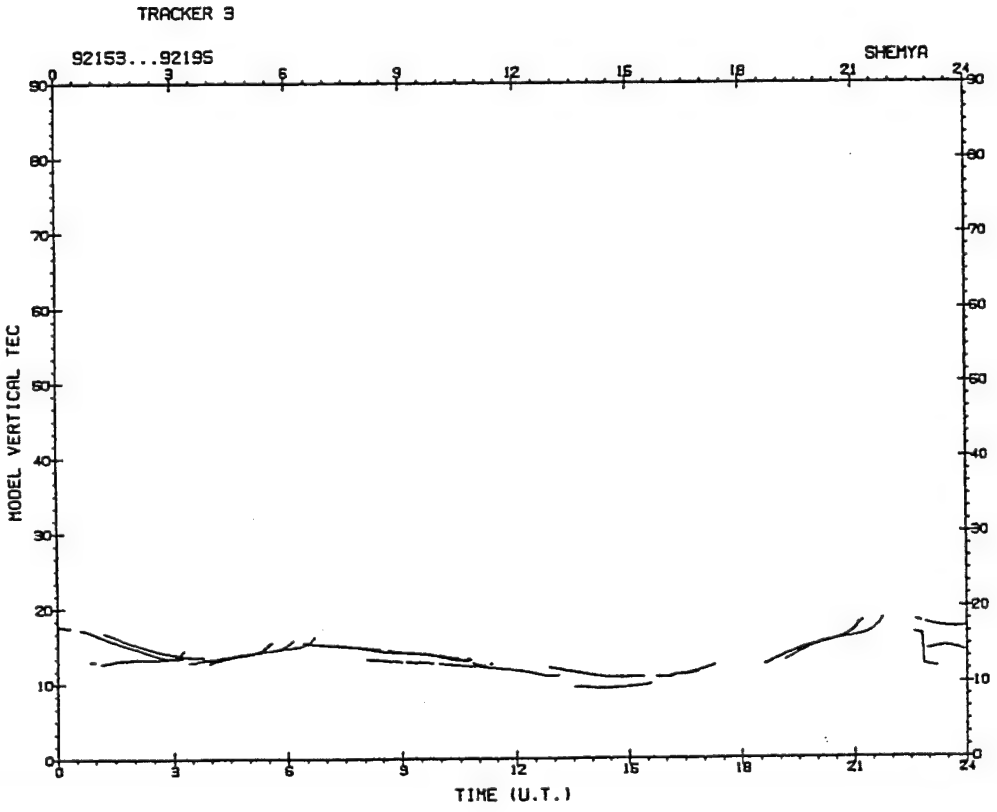

Figure 2. Bent model-predicted behavior at Shemya.

begins to introduce distortion in the TEC curves, indicating that the accuracy of these values is better than ± 2 to 3 TEC units (see Figures 3 and 4).

Dr. Andrew Mazzella (RDP, Inc., Waltham, MA) has developed a computational algorithm that incorporates the above concepts (Ref. 3. Complete text of Reference 3 is included in Appendix 3). This automated calibration process, called Self Calibration Of pseudoRange Errors (SCORE), minimizes the difference between equivalent vertical TEC measurements from two satellites at the same IPP latitude and IPP local time by adjusting the combined satellite plus receiver correction value for each satellite. No ionospheric model is assumed. This algorithm is best suited to mid-latitude stations where there is reasonably consistent diurnal TEC behavior. In more disturbed regions, the actual time difference between two measurements with the same IPP latitude and IPP local time may result in very different ionospheric conditions, requiring adaptations in the SCORE process.

An example of the results of the SCORE process is given in Figure 5. Data collected at Hanscom on day 114, 1994, are shown plotted (top) with correct calibration and (bottom) with a set of calibration values determined for a previous system configuration using a different antenna. The correct calibration values yield a credible diurnal TEC profile, whereas distortion results from incorrect values.

Discontinuity correction of the differential carrier phase data was originally achieved during post processing using Turbo Edit, a commercially available software package. For real-time TEC calculations, ARL-UT developed a Kalman filter that was used with their RTM software controlling the TI-4100 receiver.

Measurements of the DGD, from which absolute TEC is determined, are very susceptible to contamination by multipath. The DCP is two orders of magnitude less sensitive to multipath effects. It yields a relative measure of TEC, containing a $2n\pi$ ambiguity. The DCP can be referenced to the DGD through a "phase-averaging" process to resolve the ambiguity. Phase averaging entails calculating the average value of the DGD and the average value of the DCP over a satellite pass. The difference between these two levels (DGD_{ave} - DCP_{ave}) is added to each DCP measurement, bringing the relative TEC measurements, DCP, to the level of the absolute TEC measurements, DGD. The interval of data used for phase averaging must be larger than the period of the multipath, preferably a few hours, or the phase-averaged result will be in error. This is not usually a problem when post processing data, since a GPS satellite pass can last three hours or more, but the error can be significant in real-time application.

A software multipath-modeling approach proposed by Mr. Gregory J. Bishop of Phillips Laboratory at Hanscom AFB, MA, has been investigated (Ref. 4, 5, and 6). A multipath template is created using 24 hours of DGD and DCP data. The DCP and the DGD containing multipath are phase-averaged. The phase-averaged DCP is subtracted from the DGD plus multipath to produce a point-by-point multipath template file. This template contains system noise as well as multipath. To minimize the system noise content, the template is smoothed by taking one-minute averages.

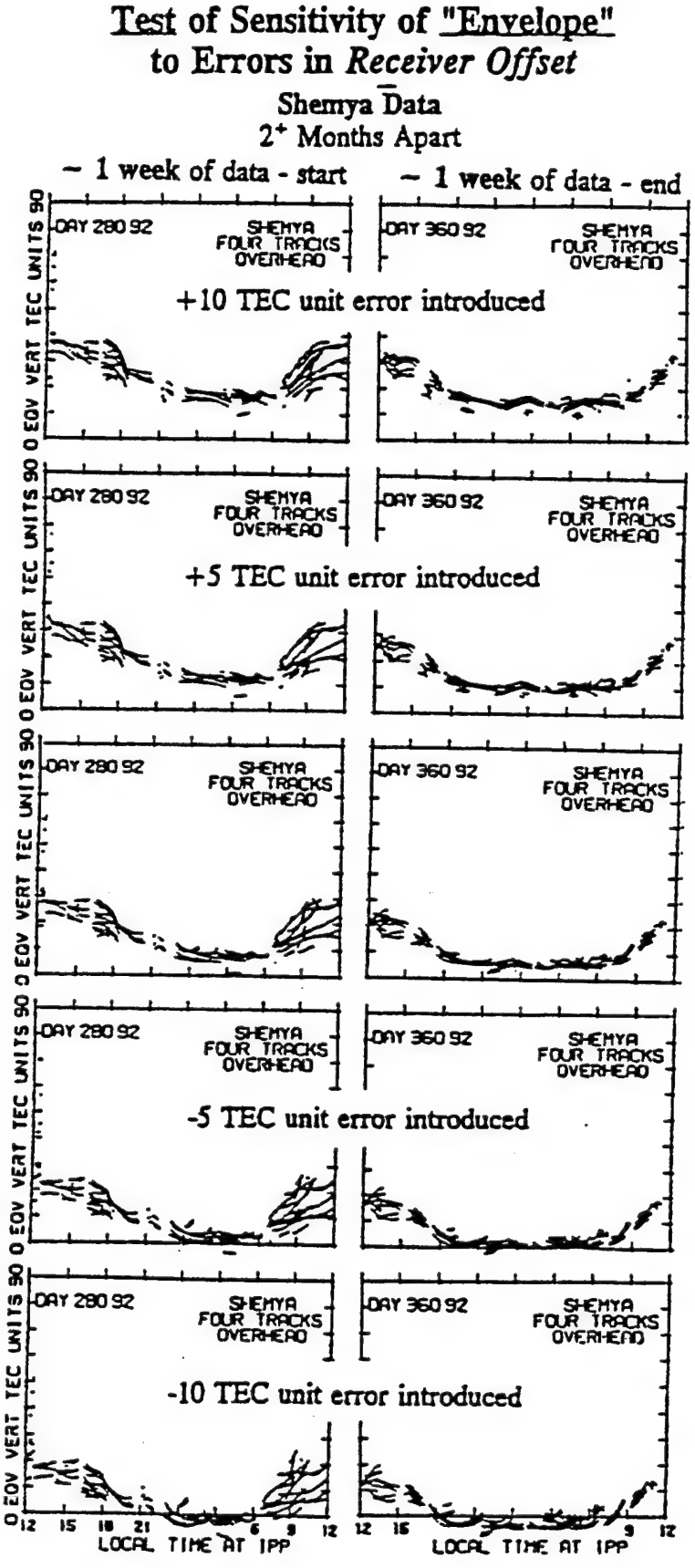

Figure 3. Shemya data showing effect of changes to receiver offset.

Test of Sensitivity of "Envelope" to Errors in T_{GD}

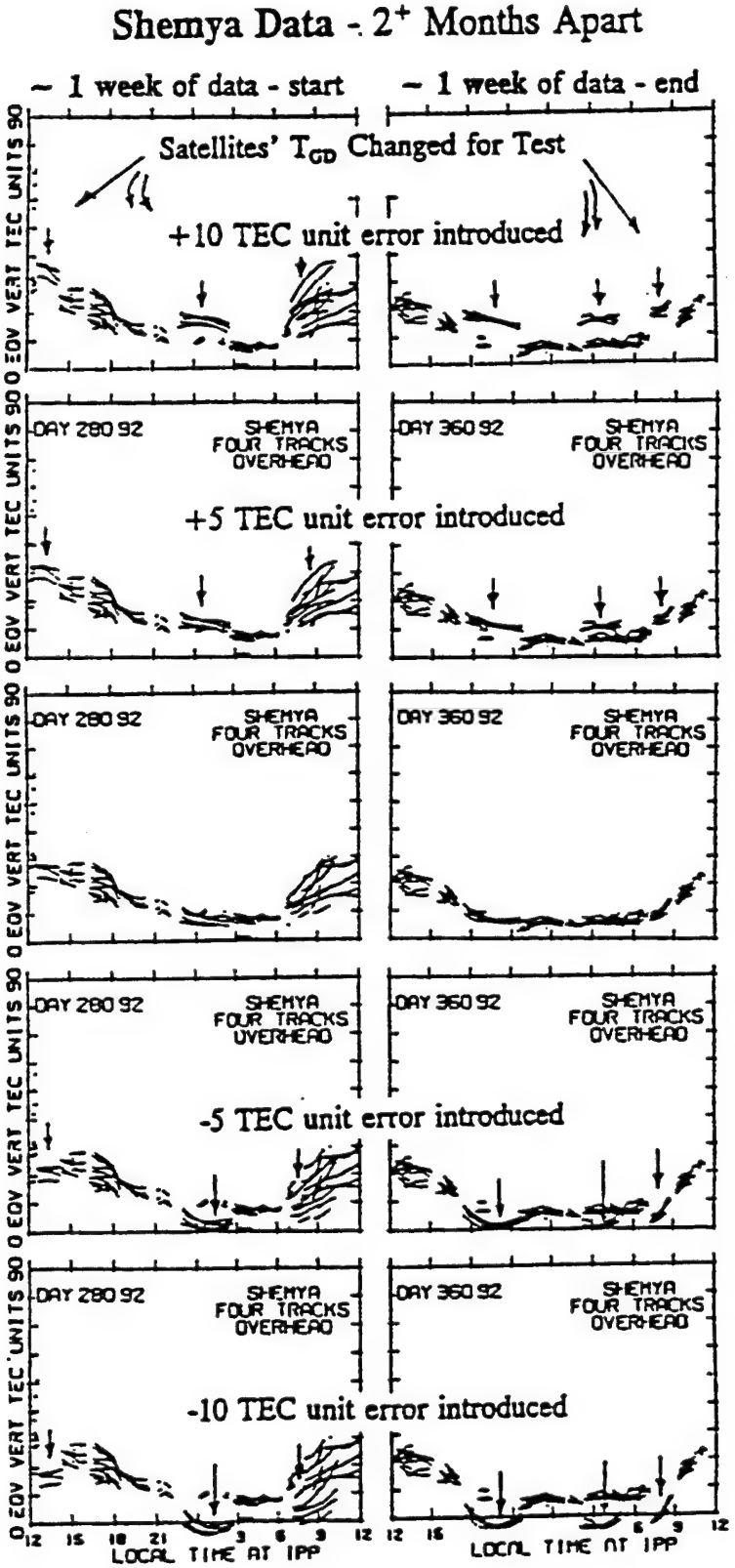

Figure 4. Shemya data showing effect of changes to satellite biases (T_{gd}).

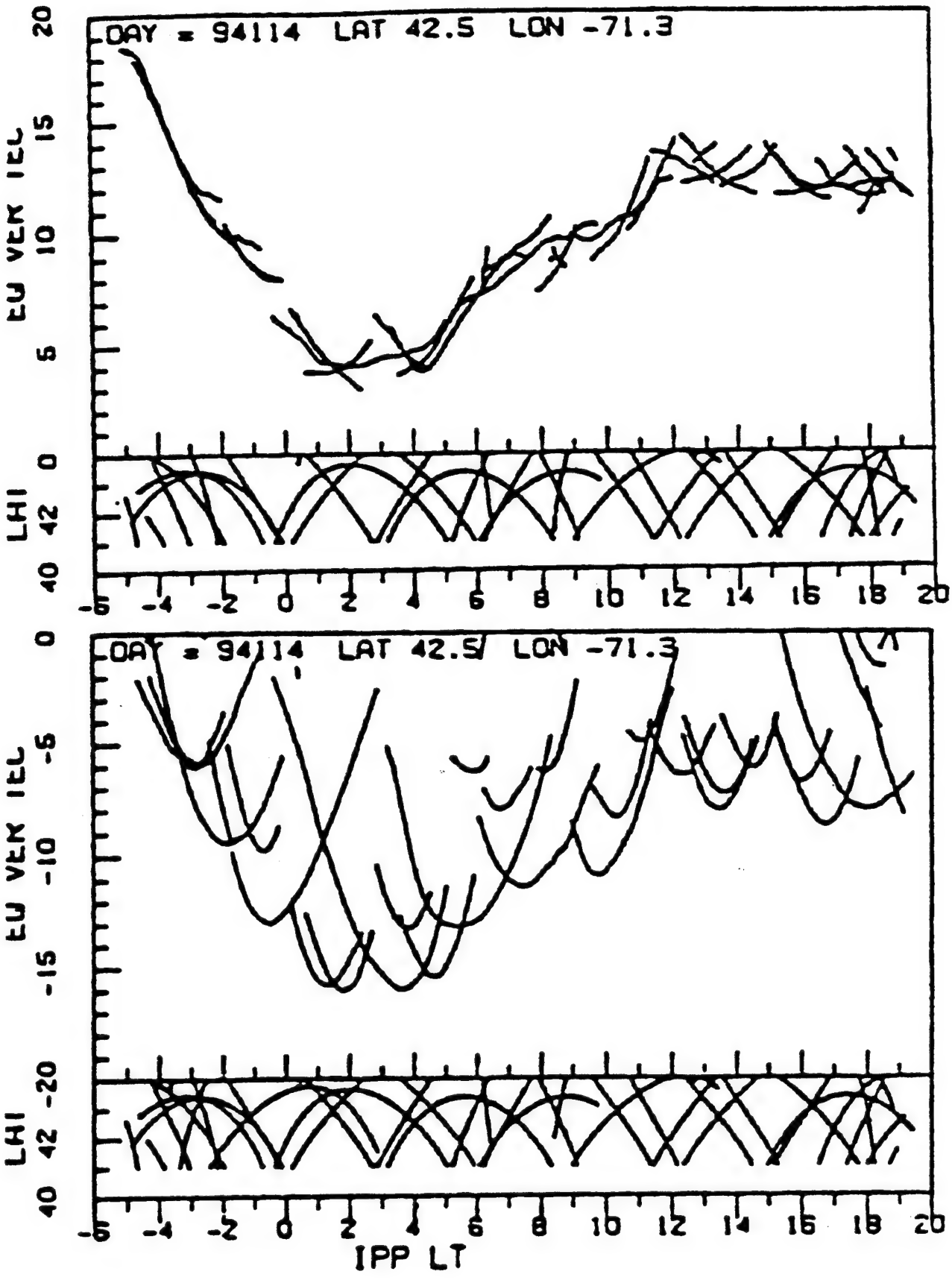

Figure 5. Correctly calibrated (top) versus incorrectly calibrated diurnal TEC data.

The correlation coefficient for templates from two different days was determined. Results showed that passes containing large multipath were highly correlated, while passes with low multipath had a much lower correlation coefficient (Ref. 6. Complete text of Reference 6 is included in Appendix 3). This is understandable since the template contains system noise, which is uncorrelated, and multipath.

A multipath template created from a day of data can be applied to data from subsequent days. Figure 6 shows 24 hours of equivalent vertical TEC from DGD data collected at Shemya, AK. Figure 7 shows the same data after the multipath template created from day 153, 1992, was applied.

Since the multipath template technique relies on daily repetition of the GPS observation geometry, the data and the template must be time aligned to compensate for the precession of the satellite orbits. The template time is shifted 3 minutes 56 seconds for each day that the subject file lags the template file. Using this simple alignment method, a multipath template yields good results for about seven days. A more precise technique based on satellite position alignment, studied by ARL-UT, significantly increases the effective life span of a template (Ref. 6).

The spatial decorrelation of a multipath template has been investigated (Ref. 6). Using the template itself, the multipath at one point was approximated by taking the template value at a given angular distance away. The multipath error, the difference between the actual template value and the approximated value, was calculated. The multipath was seen to decorrelate rapidly with spatial distance. With a five-degree spacing, the error in the approximated multipath value was sometimes as large as the actual multipath. It was shown that even a fraction of a degree change in spatial distance resulted in a noticeable change in the template, indicating the dependence of the template on satellite path. Therefore, any multipath modeling for a receive antenna's location must be capable of accurately defining the multipath down to a fraction of a degree in all possible look directions. The effectiveness and simplicity of the multipath template technique compare favorably with the more complex multipath modeling approach.

The multipath template technique was implemented by ARL-UT for use in their RTM software delivered to PL and run at Shemya, AK. The RTM configuration file contained a switch that directed the software to use a multipath template. This template was generated by NWRA personnel at PL using data collected by the RTM, and was then uploaded to the Shemya computer. Real time data collected by the RTM were first converted to RINEX format. Next, the DCP data were corrected for discontinuities by applying a Kalman filter. These corrected GPS measurements were converted to ionospheric parameters, and the multipath template was then applied to the DGD. The DCP and DGD were phase-averaged using a real-time phase-averaging algorithm, satellite bias and receiver offset adjustments were made, and the data were converted to equivalent vertical TEC.

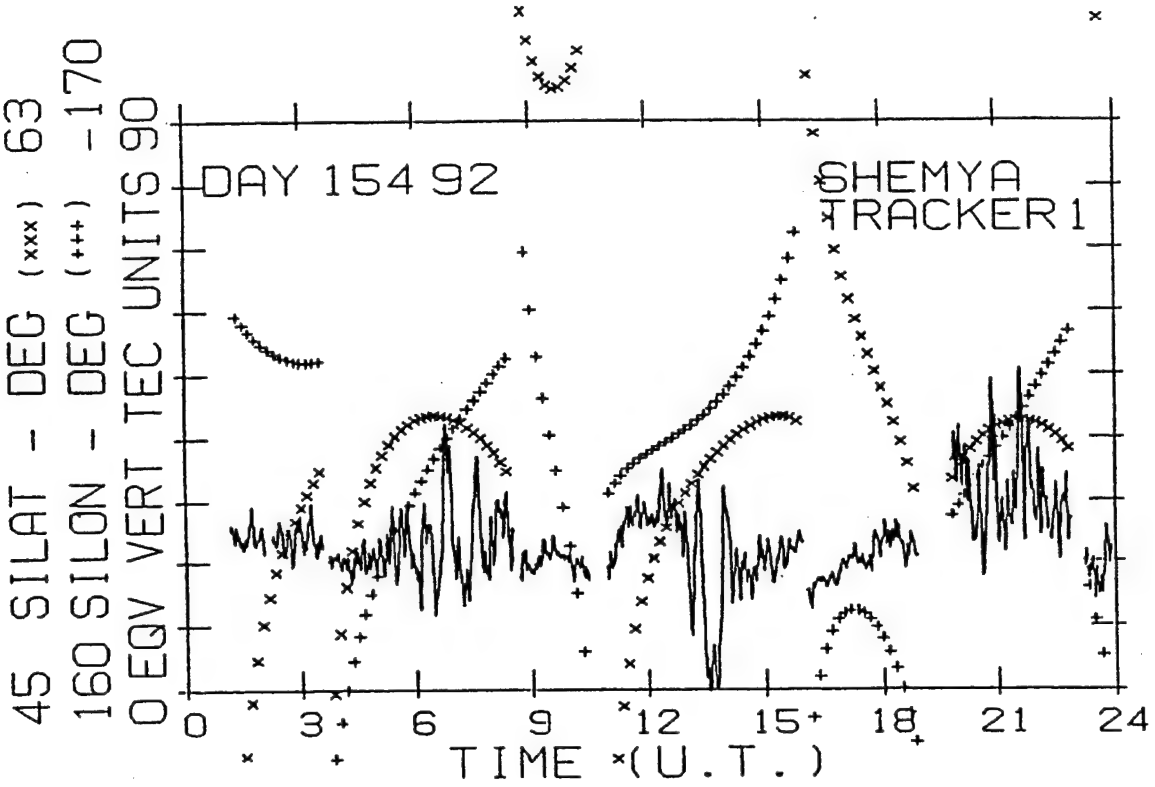

Figure 6. Day 154, 1992, TEC data from Shemya containing large multipath.

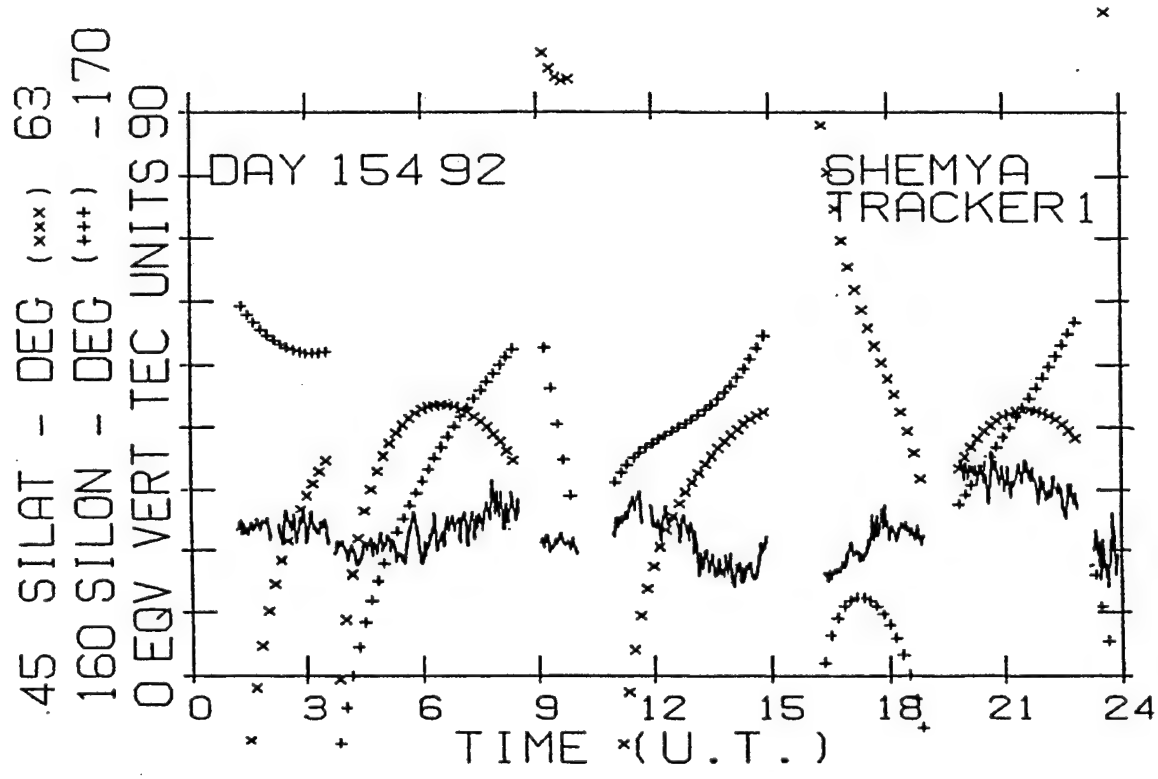

Figure 7. Day 154, 1992, TEC data after application of multipath template from day 153, 1992.

The RTM also produced a file containing one 15-minute averaged value of slant TEC, elevation, and azimuth for use by another program, the Scale Factor Generator (SFG, written by RDP). Every 15 minutes, the SFG read that file and generated a real-time ionospheric scale factor that could be used to update the radar's ionospheric correction table.

3.1.2. Hanscom

Approximately three months of RINEX formatted data were collected at Hanscom AFB using an Ashtech Z-12 multi-channel GPS receiver capable of bypassing the encrypted P code (AS) via a "codeless" processing that yields TEC data, although at lower signal-to-noise levels. Three different antennas were used with this receiver during the 16 March 1994 to 10 June 1994 period.

Figure 8 shows two days of data (90 and 91, 1994) collected using the Micropulse antenna. Data from days 95 and 97, 1994, collected with an Allen Osborne Associates antenna, are presented in Figure 9. The two overplotted curves are slant TEC from group delay (noisy curve) and slant TEC from phase. The third curve is phase-averaged, equivalent vertical TEC. In all cases for the Micropulse antenna, the group-delay data start out above the phase data and end below, and also diverge from the phase throughout the pass, while the Osborne antenna examples show no divergent behavior. Figure 10 shows day 81 data from the IGS Westford, MA, site compared to concurrent data collected at Phillips Laboratory, Hanscom, using the Ashtech Z-12 and the Micropulse antenna. Occasional, large divergences were seen in the Hanscom data but not in the Westford data. These divergences appear to be due to non-uniformities in the Micropulse antenna, as configured by Draper Laboratories.

Figure 11 illustrates multipath content in data from the two antennas for comparison. The Micropulse antenna data (day 90, left column) contain larger-magnitude, longer-period multipath components than the Osborne antenna data (day 97, right column). Studies performed on these data illustrated how factors such as multipath, antenna irregularities, drift in RF components, and interference can affect the accuracy of the GPS measurements (Ref. 7). Results of these studies demonstrated the usefulness of the SCORE approach to site-specific system calibration.

Access to the International GPS Service for Geodynamics (IGS) substantial RINEX database from its worldwide network was acquired. These data (for example, Westford, MA, data shown in Figure 10) allowed comparison and validation of data collected by NWRA during this contract period and can be used to investigate and document TEC morphology at any of the IGS sites.

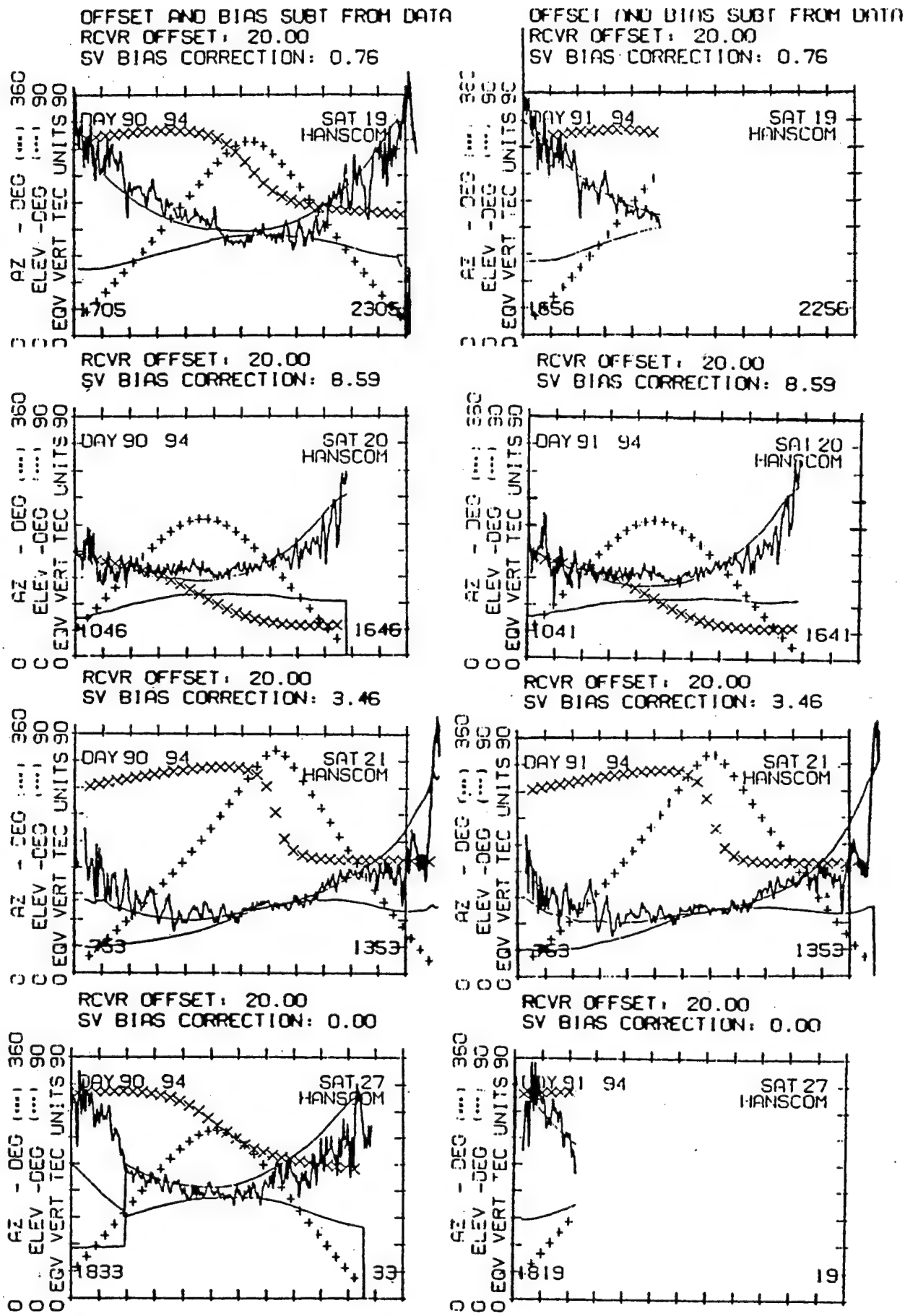

Figure 8. Ashtech Z-12/Micropulse antenna data showing divergence of group delay (noisy curve) and phase.

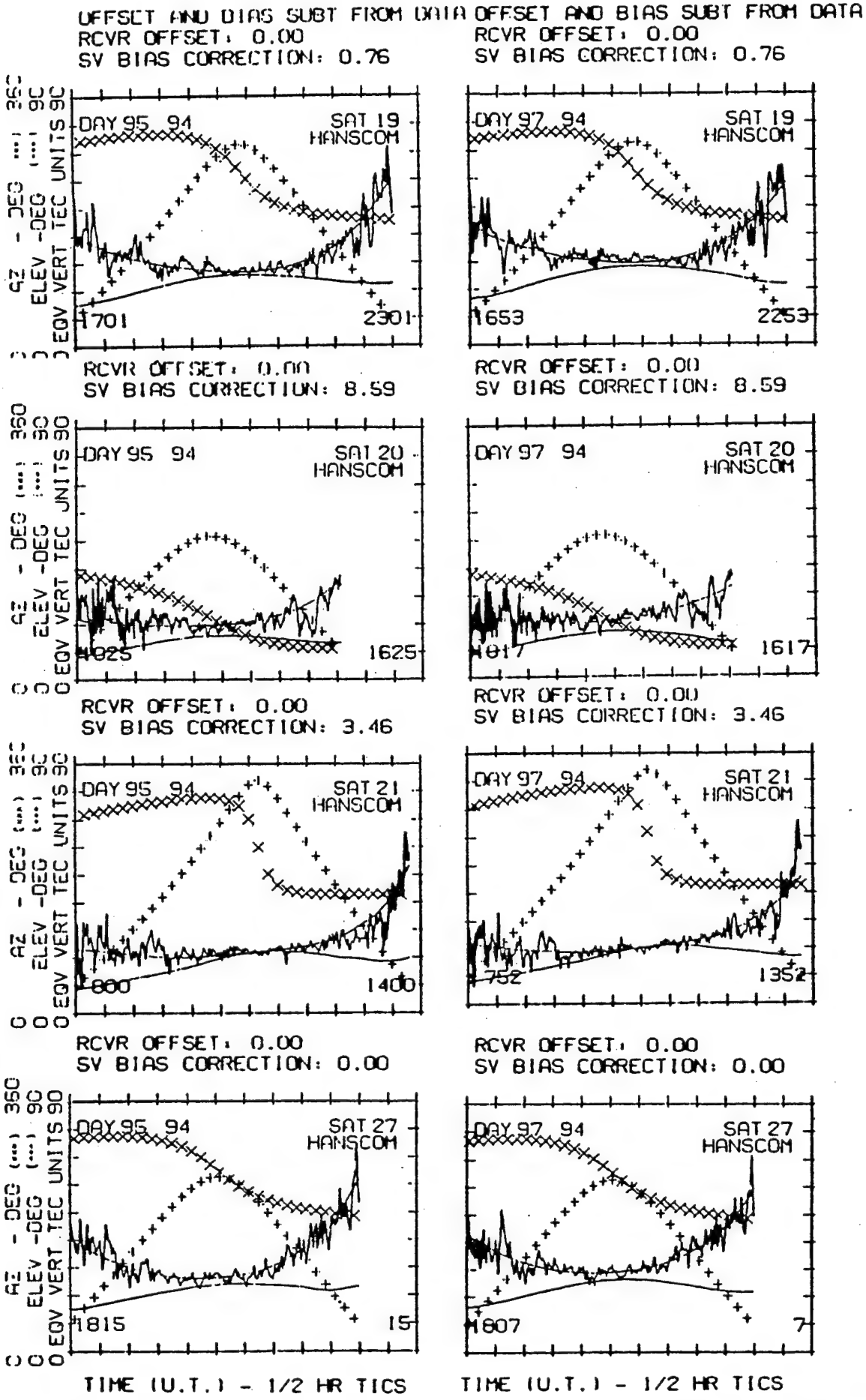

Figure 9. Ashtech Z-12/Osborne antenna data showing group delay tracking the phase.

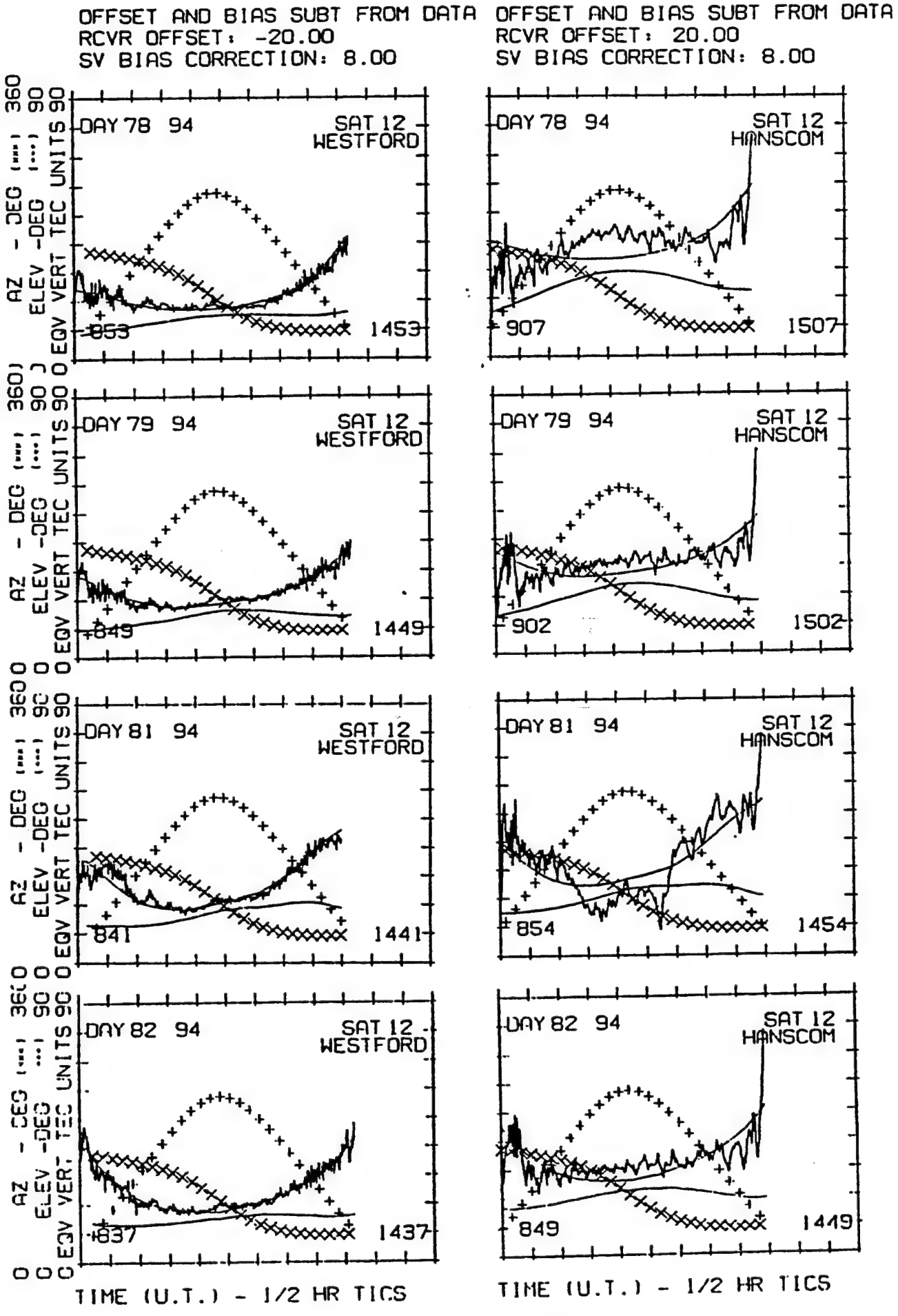

Figure 10. Data from nearby Westford, MA, (IGS) compared to Ashtech Z-12/Micropulse antenna data.

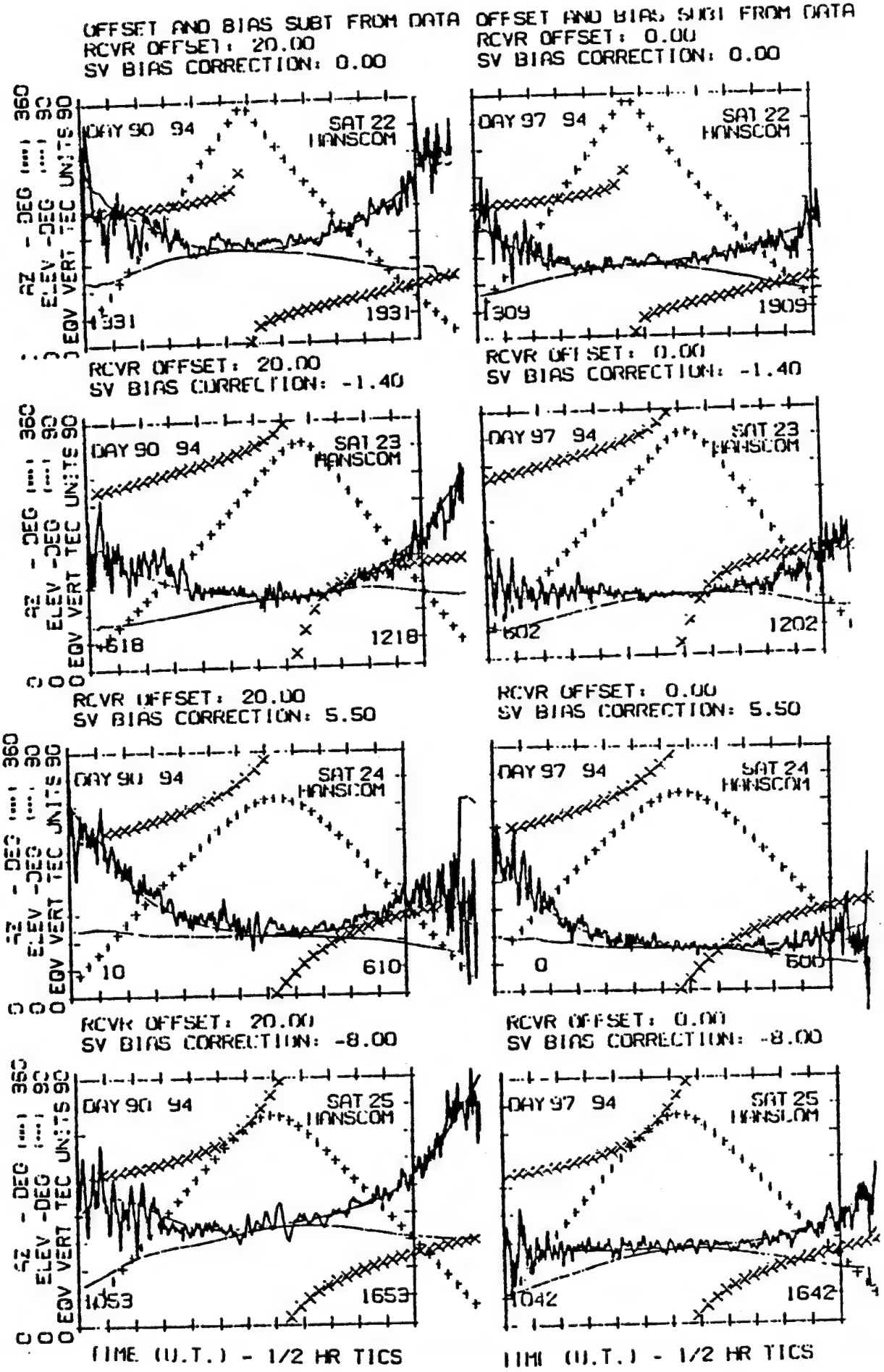

Figure 11. Larger magnitude, longer period multipath is seen in Ashtech Z-12/Micropulse antenna data (left) than in Ashtech Z-12/Osborne antenna data (right).

3.2. Shemya TEC Morphology

Analysis of the mid-latitude data from Shemya, AK, has yielded TEC morphology for that region over many months. The plots in Figure 12 show data whose IPP latitude is within ± 1 degree of the observing station. The diurnal and seasonal variation of the TEC profile is clearly evident.

3.3. Ionospheric Scintillation

The Trimble Pathfinder single-frequency GPS receiver collected data at Thule, Greenland (6-19 November 1993); Tucuman, Argentina (1-13 April 1994); and Agua Verde, Chile (26 September- 3 October 1994). The signal-to-noise ratio recorded in these measurements was converted from AMU's (Trimble defined Antenna Measurement Units) to dB and plotted. Both Tucuman and Agua Verde are in the region of the magnetic equator where ionospheric scintillation (Ref. 8), the rapid fading and enhancement of the GPS signal due to small-scale irregularities in the ionosphere, frequently occur. Figure 13 shows an example of a rapid onset of scintillation seen in the Tucuman data (Ref. 9). Some very large GPS-observed ionospheric fade conditions at Tucuman are shown in Figure 14. Such occurrences can effectively reduce satellite availability, possibly impacting GPS navigation in the region. Scintillation effects were also seen in the Thule and Agua Verde Trimble data. The Tucuman and Agua Verde scintillation occurrences were associated primarily with high geomagnetic activity and equatorial "plasma depletions", respectively. These data may thus be used for improvement or validation of scintillation models for the equatorial region with respect to these phenomena.

3.4. Assessment of Trough Signatures

The trough is a large region of lower plasma density that is a steady feature of the high-latitude ionosphere. Scintillation usually occurs poleward of the trough. The trough is typically located poleward of the middle latitudes and is seen to move equatorward during periods of high geomagnetic activity. Its signature is characterized by steepened gradients of TEC. (Typical diurnal TEC behavior at mid-latitudes exhibits flat, low levels at night, a cosine-like rapid rise at dawn, and peak values at around 1400.) The trough was seen in several examples of Shetland data from 1991-1992 (Ref. 10 and 11) during magnetic storm periods. A technique of plotting latitudinally separated data allows viewing of the apparent equatorward movement of the trough, seen from a single location. In Figure 15 (Shetland data from day 312, 1991), the trough signature is seen overhead (± one degree of the station's latitude) at 1500 hours and to the south of the station at 1630 hours. (Much of the apparent diurnal movement of the trough is due to the station's movement with respect to the trough, which is largely stationary in sun-fixed coordinates. However, as noted above, the trough does move equatorward in response to increased geomagnetic activity and poleward as this activity decreases.)

TEC data from Shetland Island, UK, were analyzed to identify signatures of the ionospheric trough region for several cases during magnetic storm activity. Occurrence of the trough in Shetland data was determined by visually inspecting the TEC plots. RDP has suggested possible approaches to developing an algorithm that could automatically detect the presence of the trough signature during data processing. These signatures will support studies of improved

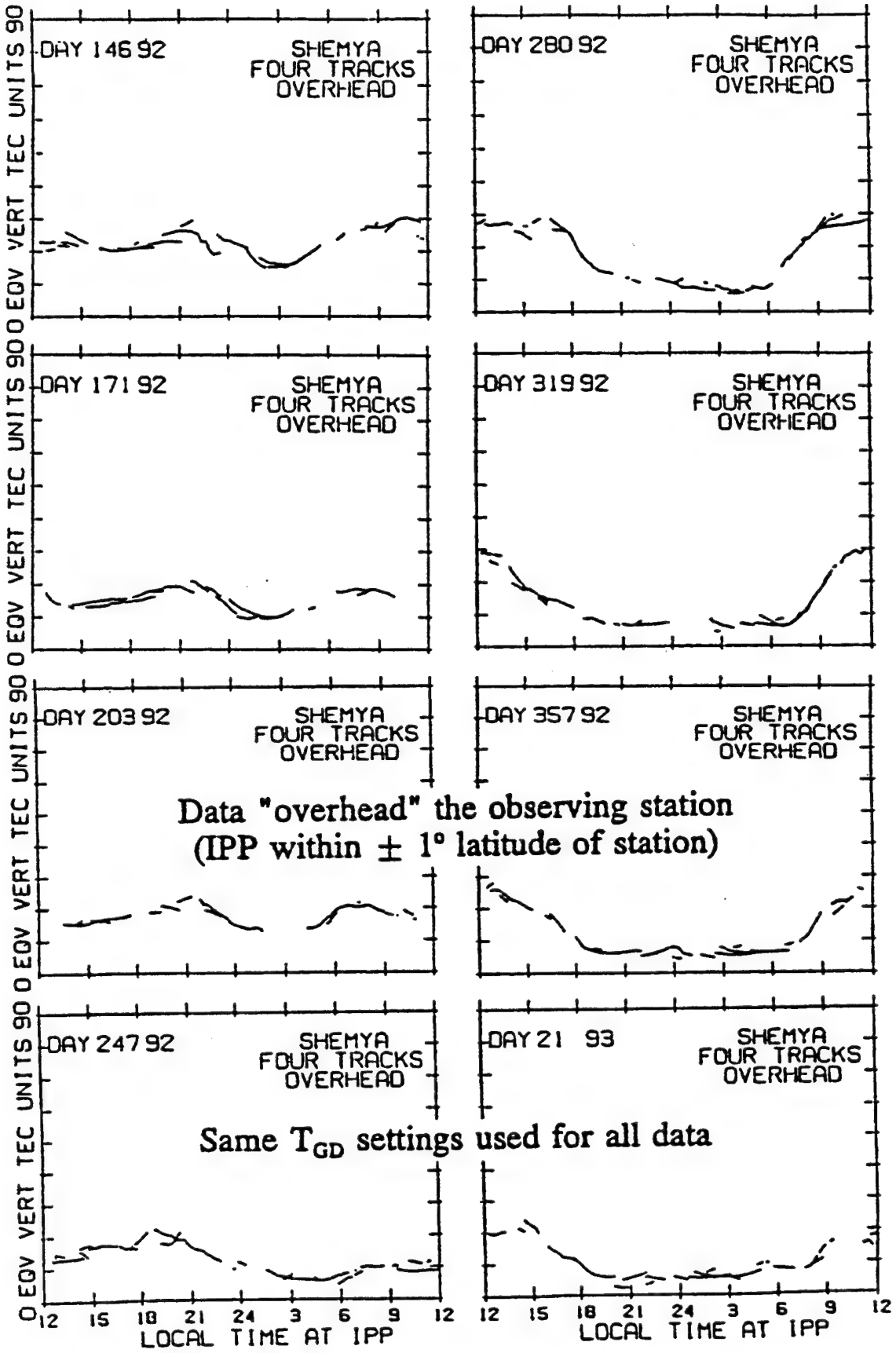

Figure 12. Shemya GPS data from a 241-day period showing seasonal evolution of the diurnal TEC profile.

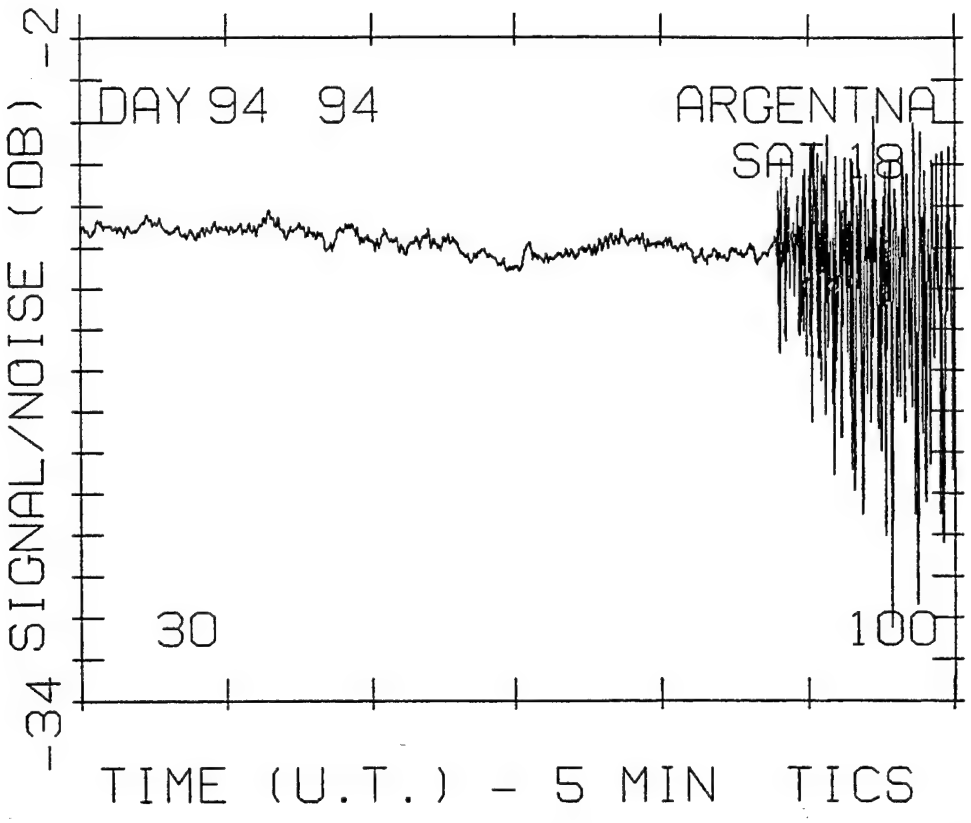

Figure 13. Onset of scintillation seen in the signal-to-noise measurements from the Trimble Pathfinder single-frequency GPS receiver taken at Tucuman, Argentina.

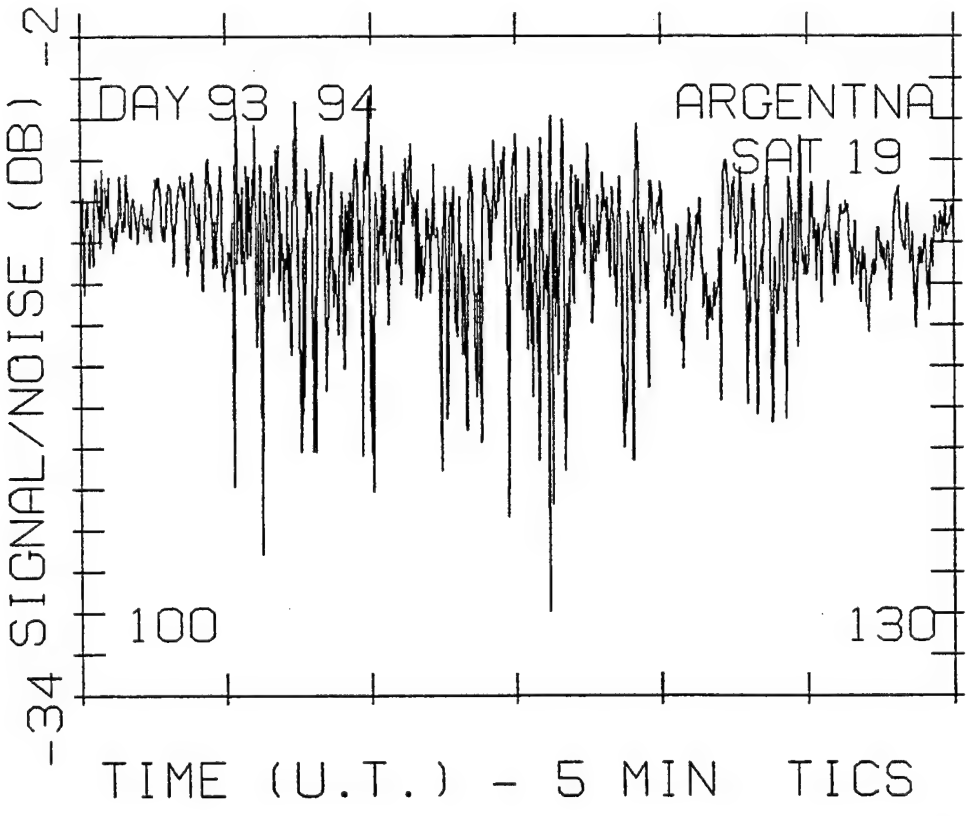

Figure 14. Example of large, GPS-observed ionospheric fade conditions at Tucuman, Argentina.

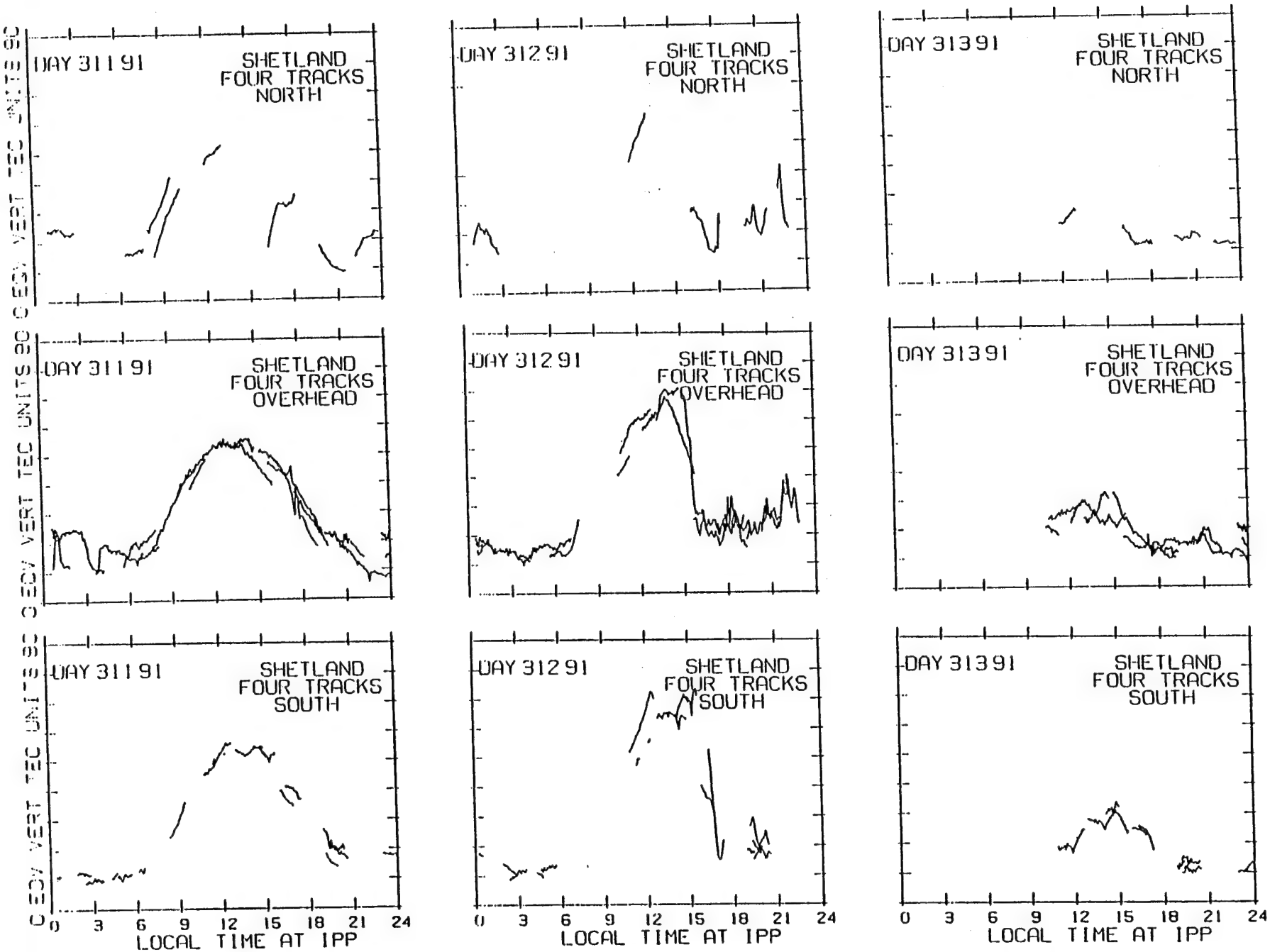

Figure 15. TEC data from Shetland Island, UK, showing the trough signature on day 312, 1991.

detection of the trough boundary with the potential for real-time application using data from the new Air Weather Service Ionospheric Monitoring System (IMS) (Ref. 12).

3.5. Ionospheric Model Assessment

The data collected by NWRA under this contract, data collected during earlier efforts, and RINEX data from the IGS worldwide network of sites can be compared to ionospheric model-predicted values of TEC. RDP, Inc., Waltham, MA, has developed analysis software for PL that performs a statistical comparison of TEC values predicted by the Bent ionospheric model to measured TEC values (Ref. 13). Their software, developed for processing on the Phillips Laboratory VAX mainframe computer, can accept both GPS and Transit satellite data. These programs were adapted by NWRA to work on IBM PC-compatibles.

The Bent ionospheric model, as implemented by the PAVPAW program, is used by US Air Force Space Forecast Center to predict TEC variation on a monthly basis for particular sites. These predictions are used to correct for TEC-induced range errors in radars. Comparison of the model-predicted values to actual TEC measurements from GPS discloses the accuracy of the model. Data collected by the Real Time Monitor system at Shemya, AK, were used in this contract effort for an initial evaluation of the Bent ionospheric model for that time and region. Two one-week periods, 158-164, 1992, and 288-294, 1992, were used in the assessment.

One day from each week was calibrated using the SCORE process to insure the accuracy of the measurements. Each week of data was then used to create a statistical database containing time, Bent model-predicted TEC, and measured TEC. (The code can be adapted to input from other models and measurement sources.) The statistics are presented in scatter plots showing model-predicted slant-path TEC values versus GPS slant-path TEC measurements (Figures 16 - 23). During production of a scatter plot, the database can be filtered according to elevation, look direction (azimuthal range), and time. For this analysis, the data were binned according to elevation (high>20°, low<20°), look direction (north = -45° to 45°, west = 45° to 135°, south = 135° to 225°, east = 225° to 315°; with directions being specified counterclockwise from 0° due north), and time (0300 to 0900, 0900 to 1500, 1500 to 2100, 2100 to 2700). This yielded 32 scatter plots for each data set.

Figures 16 and 17 show the same database (158 -164, 1992) divided into high and low elevation bins. For the 1500 to 2100 time period, the model predicted lower values than were measured in the north and west look directions (azimuthal ranges as defined above), and higher values in the south. The results were mixed for the east look direction, being higher for low elevations and lower for high elevations. Likewise, Figures 18 and 19 show low and high elevation sets for days 288 - 294, 1992. The model predicted lower values than measured in the east, south, and west look directions, and results were mixed in the north. Clearly, no conclusions can be drawn from those bins that contain very little data. Initial evaluation of model performance may be obtained from the bins with good data sets. However, it is recommended that this data set and processing be extended over periods of months to fully evaluate this and other models.

A comparison may be made of Figures 19 and 20, Figures 17 and 21, and Figures 22 and 23. In each of these three cases, the same time and elevation selection for the two different

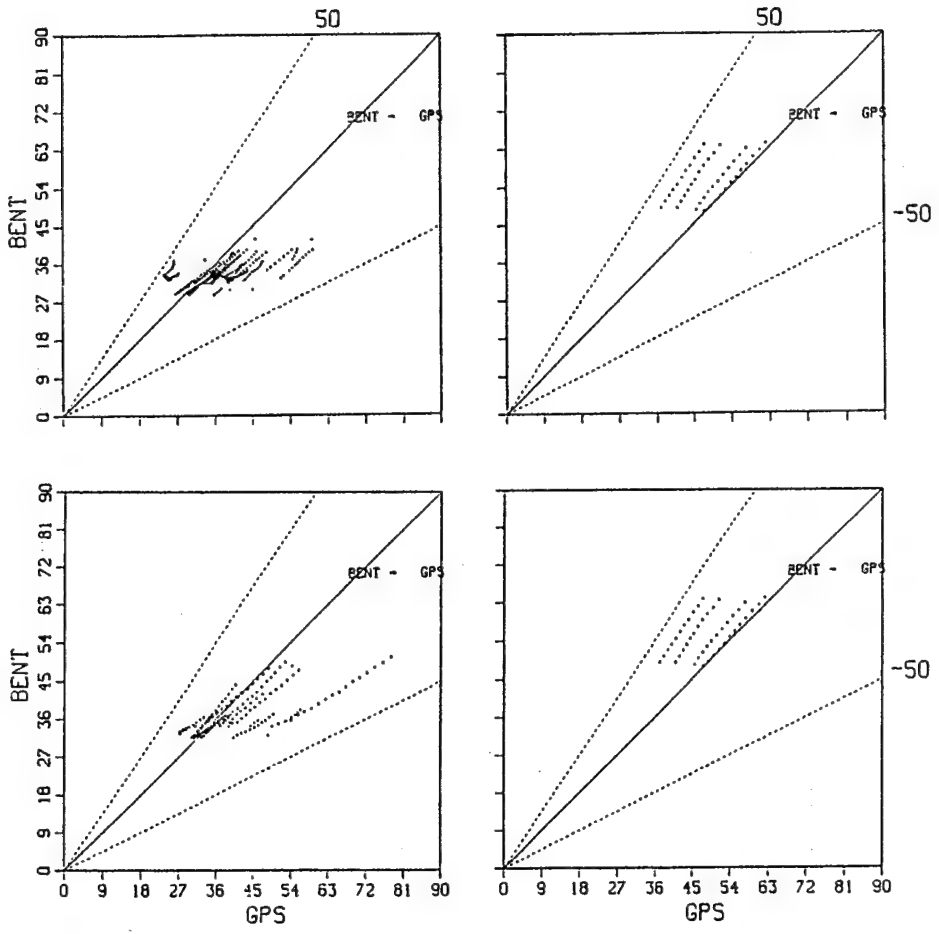

Figure 16. Comparison of monthly forecast (Bent) slant-path TEC to GPS slant-path TEC data from days 158 - 164, 1992, 1500 to 2100 hours, low elevation. Scatter plots are arranged by look direction (north, east, south, west) clockwise from top left.

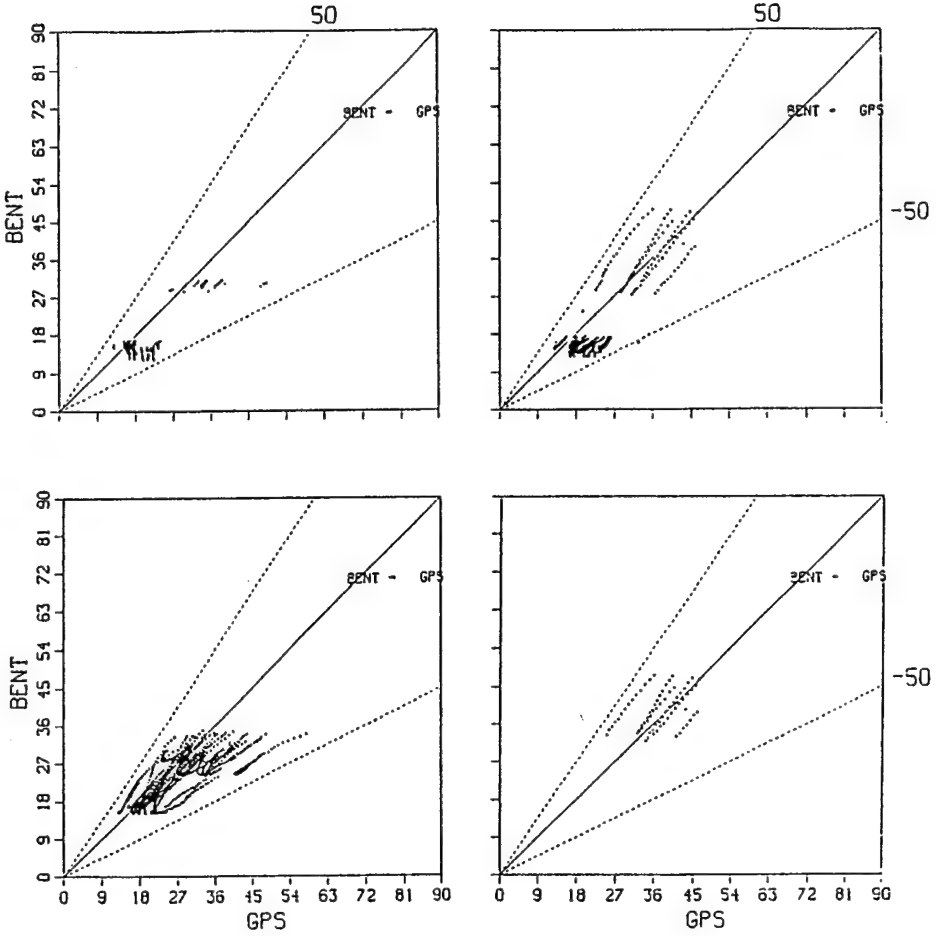

Figure 17. Comparison of monthly forecast (Bent) slant-path TEC to GPS slant-path TEC data from days 158 - 164, 1992, 1500 to 2100 hours, high elevation. Scatter plots are arranged by look direction (north, east, south, west) clockwise from top left

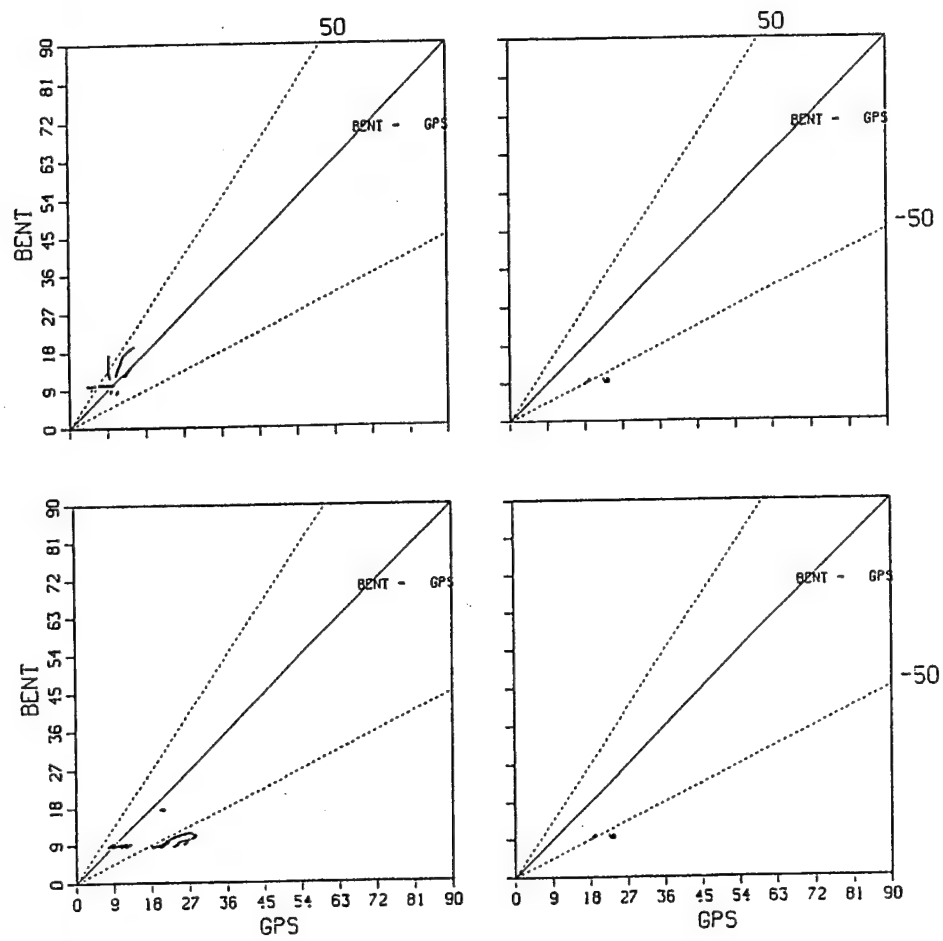

Figure 18. Comparison of monthly forecast (Bent) slant-path TEC to GPS slant-path TEC data from days 288 - 294, 1992, 2100 to 2700 hours, low elevation. Scatter plots are arranged by look direction (north, east, south, west) clockwise from top left.

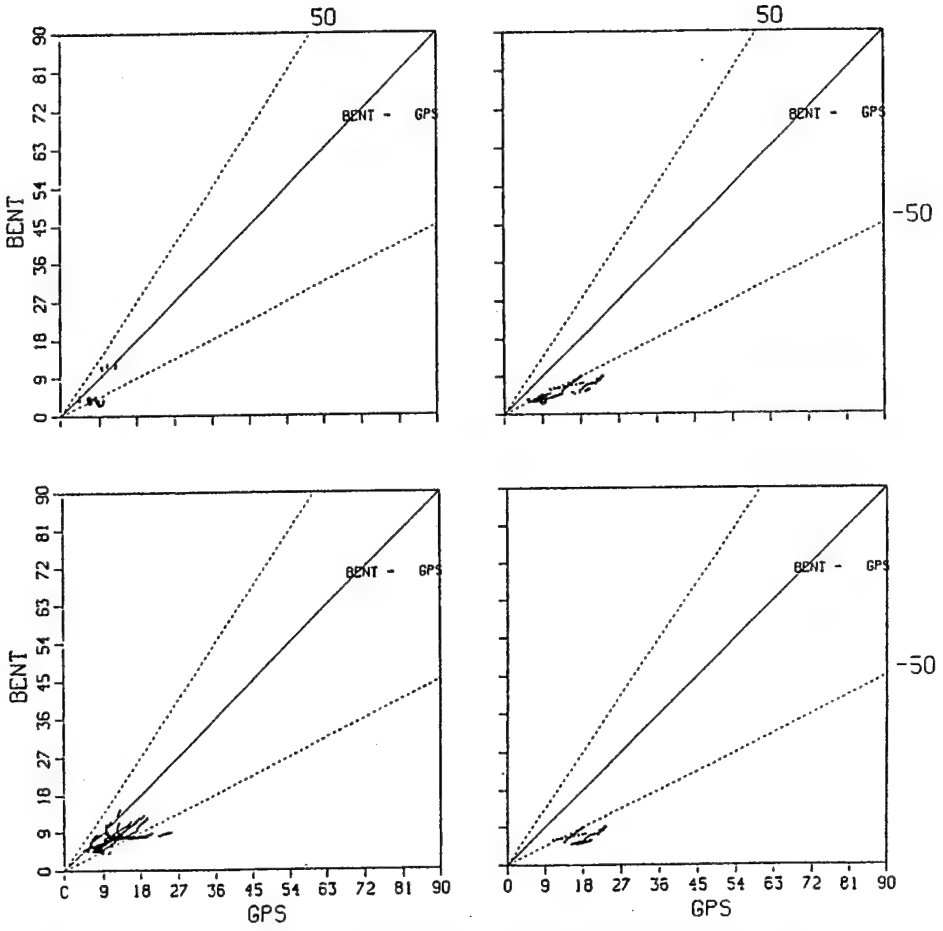

Figure 19. Comparison of monthly forecast (Bent) slant-path TEC to GPS slant-path TEC data from days 288 - 294, 1992, 2100 to 2700 hours, high elevation. Scatter plots are arranged by look direction (north, east, south, west) clockwise from top left.

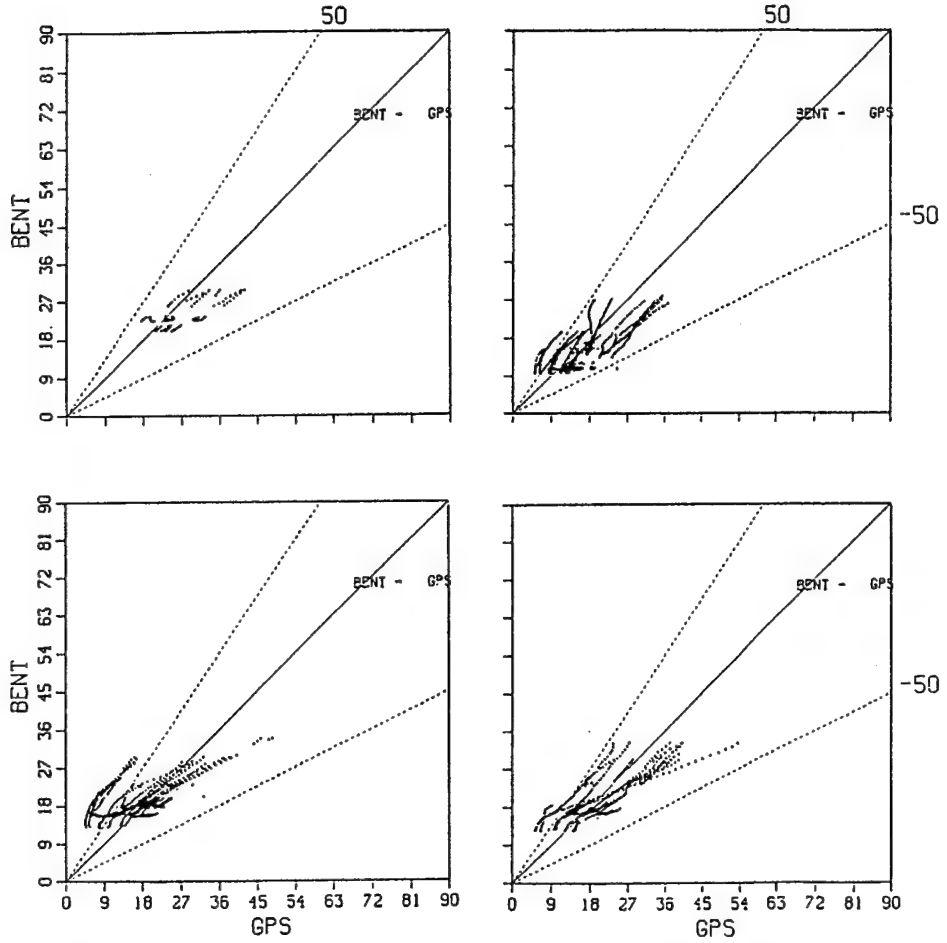

Figure 20. Comparison of monthly forecast (Bent) slant-path TEC to GPS slant-path TEC data from days 158 - 164, 1992, 2100 to 2700 hours, high elevation. Scatter plots are arranged by look direction (north, east, south, west) clockwise from top left.

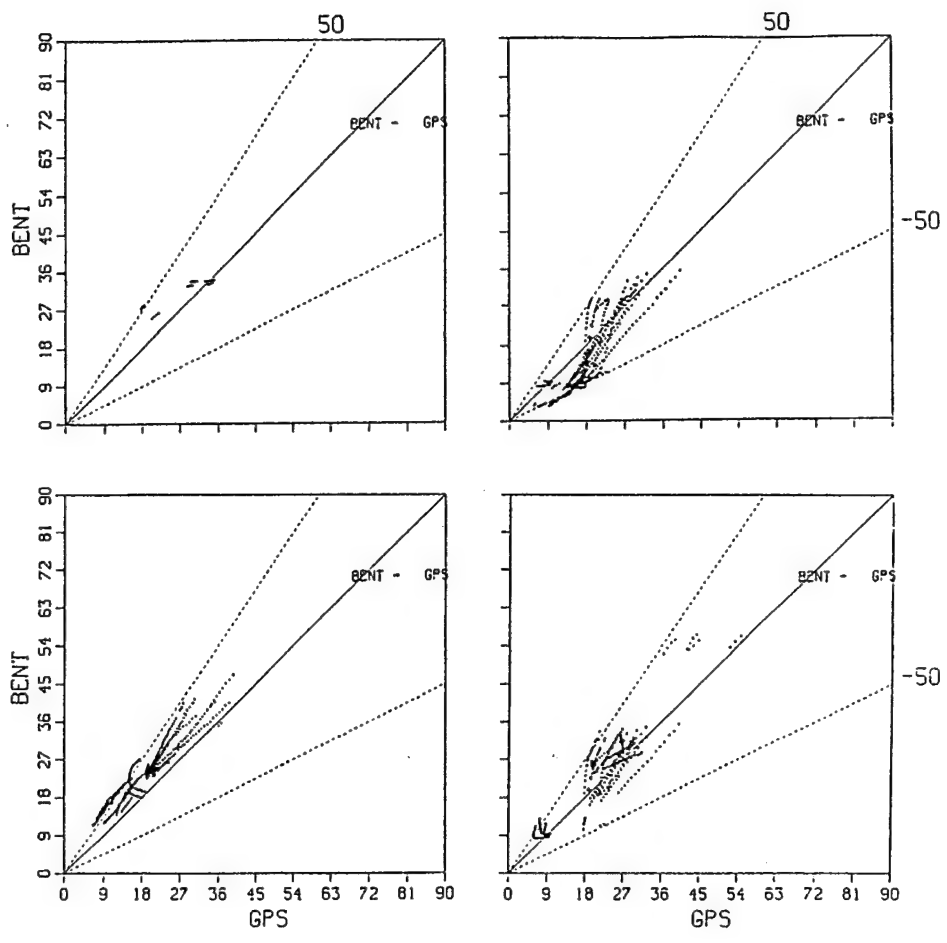

Figure 21. Comparison of monthly forecast (Bent) slant-path TEC to GPS slant-path TEC data from days 288 - 294, 1992, 1500 to 2100 hours, high elevation. Scatter plots are arranged by look direction (north, east, south, west) clockwise from top left.

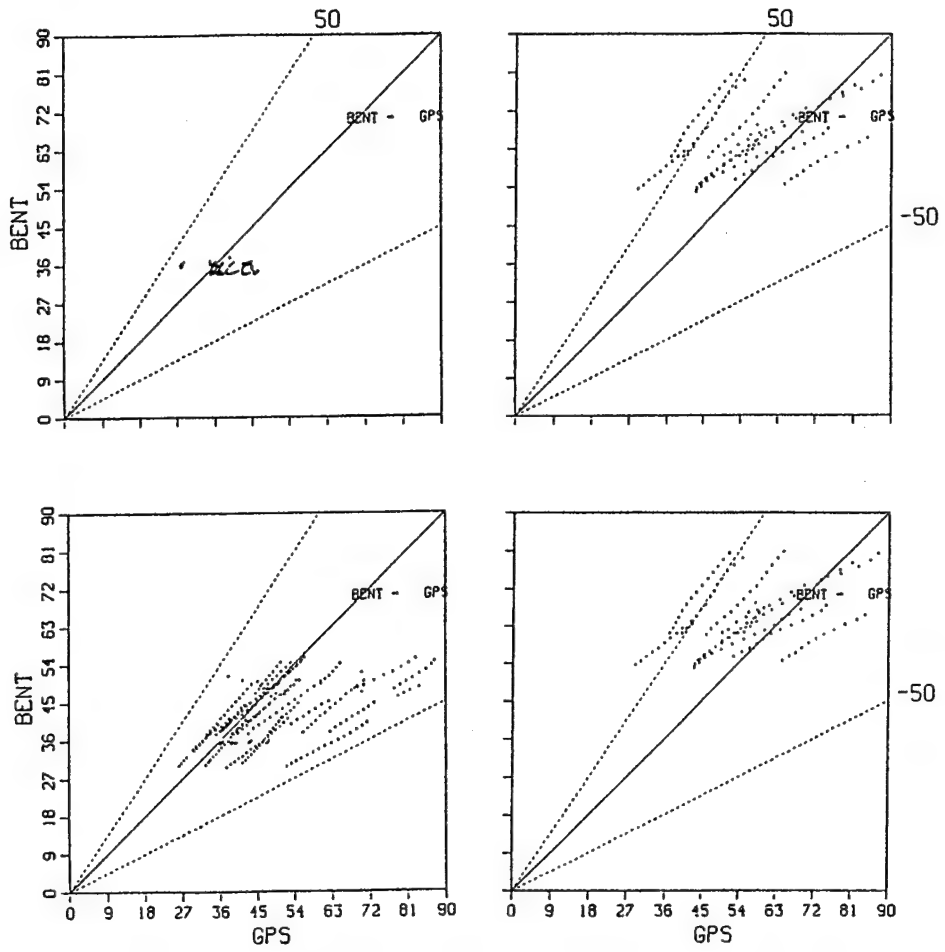

Figure 22. Comparison of monthly forecast (Bent) slant-path TEC to GPS slant-path TEC data from days 158 - 164, 1992, 900 to 1500 hours, low elevation. Scatter plots are arranged by look direction (north, east, south, west) clockwise from top left.

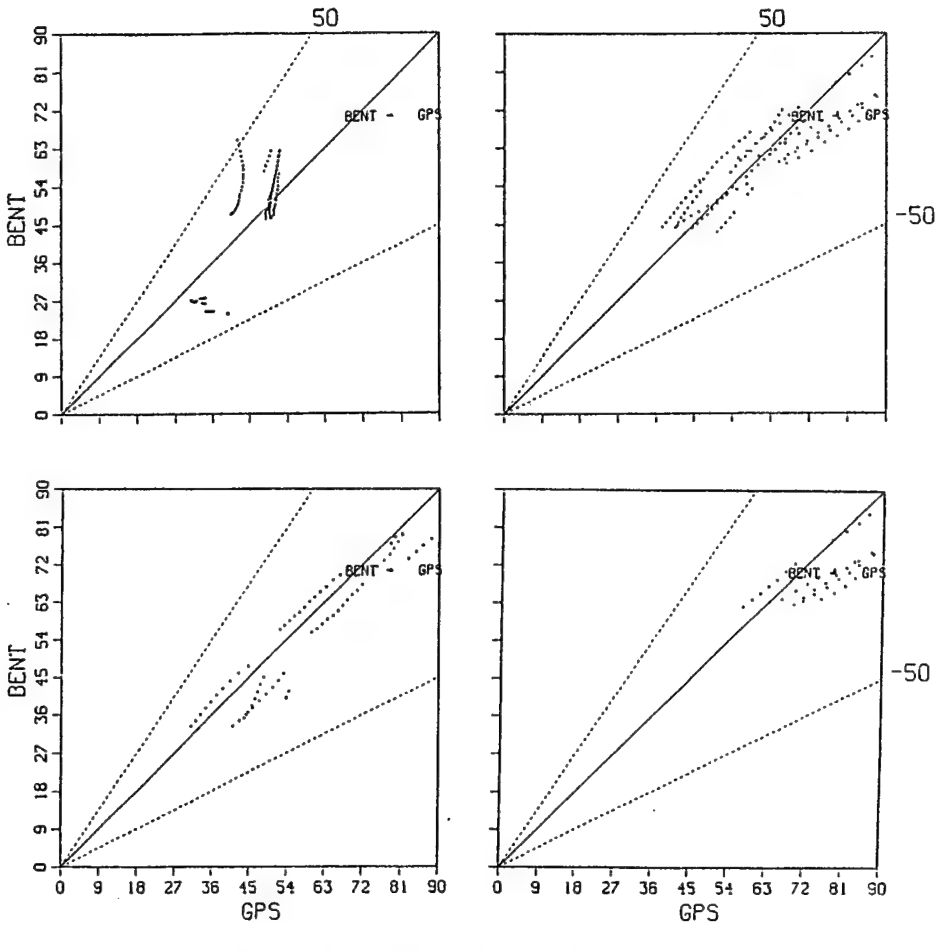

Figure 23. Comparison of monthly forecast (Bent) slant-path TEC to GPS slant-path TEC data from days 288 - 294, 1992, 900 to 1500 hours, low elevation. Scatter plots are arranged by look direction (north, east, south, west) clockwise from top left.

seasonal data sets are shown. There is no clear pattern to the agreement or disagreement of the pairs. Where there are sufficient data in a bin to provide an initial evaluation of the model performance, a clear seasonal change is indicated. It is recommended that additional data be included in the seasonal comparisons to confirm these indicated changes.

The overview of the results of this analysis are shown in Tables 1 - 4. For each bin, a symbol indicates whether the model predicted mostly lower (↓), higher(↑), or evenly distributed high and low values (–), compared to the GPS measurements. In some cases, all the data were filtered out of a particular bin (×). The model values were lower than the measured values in slightly more than half of the bins. For the night-time (2100 - 2700) and morning (0300 - 0900) cases, model predictions typically were lower than the measurements for both low (<20°) and high (20° to 90°) elevations. Most of the data points fell within the ±50% error bars shown on the plot, which is consistent with the expected accuracy of the Bent model.

These results indicate that the model could be improved for the Shemya region. Where TEC values are large, the percentage error translates to a larger error in TEC value and, therefore, a poorer correction-to-range error. Properly calibrated, real-time TEC monitors providing real-time correction factors could augment model predictions and significantly improve the accuracy of range-error corrections.

Table 2
Model Evaluation Results
Days 158 - 164, 1992, Low Elevation (<20°)

Time	North -45°to 45°	West 45° to 135°	South 135° to 225°	East 225° to 315°
0300 - 0900	↓	↓	×	×
0900 - 1500	↓	↓	↑	↑
1500 - 2100	↓	↓	↑	↑
2100 - 2700	↓	↓	↓	×

Table Symbols Legend

↓ predicted values generally less than measured.

↑ predicted values generally greater than measured.

– predicted values distributed equally as greater than and less than measured.

× all data filtered out - no points in this bin.

Table 3
Model Evaluation Results
Days 158 - 164, 1992
High Elevation (20° to 90°)

Time	North -45°to 45°	West 45° to 135°	South 135° to 225°	East 225° to 315°
0300 - 0900	↓	↓	↓	↓
0900 - 1500	–	–	↑	↑
1500 - 2100	↓	↓	↑	↓
2100 - 2700	↓	↑	↑	–

Table 4
Model Evaluation Results
Days 288 - 294, 1992
Low Elevation (<20°)

Time	North -45°to 45°	West 45° to 135°	South 135° to 225°	East 225° to 315°
0300 - 0900	↓	↓	↓	↓
0900 - 1500	↑	↓	↓	↓
1500 - 2100	–	–	↑	×
2100 - 2700	↑	↓	↓	↓

Table 5
Model Evaluation Results
Days 288 - 294, 1992
High Elevation (20° to 90°)

Time	North -45°to 45°	West 45° to 135°	South 135° to 225°	East 225° to 315°
0300 - 0900	↓	↓	↓	↑
0900 - 1500	↓	–	↑	↑
1500 - 2100	↑	↑	↑	↓
2100 - 2700	↓	↓	↓	↓

Radar data files from the Ballistic Missile Early Warning System (BMEWS) radar at Fylingdales, England, were analyzed to determine if intensity scintillation (S_4) is seen by the radar. The intensity scintillation index, S_4, is defined as the square root of the variance of received power divided by the mean (Ref. 14). The percentage occurrence of scintillation versus latitude seen in the radar measurements of a calibration sphere at 430 MHz was compared to scintillation occurrence versus latitude studies from Transit satellite observations at 150 MHz from nearby Whitby, England. The Transit data were collected and analyzed by University College of Wales, Aberystwyth (UCW). Because the radar measurements are at a higher frequency than the Transit measurements, it is necessary to scale the scintillation data for accurate comparison. The scaling is performed according to the WBMOD scintillation model (Ref. 15).

The radar data are a measurement of a two-way path. Therefore, a scaling must be done so that the values are effectively one-way measurements. The relationship between two-way and one-way S_4 is given by:

$$S_4^2 = 4S_m^2 + 2S_m^4/(S_m^2 + 1) \qquad (1)$$

where S_m is the effective one-way path (Ref. 16).

Studies have shown that S_4 is frequency dependent, and a frequency scaling is performed to translate from the 430 MHz for the radar data to 150 MHz for Transit (Ref. 15). First, a transformation from significant to weak scatter S_4 at 430 MHz is made according to:

$$S_4^2 = 1 - e^{-S4weak^{**}2} \qquad (2)$$

Once in the weak-scatter domain, frequency scaling is applied.

$$S_4[\text{Transit}]/S_4[\text{radar}] = \{f(\text{radar})/f(\text{Transit})\}^{1+q/4} \quad (3)$$

where q is the one-dimensional power-law index of the irregularities' spatial spectrum. Then the inverse transformation back to significant scatter is performed.

Initial results indicated that the radar was seeing scintillation at the same times and latitudes as the Transit observations. However, the actual percentage occurrence values did not agree closely. Several factors may have contributed to this disagreement. The primary factor is that the Transit observations typically were along a different longitude path and offset in time by one half to one hour. Thus, better statistical agreement requires a larger database than was used. Also, the radar measurements for any given pass of the calibration sphere frequently contained a change of radar face that introduced a discontinuity resulting in S_4 values large enough to contribute to the statistics. Finally, the radar system noise appeared to introduce a range-dependent bias.

A case set of TEC and scintillation data from Thule was analyzed for comparison to concurrent data from ionospheric sounders and incoherent scatter radar, to confirm GPS measurement (Ref. 17. Complete text of reference is included in Appendix 3). These Thule data, collected in 1989 during solar-maximum activity, may now be employed to validate predictions of physics-based polar ionosphere models.

4. CONCLUSIONS

NWRA developed a data archive of TEC data through operation and maintenance of GPS satellite receiver equipment at Shemya, AK; Hanscom AFB, MA; Thule AB, Greenland; Tucuman, Argentina; and Agua Verde, Chile. Scintillation data can also be extracted from much of the database. The Shemya, AK, data provide a valuable resource for characterizing TEC morphology and variability with look direction at this site. These data may now be used in comparison of measured to model-predicted values, permitting evaluation of current models for validation or improvement.

Valuable techniques were developed to improve data quality. The multipath template technique effectively removes multipath contamination from the DGD data in a real-time data-collection scheme. The automated SCORE process is capable of calibrating an installed receiver system for the combination of all system components' contributions to pseudorange error.

Analysis of the NWRA database has produced ionospheric trough boundary signatures in the sub-auroral European sector. These signatures will support studies aimed at real-time detection of the trough boundary.

A database was developed of amplitude scintillation data from both radar and Transit navigation satellites located in the vicinity of York, England. These data will support validation and improvement of scintillation modeling in that region.

The TI-4100 GPS receiver system located at Shemya, AK, demonstrated the feasibility of a GPS-based ionospheric monitor producing real-time ionospheric scale factors for updating of the Cobra Dane radar's ionospheric correction tables via direct input from an independent, on-site ionospheric sensor. A comparative morphological study of these data was performed versus predictions from the Bent model. This study yielded an initial assessment of the seasonal and directional variation in ionospheric specification accuracy of the Bent model, specific to the Shemya site.

REFERENCES

1. Llewellyn, S.K., and Bent, R.B., "Documentation and Description of the Bent Ionospheric Model," AFCRL-TR-73-0657, 1973, AD 772733.

2. Bishop, G.J., and E.A. Holland, "Apparent Good Temporal Stability of the GPS Group Delay Correction Term Seen in Two Large Sets of Ionospheric Delay Data," Abstract G51A-7, Supplement to EOS, October 26, 1993.

3. Bishop, G.J., D. Walsh, P. Daly, A.J. Mazzella, E.A. Holland, "Analysis of the Temporal Stability of GPS and GLONASS Group Delay Terms Seen in Various Sets of Ionospheric Delay Data," in Proceedings of ION GPS-94, September, 1994.

4. Bishop, G.J., and E.A. Holland, "A Simple Approach to Reducing Severe Multipath Errors in GPS Ground-Based Measurements of Ionospheric Delay," Abstract G12B-9, Supplement to EOS, 20 April 1993.

5. Bishop, G.J., and E.A. Holland, "Multipath Impact on Ground-Based Global Positioning System Range Measurements: Aspects of Measurement, Modeling, and Mitigation" in "Multiple Mechanism Propagation Paths (MMPPs): Their Characterization and Influence on System Design," Proceedings of AGARD EPP 53rd Symposium, Oct 1993, Paper 29.

6. Bishop, G.J., D.S. Coco, P.H. Kappler, and E.A. Holland, "Studies and Performance of a New Technique for Mitigation of Pseudorange Multipath Effects in GPS Ground Stations," in Proceedings of ION National Technical Meeting, San Diego, CA, Jan., 1994.

7. Bishop, G.J., D.S. Coco, P.H. Kappler, and E.A. Holland, "A Review of Some Issues in Analysis of GPS Data for Extraction of Accurate Ionospheric Measurements," in Proceedings of the 11th International Beacon Satellite Symposium, URSI Beacon Satellite Group, University of Wales, Aberystwyth, July, 1994.

8. Fremouw, E.J., "Transionospheric Probing and Propagation," Media Effects on Electronic Systems in the High-latitude Region, (AGARD Lecture Series No. 162) NATO, Paris, 1988.

9. Bishop, G.J., S. Basu, E.A. Holland, and J.A. Secan, "Impacts of Ionospheric Fading on GPS Navigation Integrity," in Proceedings of ION GPS-94, September, 1994.

10. Bishop, G.J., I.K. Walker, C.D. Russell, and L. Kersley, "Total Electron Content and Scintillation Over Northern Europe", in Proceedings of the 1993 Ionospheric Effects Symposium, Alexandria, VA, May, 1993.

11. Andreasen, C.C., E.A. Holland, J.A. Secan, and J.M. Lansinger, "Comparative Investigation of High-Latitude Ionospheric Structure and Effects Near Solar Maximum," PL-TR-93-2088, 31 March 1993, ADA2 73799.

12. Bishop, G.J., D.O. Eyring, K.D. Scro, S. Deissner, D.J. Della-Rosa, W. Cade, N. Ceaglio, M. Colello, "Air Force Ionospheric Measuring System Supports Global Monitoring and Mitigation of Effects on AF Systems," in Proceedings of ION GPS-94, September, 1994.

13. Mazzella, A.J., J.G. Casserly, M.B. Delorey, J.R. Hughes, "Ionospheric Model Assessment Using TRANSIT Data," RDP-TR-9101, March, 1991, PL-TR-91-2162, ADA2 44455.

14. Aarons, J., "Global Morphology of Ionospheric Scintillations," Proceedings of the IEEE, Vol. 70, No. 4, April 1982.

15. Secan, J.A., E.J. Fremouw, and R.E. Robins, "A Review of Recent Improvements in the WBMOD Ionospheric Scintillation Model," The Effect of the Ionosphere on Communication, Navigation, and Surveillance Systems, J.M. Goodman, ed., Naval Research Laboratory, Washington, 1987.

16. Fremouw, E. J., and A. Ishimaru (1992), "Intensity Scintillation Index and Mean Apparent Radar Cross Section on Monostatic and Bistatic Paths," *Radio Science 27*, (4), 539-543.

17. Bishop, G.J., T.W. Bullett, and E.A. Holland, "GPS Measurements of L-Band Scintillation and Total Electron Content in the Northern Polar Cap Ionosphere at Solar Maximum," in Proceedings of the 11th International Beacon Satellite Symposium, URSI Beacon Satellite Group, University of Wales, Aberystwyth, July 1994.

APPENDIX 1
PROGRAM DESCRIPTIONS

Research software was written to process and analyze data collected during this contract period. Programs were developed to implement valuable data-quality improvement techniques. Below is a description of these programs. Modern GPS receivers usually supply the software for initial processing of the raw data into some standard format, typically RINEX, and these manufacturer-supplied programs will not be listed here.

RINEX DATA FILE PROCESSING

RINEX data files are produced by the Ashtech Z-12 GPS receiver software and by the TI-4100 four-channel GPS receiver software, RTM. Data from IGS also are in RINEX format. These files typically contain GPS measurement data, namely L1, L2, P1, and P2. For analysis purposes, these measurements are converted to ionospheric parameters, SR-slant TEC from code and SP-slant TEC from carrier phase, also in RINEX format. From the RINEX file of ionospheric parameters, individual satellite pass files are extracted. These contain a file header with satellite number, Julian date, and year, and data records with time, SR, and SP. The pass files can be processed into equivalent vertical TEC and plotted. The programs that perform these conversions are listed below.

RINMTI.FOR (ARL-UT): converts RINEX files of GPS measurement parameters into RINEX files of ionospheric parameters.

RNX2PASS.FOR: extracts individual satellite pass files from a RINEX file of ionospheric parameters.

PAS2PLOT.FOR: "phase averages" the slant TEC from phase and from code, converts to equivalent vertical TEC, and outputs one of the following: pass-file plots, 24-hour plots, or 24-hour overplots of multiple days of data, as selected by the user.

PAS2DPLT.FOR: similar to pas2plot.for, except that a latitude range (north, overhead, or south of the observing station) is selected and only data from satellites whose IPP latitude is in the selected region are plotted.

RNXCNVT.FOR: extracts the data contained in the RINEX files generated by the RTM software and reformats these data to single-channel file format. This format simulates the output of the older STEL-5010 single-channel GPS receivers, so that these data may be processed and analyzed using programs written for the STEL-5010 data.

MULTIPATH MITIGATION

The multipath template technique was developed for data files in the single-channel file format. With this format, several sequential pass files are contained in one large file. The data sampling rate is 1 sample every 6 seconds. The slant TEC from code and the slant TEC from phase are in two separate files, the DGD and the DCP files, respectively. The DCP and the DGD containing multipath are phase-averaged. The phase-averaged DCP is subtracted from the DGD plus multipath to produce a point-by-point multipath template file. This template contains system

noise as well as multipath. To minimize the system noise content, the template is smoothed by taking one-minute averages.

SHTSHEM4.FOR: phase averages the DGD and DCP files in single-channel file format.

MULTI1.FOR: inputs are the DGD and the phase-averaged DCP files. The output is a point-by-point multipath template file.

SMTHDATA.FOR: program used to smooth the template (to minimize system noise). The averaging interval is specified by the user at run time as an integral number of samples to be smoothed.

MULTI2A.FOR: applies a multipath template to a DGD file from a subsequent day, removing the multipath. A template is typically effective for one week.

TMPLPLT1.FOR: plots the multipath template after smoothing by averaging over 1-minute intervals (10 samples).

TMPLPLT5.FOR: same as tmplplt1, except the averaging interval is 5 minutes (50 samples).

TRIMBLE SINGLE FREQUENCY GPS RECEIVER DATA

Trimble supplies software for processing the raw data files to an ASCII format. Each record of measurement data in the ASCII file contains time, a signal-to-noise parameter, pseudorange, and doppler values. Programs were written to extract individual satellite pass information from the ASCII file and to plot the signal-to-noise as dB versus time.

RDTRMBL5.FOR: extracts individual satellite pass information from the ASCII file to separate pass files.

PLTRMBL2.FOR: output is a 24 hour plot of pass file in dB versus time.

PLTRMBL3.FOR: same as pltrmbl2.for, except the plot is to screen, not printer, and plot may be annotated. Hard copy is optional.

TRMDIAG3.FOR: plots the pass file (dB vs. Time) in half-hour segments on an expanded scale for analysis. A start time for the plot may be specified.

TRMDIAG4.FOR: same as trmdiag3.for, except plot is to screen, not printer, and plot may be annotated. Hard copy is optional.

TRMREFMT.FOR: output is a reformatted pass file in which the signal-to-noise parameter, originally specified in Trimble's Antenna Measurement Units (AMU), is given in dB. No plotting is done.

THULE STEL-5010 DATA

NWRA has a large archive of TEC and scintillation data from GPS observations made at Thule, Greenland, during the 1989-1990 period of solar-maximum activity. These data can be used in conjunction with observations made by others using different ionospheric sensing equipment for scientific study.

DAT2TEC2.FOR: generates a data file from the DGD and DCP single-channel formatted files, containing time, equivalent vertical TEC, IPP latitude and longitude of the observation, and great circle distance from Qaanaaq, Greenland. The output data file is used for comparison to ionospheric sounder data from Qaanaaq.

SHEMYA DATA, MODEL COMPARISON

The analysis software developed by RDP, Inc., for statistical comparison of TEC values predicted by the Bent ionospheric model and measured TEC values was adapted to work on an IBM-compatible PC. A data file is generated containing the actual TEC measurements and model-predicted TEC, along with time and satellite location information. The statistical comparison of the two quantities is shown as a scatter plot of Bent model predictions versus GPS measurements. The data may be filtered according to time, look direction, and elevation for detailed analysis.

TRANGPS6.FOR: reformats the GPS data in single-channel file format into the format needed by the TEC statistical analysis program.

TECSTAT.FOR: generates the database of model and measured TEC, using ETAC's (USAF Environmental Tactical Application Center) implementation of the Bent ionospheric model for prediction of TEC variation on a monthly basis.

TRNANAL6.FOR: produces scatter plots of model predicted vs GPS measured values. Data for plotting can be filtered according to time, look direction, and elevation.

RADAR DATA

Radar data files, measurements of a radar calibration sphere and of Transit satellites, were archived by the BMEWS radar at Fylingdales, England. Data from the first three months of 1993 were analyzed by NWRA and compared to Transit data collected at nearby York, England, and analyzed by the University of Wales, Aberystwyth, to determine whether scintillation is being seen by the radar.

LAT_LON5.FOR: produces an output file of the radar target's (calibration sphere or Transit satellite) sub-satellite latitude and longitude at specified time, from the two line element set.

CGMLL.FOR: input is the lat/lon file from lat_lon5.for and the output is an analogous file with corrected geomagnetic latitude and longitude, in geodetic coordinates.

PLOTRADR.FOR: plots a data file as radar cross section (rcs) in square meters, rcs in dBsm, or S_4, versus either time or latitude.

PLTRADR7.FOR: creates the data file used in the percentage occurrence analysis. The radar data files are detrended, scaled from 2-way to 1-way path, scaled from radar frequency to Transit frequency, paired with latitude and longitude information from lat_lon5.for, and written to an output file. No plotting is done.

PLTRADCG.FOR: same as pltradr7.for, except the lat/lon information is corrected geomagnetic lat/lon from the cgmll.for output.

BINNING4.FOR: calculates and plots the percentage occurrence of scintillation above a specified value versus latitude, from data files generated by pltradr7.for.

BINTIM.FOR: determines and plots the distribution of data points versus time in 15-minute bins. Used to analyze the time distribution of a data set.

SCORE

The SCORE (Self Calibration of pseudoRange Errors) process comprises the following programs, written by Dr. Andrew Mazzella, RDP, Inc. Using dual-frequency, GPS-measurement data, the process can determine a correction value for each satellite equal to the combined satellite plus receiver system bias. Properly formatted GPS data from any system can be analyzed, resulting in a system-specific calibration.

GENIPPDB.FOR: generates a database of time, equivalent vertical TEC, IPP latitude and longitude, and IPP local time, for input to the bias determination program.

GPSBIAS.FOR: input is the database from genippdb.for. This program runs the bias determination algorithm and outputs a file of satellite plus receiver system biases for each satellite in the input database.

RUNBIAS.BAT: batch file for the automated SCORE processing.

IPPDBPLT.FOR: program to plot the IPP database files. Output plot displays both equivalent vertical TEC versus IPP local time and latitude versus IPP local time on separate axes.

GLONASS DATA

A sample set of GLONASS data was provided by the University of Leeds, England, for testing with the SCORE algorithm. Programs were written to reformat and plot the data and to generate an input data base.

GLONASS.FOR: reads the data files from Leeds and reformats them to an extended pass-file format that also includes azimuth and elevation information.

GLNSDPLT.FOR: plots the GLONASS pass files, equivalent vertical TEC versus time.

XPF2IPP.FOR: generates the IPP database for input to SCORE processing using the extended pass-file format of the GLONASS data.

APPENDIX 2
DATA COLLECTION LOG

The following table lists dates, locations, and receiver type used for data collection during this contract period.

DATA COLLECTION TABLE

Receiver type ⇒ Site ⇓	TI-4100 4-channel GPS receiver	Trimble Pathfinder single-frequency GPS receiver	Ashtech Z-12 y-code GPS receiver	STEL-5010 single-channel GPS receiver	ITS-10S Transit receiver
Shemya, AK	May 1992 to January 1994 85% coverage				
Hanscom AFB, MA	July 1993 to December 1993 30 % coverage		March 1994 to June 1994 95% coverage		14 October to 28 October, 1993 80% coverage
Thule, Greenland		6 November to 19 November, 1993 95% coverage		6 November to 19 November, 1993 95% coverage	6 November to 19 November, 1993 80% coverage
Agua Verde, Chile		26 September to 3 October, 1994 95% coverage			
Tucuman, Argentina		1 April to 13 April, 1994 95% coverage			

APPENDIX 3

SUPPLEMENTAL DOCUMENTS

References 3, 6, and 17 listed below are included in this appendix.

3. Bishop, G.J., D. Walsh, P. Daly, A.J. Mazzella, E.A. Holland, "Analysis of the Temporal Stability of GPS and GLONASS Group Delay Terms Seen in Various Sets of Ionospheric Delay Data," in Proceedings of ION GPS-94, September, 1994. This paper was originally presented at the 7th International Technical Meeting of The Satellite Division of The Institute of Navigation at the Salt Lake Convention Center, Salt Lake City, Utah, 20 - 23 September 1994.

6. Bishop, G.J., D.S. Coco, P.H. Kappler, and E.A. Holland, "Studies and Performance of a New Technique for Mitigation of Pseudorange Multipath Effects in GPS Ground Stations," in Proceedings of ION National Technical Meeting, San Diego, CA, Jan., 1994. This paper was originally presented at the 1994 National Technical Meeting of the Institute of Navigation, "Navigating the Earth and Beyond," at the Catamaran Resort Hotel, San Diego, CA, 24 - 26 January 1994.

17. Bishop, G.J., T.W. Bullett, and E.A. Holland, "GPS Measurements of L-Band Scintillation and Total Electron Content in the Northern Polar Cap Ionosphere at Solar Maximum," in Proceedings of the 11th International Beacon Satellite Symposium, URSI Beacon Satellite Group, University of Wales, Aberystwyth, July 1994. This paper was originally presented at the 11th Meeting of Working Group G2 of the International Union of Radio Science (URSI) on Studies of the Ionosphere using Beacon Satellites, University of Wales, Aberystwyth, UK, 11 - 15 July 1994.

Studies and Performance of a New Technique for Mitigation of Pseudorange Multipath Effects in GPS Ground Stations

Bishop, G.J., D.S. Coco, P.H. Kappler, and E.A. Holland

from Proceedings of ION National Technical Meeting, San Diego, CA, Jan., 1994

BIOGRAPHIES

Mr. Bishop is a project engineer in the Ionospheric Effects Division of the USAF Phillips Laboratory (PL). PL develops and transitions technologies in the areas of military space and missiles, directed energy, and geophysics. Mr. Bishop's work areas include mitigation of ionospheric effects on AF systems, and application of GPS to ionospheric monitoring.

Dr. Coco is a Research Scientist at the Applied Research Laboratories, the University of Texas at Austin (ARL:UT). ARL:UT is involved in DoD and civilian applications of fundamental scientific advances in electromagnetics, acoustics, and computer engineering. Dr. Coco is involved in ionospheric monitoring, GPS receiver design and evaluation, and GPS positioning.

Mr. Kappler is a Research Scientist Associate at Applied Research Laboratories, the University of Texas at Austin (ARL:UT). Mr. Kappler is involved in performance evaluation testing of GPS receivers, and analysis of multipath effects in GPS-based systems.

Ms. Holland is a support engineer with Northwest Research Associates (NWRA), Inc. NWRA is a small research and development firm that specializes in geophysical fluid dynamics. Ms. Holland is involved in design of GPS-based ionospheric monitors and application of ionospheric monitor data to morphology studies, model validation and error correction for AF systems.

ABSTRACT

In many applications multipath can be the dominant error source for the measurement of the GPS pseudorange observable. This multipath error can seriously degrade the accuracy of any application that relies on accurate measurements of the pseudorange observable, including navigation, positioning, and ionospheric monitoring.

This study focuses on the implementation and analysis of a software multipath modeling approach called the "multipath template" technique. This technique takes advantage of the daily repetition of the GPS observation geometry from a fixed ground station to create a template of the multipath error signature specific to each satellite pass. This multipath template can be applied to successive days of data to reduce the pseudorange multipath errors. This technique has the potential to reduce multipath errors in both geodetic and ionospheric applications.

Several important aspects of the multipath template technique have been investigated. These include a study of the effective lifetime of a given template and an analysis of the effects of orbital stability on implementation of the technique. The spatial decorrelation of the multipath template has been also analyzed. In addition, an algorithm for quantifying the effectiveness of the multipath template technique in near real time has been developed. Finally, an investigation has been performed on the multipath errors remaining after applying the multipath template.

IONOSPHERIC EFFECTS

The multipath template technique is illustrated in this paper by its application to measurement of GPS ionospheric pseudorange errors. The second frequency in the two-frequency GPS signal format (1.228 MHz, referred to as L2, while the L1 signal is at 1.575 GHz) was incorporated mainly to permit GPS receivers to measure the group delay of GPS signals due to the ionosphere. The group delay represents a range error to the satellite being observed and affects the navigation solution of the GPS receiver. The physical parameter causing the signal group delay is the ionospheric total electron content (TEC) along the raypath to the satellite. TEC is defined as the total integrated quantity of electrons contained in a column of one meter-squared cross-section

centered on the raypath. TEC is typically expressed in "TEC Units", (TECU) where one TECU = $1x10^{16}$ electron/m^2. A GPS receiver measures the differential group delay (DGD) between the precise code streams on L1 and L2, which may be scaled to give TEC or absolute ionospheric group delay on either GPS frequency. TEC is typically the largest contributor to GPS range errors, and normally exhibits a diurnal variation with a peak near 1400 local time and low values at night, exceptions being in disturbed ionospheric regions such as the auroral zone.

GPS MULTIPATH MITIGATION

Multipath contamination, occurring when a GPS receiver acquires reflected signals from the ground or objects near the antenna, can exceed the GPS TEC measurement. This occurs in non-ideal antenna locations such as typical building rooftops having vents, antennas, etc., and in observing GPS satellites at elevation angles near or below 15°. Since GPS multipath can be an important error source in GPS navigation as well as in ionospheric and geodetic measurements, several techniques have been proposed for multipath mitigation [1].

Probably the most common multipath mitigation techniques are the use of an antenna that is desensitized (tapered) at low elevation angles, and smoothing the GPS DGD with differential carrier phase (DCP), referred to as "phase averaging". Tapered antennas reduce multipath, but also sacrifice coverage of GPS satellites, reducing availability for navigation calculations, and shrinking the area of the ionosphere that can be monitored from a single site. Phase averaging takes advantage of the fact that GPS DCP (a relative measure of TEC) is two orders of magnitude less sensitive to multipath than the DGD [2].

Figure 1 illustrates the application of the phase averaging process. The data was acquired at Shemya, Alaska, in a severe multipath environment typical of many installations. (A non-tapered antenna was mounted on a six-foot pole above a reflective roof, with railing and other antennas nearby.) The smooth line in Figure 1 is the DCP, fitted to the DGD data. Close examination of this data shows that if the interval of data available for phase averaging is of the same order as the period of large multipath, the phase averaging process may have significant, oscillating errors. This concern may be minimized if satellites are tracked as long as possible, and the phase averaging product is not used until a long period of data has been collected. To make sure the phase data will be useable over such long intervals, techniques have been developed that are very efficient at correcting phase discontinuities [3]. Another concern is the observation that multipath is not zero-mean [4, 5]. However, as we show in a following section, the mean error tends to be quite small in real environments where there are a variety of reflectors, with reflection coefficients that vary as the satellite moves.

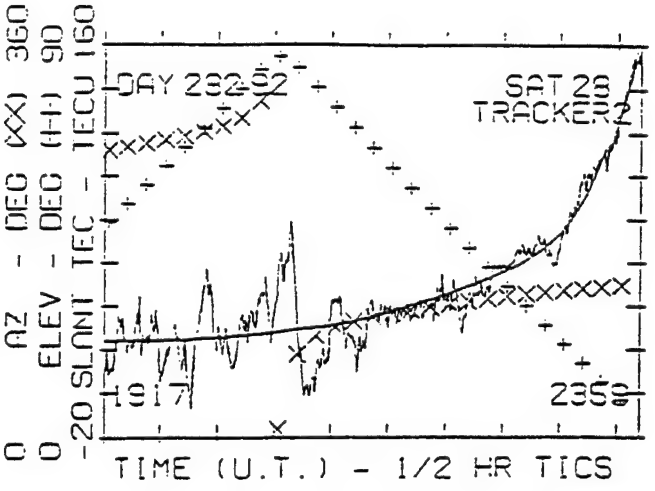

Figure 1. Single GPS pass with severe multipath, illustrating "phase averaging" process.

For real-time applications a phase-averaging product may not meet accuracy requirements until a data set from that satellite has been accumulated for much more than an hour. This could mean, for example, that although an untapered antenna would allow acquisition of satellites just above the horizon, the data from *rising* satellites would be inaccurate, possibly over a region as great as would have been lost to antenna tapering. However, *setting* satellites' data could be accurate, if the satellite was initially acquired well above the horizon.

MULTIPATH TEMPLATE TECHNIQUE

A simple multipath mitigation technique [1], that overcomes the real-time limitations of phase-averaging, has been developed by PL for ground-based applications. This technique takes advantage of the fact that the observation geometry of a satellite repeats almost exactly on successive days. Since this is the case, a 'template' model [6] of multipath may be constructed from each GPS satellite pass on a given day, and then used to remove multipath from the delay measurements on the following day(s). This is done by using the phase-averaging process to fit the DCP TEC measurements to the DGD TEC, and then subtracting this referenced DCP data from the original DGD data. This process yields a template consisting of the multipath structure for that satellite pass (with absolute level accurate to the degree that the multipath is zero-mean for that pass) and the system noise for that pass. To eliminate system noise either one-minute smoothing of the template or averaging of two successive days' templates has been performed.

Figure 2 (after [1]) illustrates the application of the template technique to "remove" multipath. The upper plot shows five minute smoothed DGD TEC for seven satellite passes over an entire day. In the lower plot a template derived from the previous day's data has been subtracted prior to smoothing, thus "removing" the multipath. The resulting data in this lower plot is DGD TEC data, it has not been phase averaged.

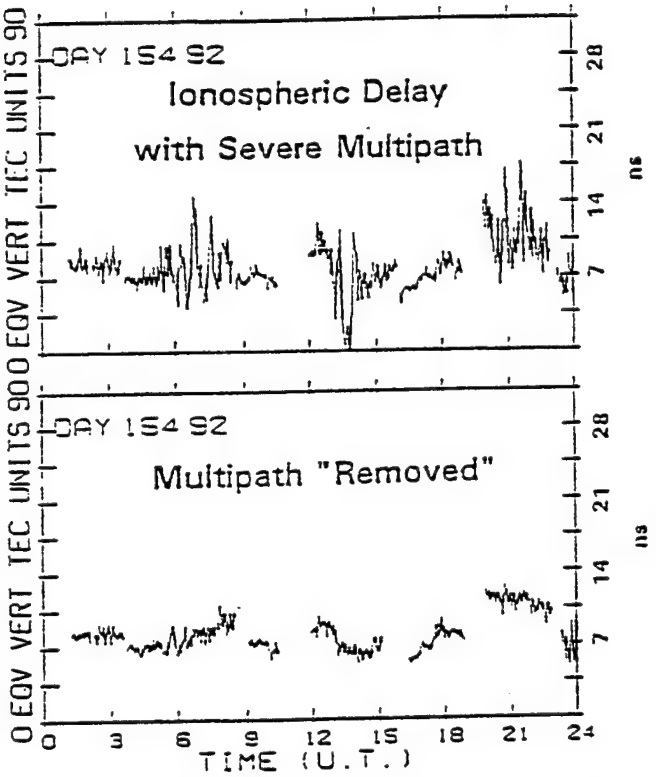

Figure 2. Illustration of application of "multipath template" technique to reduce the effects of severe multipath, (after [1]).

GPS TEC BIAS: THE DIFFERENTIAL GROUP DELAY CORRECTION TERM, T_{GD}

An important potential error source in GPS TEC measurements is the GPS differential group delay correction term, T_{GD}. T_{GD} is the difference in transmit time (at each satellite) between the GPS code on the two frequencies, and is broadcast as a clock correction for the single-frequency GPS user, [7]. However, any error in the broadcast T_{GD} appears as an error in the ionospheric delay correction (and thus in GPS range) for the two-frequency user. An error in T_{GD} can be within specification of the GPS-ICD and still be greater than the ionospheric delay, in many cases.

PL and NWRA have obtained a large data base of two-frequency GPS TEC measurements of, using a TI-4100 receiver for one year at the Shetland Islands UK, 1991-92, and subsequently at Shemya, Alaska, 1992-93, with ARL:UT. These data sets were analyzed to remove the combined effects of receiver offset and satellite biases, using an iterative technique developed, and lately refined, by PL and NWRA, [8].

The analysis of each data set also yielded relative corrections for T_{GD}, (relative, since the combination of receiver and satellite effects is identified in the analysis), for the satellites in each data set.

Figure 3 compares these T_{GD} data sets, with each T_{GD} value differenced against that for satellite PRN 19, and then differenced against the same (T_{GD} PRN x - T_{GD} PRN 19) measure from pre-launch T_{GD} data. Therefore what is plotted is the *change* from the pre-launch differences seen in the PL Shetland data, and again in the PL Shemya data. The largest T_{GD} change shown in this data is *less than 2 ns* for each satellite. Since that 2 ns is the maximum change over 2 years for the *difference* between two T_{GD} values, this would imply that the typical T_{GD} change for one of these satellites over this period was closer to 1 ns. This is good news for stability of the T_{GD} values since the PL data covers nearly two years, and, obviously, pre-launch data goes back still further. In five of the seven cases in Figure 3, the Shemya (one year later) data's difference value was *further* from the pre-launch values than was the Shetland (earlier) data. It is possible, however, that improvements in PL data analysis techniques between the Shetland and Shemya analyses contributed to these changes.

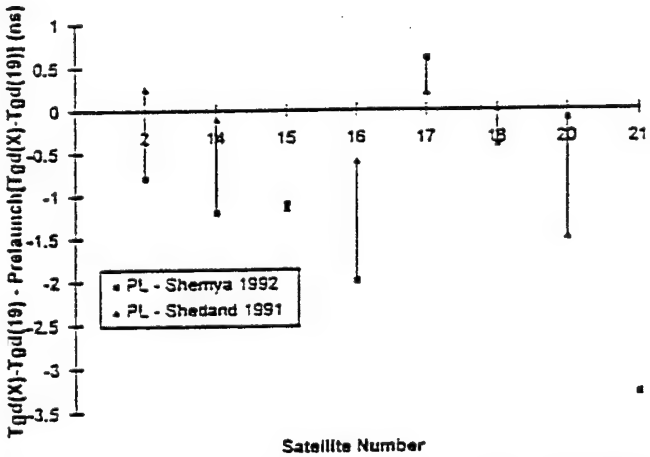

Figure 3. Comparison of GPS group delay correction terms, T_{GD}, derived from two large data sets: T_{GD} for PRN x is differenced vs PRN 19, then that value is differenced vs pre-launch data.

This data suggests that the typical change to be expected in T_{GD} for a given satellite over one to two years would

be about 1 ns, that there *is* an actual change taking place, and that the change tends to carry T_{GD} *away* from pre-launch values. From these results, it would also seem likely that both the short and long-term stability of T_{GD} is adequate for many ionospheric monitoring applications.

PL DISPLAY TECHNIQUE FOR GPS TEC DATA

In monitoring ionospheric TEC it would be ideal to measure TEC variation from a given site looking directly overhead (vertical) throughout a day. However, except for observation of geostationary satellites from the equator, such an observing mode is not possible. In fact for GPS, the signal passes through a longer distance in the ionosphere at lower elevation angles, resulting in a larger TEC value than would be seen looking *directly up* through the ionosphere at the point of penetration. This "slant" TEC value is usually geometrically scaled to an "equivalent vertical" TEC value, for study. In addition, the GPS observation point moves to different parts of the sky where different time zones (actual time of day in the ionosphere) and ionospheric regions may be seen [9]. If plotted directly vs time, the GPS diurnal record can thus be very discontinuous as the observation switches between satellites. Comparisons with ionospheric model predictions confirm that the discontinuities are valid [10], but such a plot is difficult to interpret.

PL has developed a display technique to facilitate analysis of GPS TEC data [10]. First, only those data where the ionospheric penetration point (IPP) is within $\pm 1°$ of latitude of the observing station are plotted. Secondly, to eliminate the effect of looking into different time zones, the abscissa plots local time *at the IPP*. The resultant plot (see Fig. 4) gives a very close approximation to diurnal TEC "overhead" the station, with small perturbations due to longitudinal TEC differences.

SENSITIVITY AND STABILITY OF GPS TEC DATA FROM SHEMYA ALASKA

Figure 4 gives excerpted diurnal "overhead" plots from a 241 day period of the GPS data taken by PL and ARL:UT at Shemya. A clear diurnal pattern, evolving with the seasons, is evident throughout the period. This data set was analyzed using constant settings for receiver offset and satellite T_{GD} values. Variations seen in this data appear consistent with typical spatial and day-to-day ionospheric variations. Thus any variation in T_{GD} or receiver offset should be below these levels.

As a check on whether variation in T_{GD} should be visible in the data set, perturbations were deliberately introduced and the data re-plotted. Figure 5 shows the data from two *single day* plots, more than two months apart, with changes of $+10$, $+5$, 0, -5 and -10 TECU introduced in the T_{GD} values for three of the satellites. The 5 TECU changes are clearly visible. Examination of the effects of the changes in Figure 5 suggests that much smaller changes should be detectable.

DATA FORMAT AND TIME ALIGNMENT

The multipath template is created using 24 hours of off line data in a Phillips Laboratory (PL) data format. For use with real time data in RINEX format, code was written to convert from RINEX to PL format and from PL format to RINEX. A multipath template created from a day or days of data, can be applied to data from subsequent days. Since the process relies on daily repetition of the GPS observation geometry, the data and the template must be time aligned to compensate for the precession of the satellite orbits. The template time is shifted 3 minutes 57 seconds for each day that the subject file lags the template file. Using this simple alignment method, a multipath template yields good results for about 7 days. A more precise technique based on satellite position alignment promises to significantly increase the effective lifespan of a template.

EFFECTIVE MULTIPATH TEMPLATE LIFETIME

The effective lifetime of the template depends on GPS orbital geometry stability and the nature and stability of the reflectors at the specific site. If it can be shown that the multipath template for a given environment retains a high level of effectiveness over an extended period of time then it would be possible to use a single template over that time period. If template effectiveness is short-lived, the resulting requirement for frequent updates would limit the value of the technique.

Currently, generating a multipath template requires some human interaction to maintain a consistent high level of quality control. Thus it is usually not practical to generate multipath templates on a daily basis for isolated field sites, from which it is difficult and expensive to retrieve the required data. Fortunately, our investigations, as discussed below, have shown that multipath templates maintain their effectiveness over several weeks or more so that only infrequent updates are required.

To investigate the effective lifetime, we processed a selection of data from a 42 day period at Shemya. We calculated a TEC multipath template for each day, and its cross-correlation with the template the beginning day in the series. As expected, the cross-correlation function peaked at the point where the geometry repeated (nominally 3 min 57 sec earlier per day).

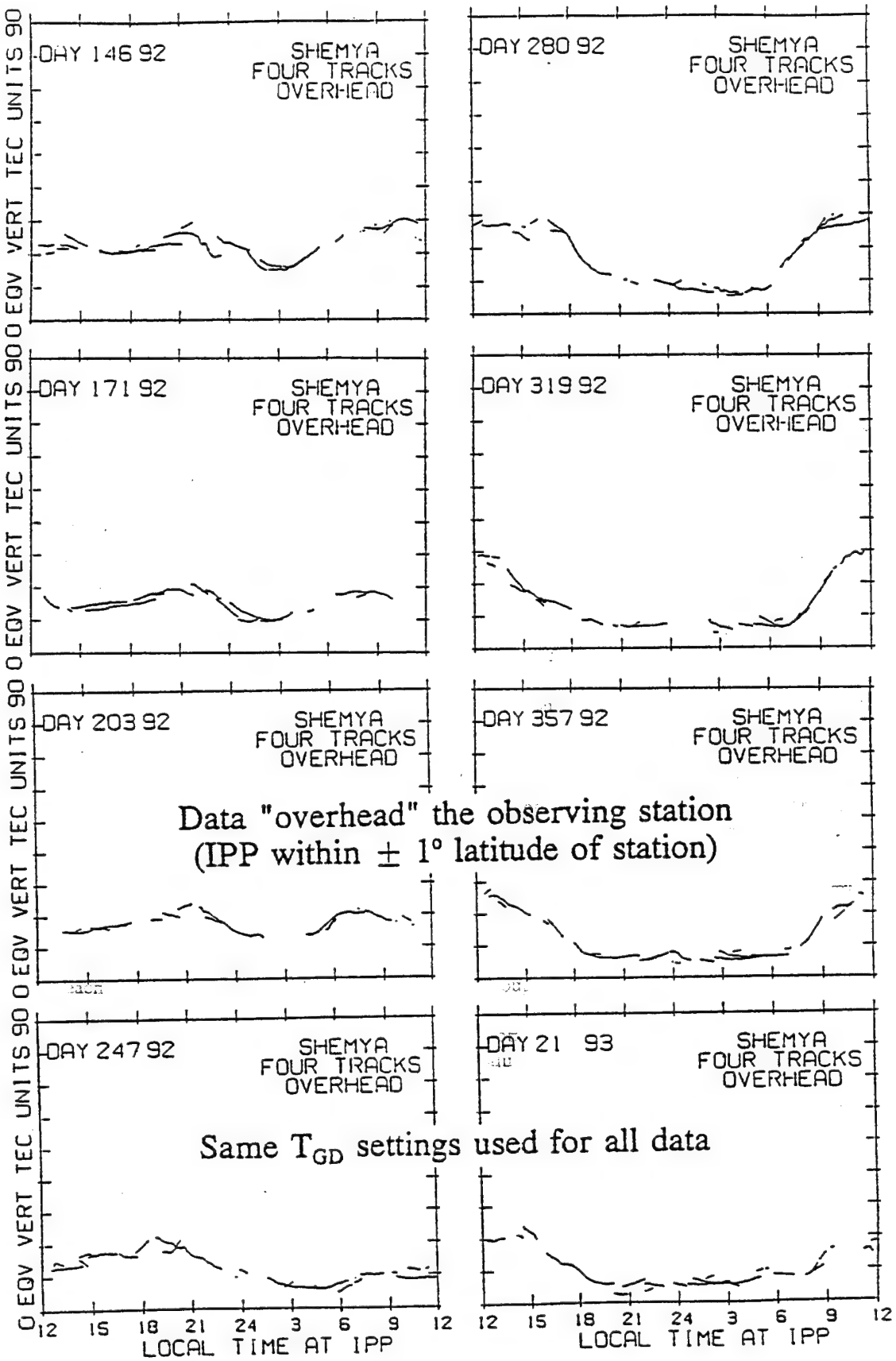

Figure 4. Excerpted diurnal "overhead" plots from a 241 day period of the GPS data taken by PL and ARL:UT at Shemya, Alaska, 1992. A clear diurnal pattern, evolving with the seasons, is evident throughout the period.

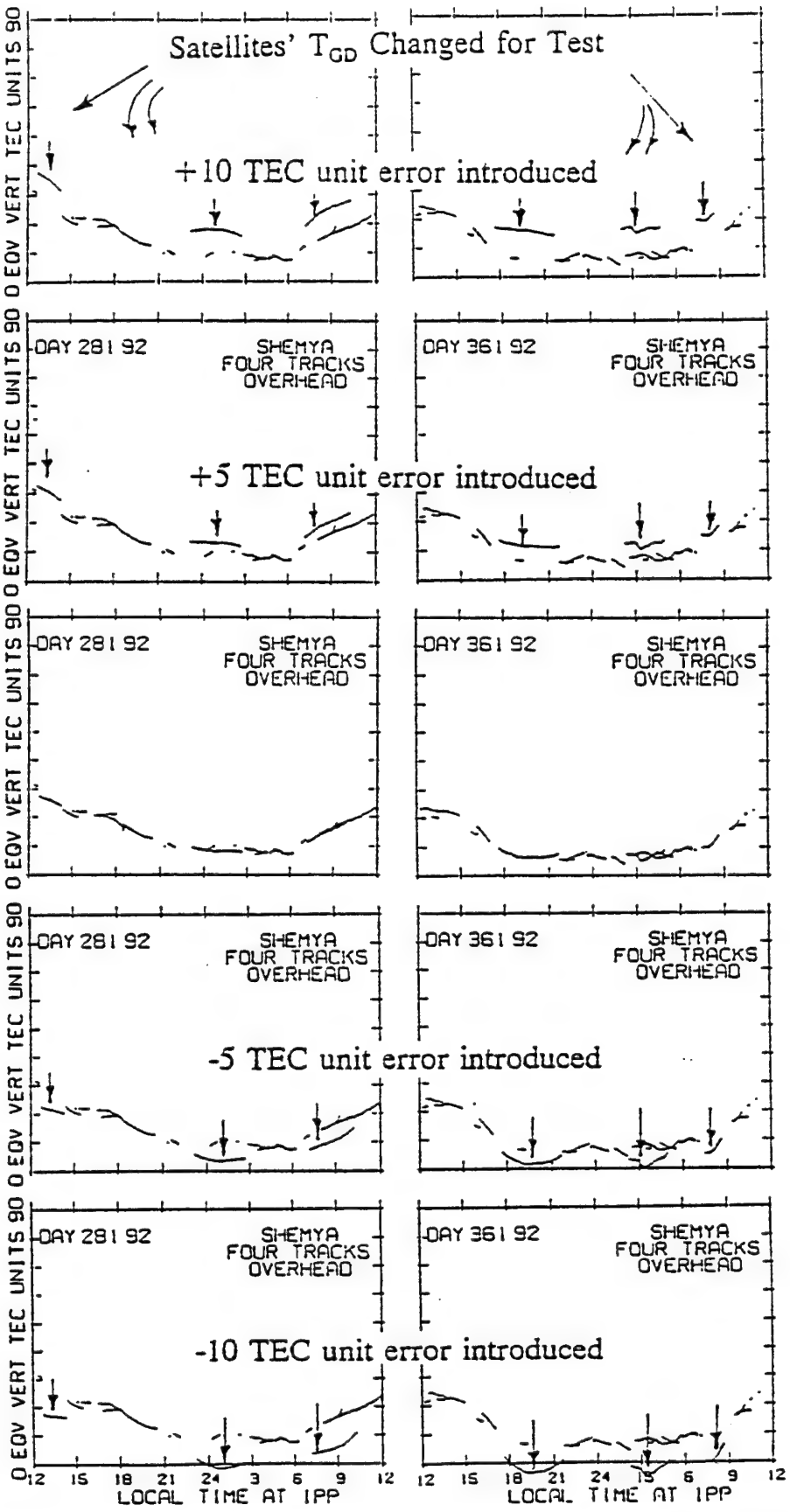

Figure 5. Shemya, Alaska data from two *single day* plots, more than two months apart, with changes of +10, +5, 0, -5 and -10 TECU introduced in the T_{GD} values for three of the satellites. The 5 TECU changes are clearly visible.

The peak correlation values for these data for two different satellites are plotted as a function of the offset from the reference day in Figure 6. This plot demonstrates that the effectiveness of the template is maintained at a fairly high level for the entire 42 day period for both satellites. The correlation value for PRN 11, having a relatively high level of multipath ($\sigma \approx 9$ TECU), shows a slow gradual decrease over this time period. But the correlation value for PRN 3, with a relatively low level of multipath ($\sigma \approx 6$ TECU) is lower, but relatively constant. The higher correlation values associate with the higher multipath level [1] because the template contains both multipath errors, which will correlate, and random system noise, which will not correlate.

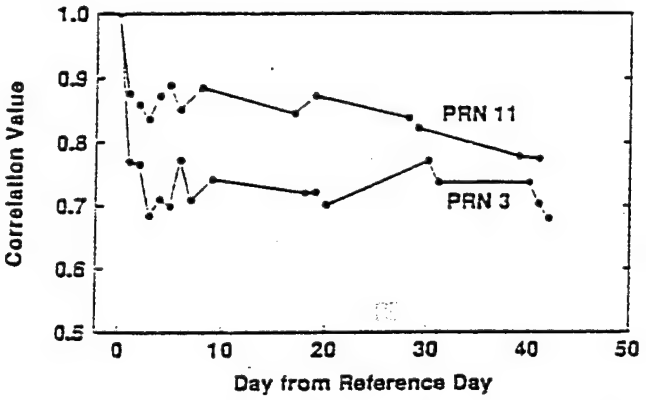

Figure 6. Peak correlation values of multipath template vs template from first day, over a 42-day period at Shemya, Alaska; PRN 11 - high multipath, PRN 3 - low.

ESTIMATING THE TIME SHIFT

One of the main reasons that the template technique is feasible is because the GPS satellite geometry repeats itself on a daily basis. Due to the difference between sidereal time and Universal Time, the geometric configuration of the GPS satellites is shifted by approximately 237 seconds per day. This nominal time shift has been used for implementing the template in the early versions of the software when the template was only applied over a time period of a few days, but a more precise alignment method is required for using a single template over longer time periods.

To investigate how close the nominal 237 sec/day comes to describing the actual shift for GPS satellites we collected a set of six broadcast ephemerides over a one year period and calculated the true time shift. The true time shift is simply the time difference that produces the same satellite geometry for a given satellite. The deviation of the true time shift from the nominal time shift for a typical satellite is shown in Figure 7 where the reference day is Jan. 30, 1992. This plot shows that the deviation, even after only 60 days, is over 200 seconds.

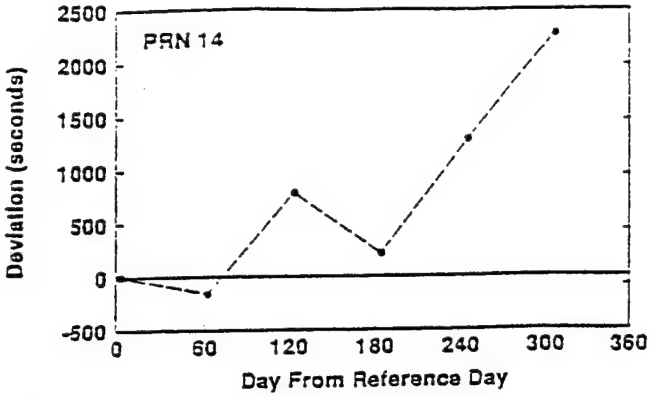

Figure 7. Deviation of true GPS day-to-day time shift, normalized vs nominal 237 second shift, for a typical satellite, calculated from broadcast ephemerides.

In practice, the accuracy to which time shift must be known depends upon the width of the cross-correlation function of the template and the multipath error on the day for which the template is to be applied. The half widths for the Shemya data discussed in the previous section are in the 1 to 2 minute range. This means that the time shift accuracy has to be less that 1 minute, otherwise the template is likely to degrade the pseudorange accuracy rather than improve it.

In our investigations we have found that we can use the nominal 237 seconds per day time shift for time periods up to about 7 days [1], but a more sophisticated approach is required for longer time periods. If the template is to be used beyond a 7 day time period then the time shift must be estimated directly from a comparison of the satellite positions for the two days. This approach can be implemented in a real time system fairly easily if the system has access to the broadcast ephemeris.

We have found that generating a time shift from a comparison of satellite positions provides sufficient accuracy for time periods up to one year. However, if the satellite orbits are modified significantly this simple time shift method may not be sufficient. The easiest approach to this problem is to specify a maximum tolerance (see spatial decorrelation section, below) for the difference in the satellite geometry and alert the user if the difference exceeds this tolerance. A new template will need to be generated if the satellite geometry cannot be duplicated.

SPATIAL DECORRELATION OF MULTIPATH TEMPLATE

A measure of the spatial decorrelation of the multipath template may be obtained from the template itself, by plotting the change in multipath over a fixed spatial distance. To illustrate this, the data set of Figure 1 was analyzed to obtain and plot multipath difference using a data point spaced 5, 2, 0.5 and 0.25 degrees away in spatial angle. Figure 8 shows the template and the plots of multipath difference for the 2° and 0.5° cases. It is clear that even at 2° spacing the multipath is decorrelated, since the difference is as large as the original multipath. It appears that the threshold of "tolerance for the difference in satellite geometry" (mentioned above in regard to estimating the time shift) is less than 0.5°, since at this spacing the differences begin to drop off. Stated another way, a fraction of a degree change in satellite path produces a readily discernable change in the multipath template.

QUANTIFYING TEMPLATE EFFECTIVENESS IN NEAR REAL-TIME

The effectiveness of the template can be addressed fairly easily in postprocessing applications by inspecting the day-to-day correlation of the DGD TEC - DCP TEC data after the template has been applied to the DGD data. However, evaluating effectiveness presents a challenge in real-time applications, especially in those applications where the previous day's data is not available.

Several statistical techniques for single day, near-real-time identification of pseudorange multipath have been investigated at ARL:UT. The most promising technique at this time is a spectral ratio technique which uses the ratio of the high and low frequency components of the power spectral density function of DGD TEC - DCP TEC measurements. The DGD TEC - DCP TEC data has two primary noise sources, the receiver system noise and the multipath error. The system noise is generally random in nature and thus contains mostly high frequency components. The multipath error, on the other hand, usually exhibits a significant low frequency component. Although it is not possible to isolate each of these errors completely using a spectral technique, we have found that the power spectrum is a very useful tool in identifying multipath signatures in near real-time.

The spectral ratio for a given segment of data is calculated by integrating the spectral density function below and above a selected cutoff frequency, and then dividing the low frequency value by the high frequency value. We have found that a cutoff frequency of 0.008 Hz, corresponding to a period of 2 minutes, produces a spectral ratio that is a useful indicator of multipath error. The optimum cutoff value, however, depends somewhat on the antenna environment and the receiver.

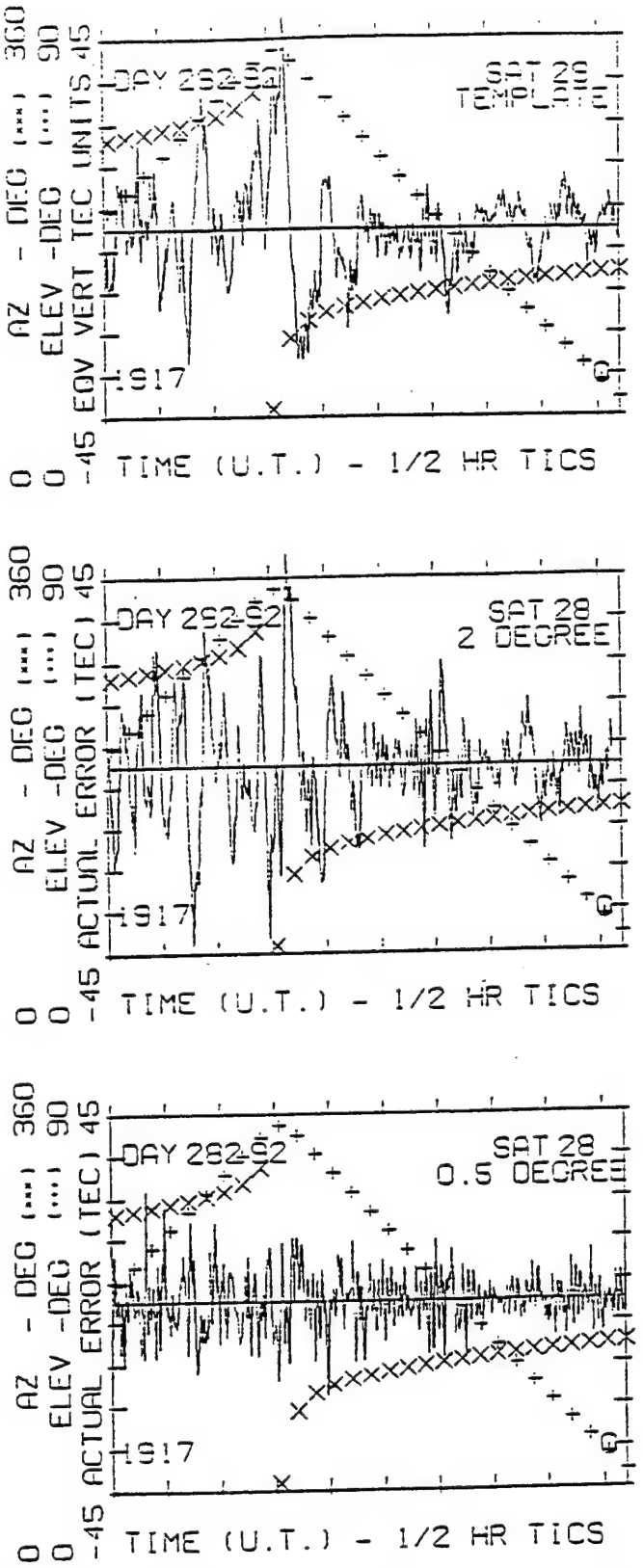

Figure 8. Spatial decorrelation of the multipath template obtained from the template itself, by plotting the multipath difference over a fixed spatial distance. Shown are: template and 2° & 0.5° cases.

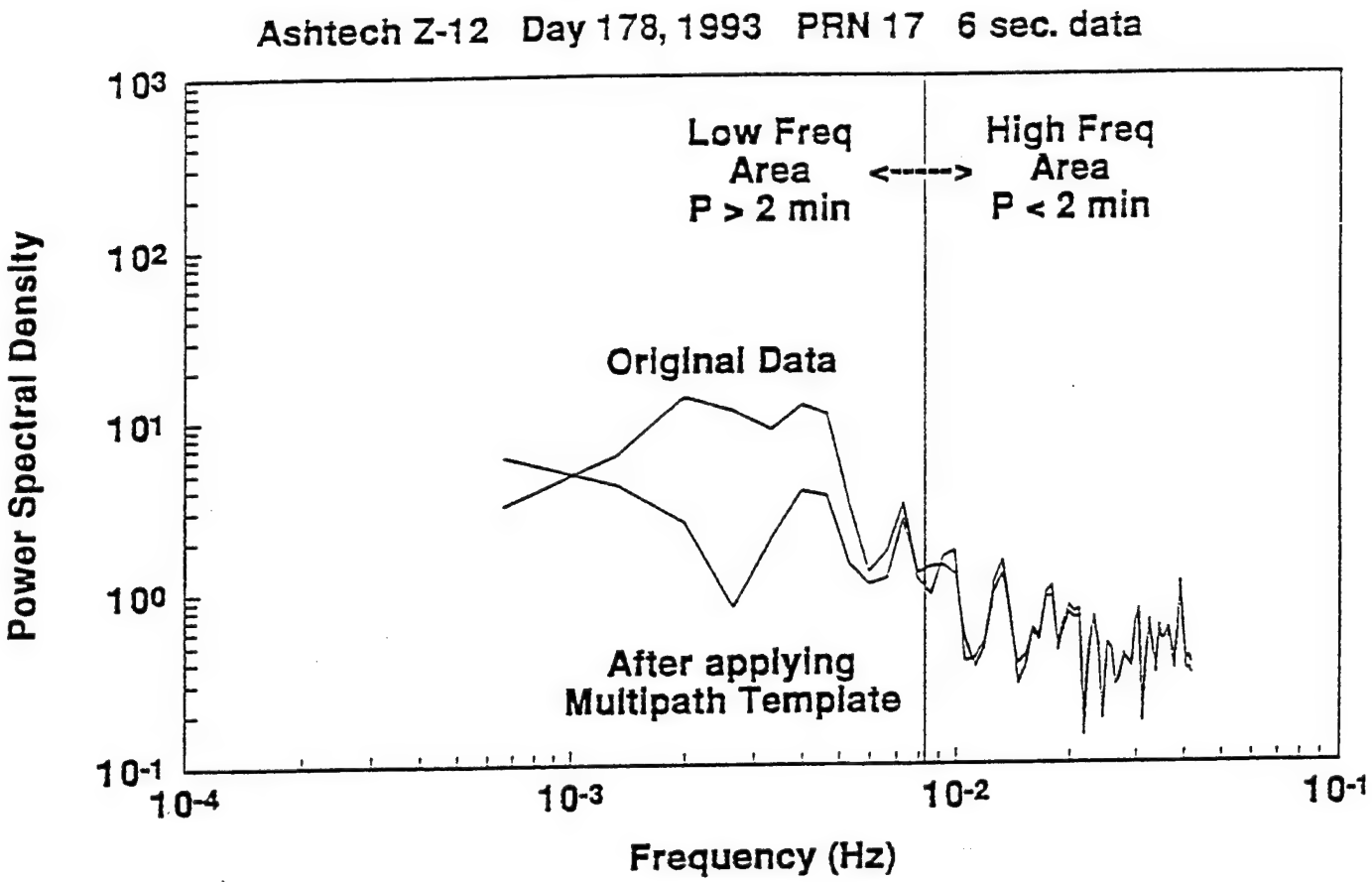

Figure 9. Power spectral density plot for DGD TEC - DCP TEC before and after applying multipath template.

Figure 9 shows the power spectral density functions for DGD TEC - DCP TEC data taken with an Ashtech Z-12 on the ARL:UT rooftop. The original data is shown along with the data after the multipath template has been applied. The template reduces the spectral values significantly in the low frequency region but not in the high frequency region. This indicates that the template is reducing the low frequency multipath contributions. Thus the spectral ratio parameter would show a corresponding decrease when applied to real-time data which had been *successfully* freed of multipath by the template technique.

To study the effectiveness of this technique we show the spectral ratios calculated for a data set similar to that in Figure 9, also from the ARL:UT rooftop. The multipath template (unsmoothed DGD TEC - whole pass phase averaged DCP TEC) data is shown in the top of Figure 10, with standard deviation (calculated after one-minute smoothing the template to reduce system noise), spectral ratio, and DCP "offset" (used to shift DCP to fit onto the DGD in the phase averaging process, here normalized to the offset derived using the entire satellite pass), plotted below. Values are plotted for each minute, computed from 4, 9, and 34 - minute sliding windows. There are two regions of strong low frequency multipath apparent in this data, one at about 23.25 hours and the other at 23.75 hours. Both of these regions are detected in both the standard deviation and spectral ratio plots, but the spectral ratio plot is more sensitive to the long-period multipath that can cause in residual errors for the template technique.

MULTIPATH ERRORS REMAINING AFTER TEMPLATE APPLICATION

As noted above, multipath is technically not zero-mean [5]. Although multiple-reflector situations may approximate zero-mean multipath, there will still be some residual error after application of a template. To examine how such error would behave it is instructive to look at a typical example where the phase-averaging process used to derive the template is performed using sliding-window subsets of a pass. The phase-average process generates a "DCP offset" (see above - Figure 10) used to fit the phase data to the group delay data. When calculated for a "sliding-window" subset of the pass, the offset will show variation related to the non-zero mean of the multipath in that window. Comparing the sliding-window offsets' behavior to the offset derived by using the entire pass gives a general bound on the amount of error that the

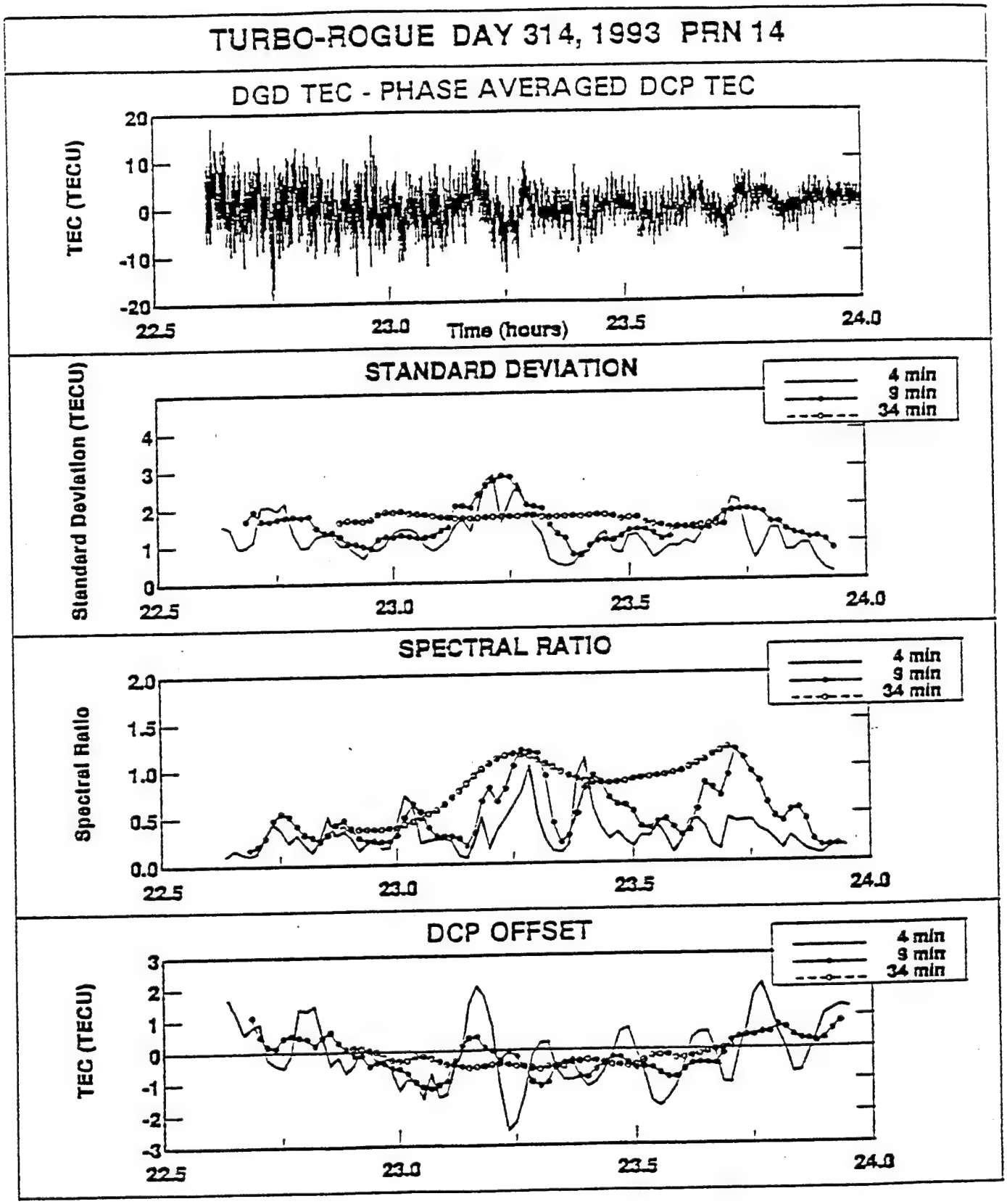

Figure 10. Multipath template (unsmoothed DGD TEC - whole pass phase averaged DCP TEC) data, standard deviation (calculated after one-minute smoothing the template to reduce system noise), spectral ratio, and DCP "offset" (used to shift DCP to fit onto the DGD in the phase averaging process, here normalized to the offset derived using the entire satellite pass). Values are plotted for each minute, computed from 4, 9, and 34 - minute sliding windows.

template technique could produce, an example is given in the bottom plot of Figure 10.

It may be seen that the offset in Figure 10 varies up to about 2 TECU from the whole-pass offset (normalized to zero, here) for the shortest window, but maintains in the 1 TECU range for longer windows. This suggests that for multipath amplitudes up to 10 TECU windows of 10 minutes or greater may have residuals less than 1 TECU.

Neither the standard deviation nor the spectral ratio appears to be a perfect diagnostic of regions where a sliding window will find low multipath that yields a good match to the whole-pass offset. The 9-min window spectral-ratio seems to have less detecting capability than the 17-min, which seems non-intuitive. However, this is likely due to the window being too short to detect some longer-period multipath. In general, both diagnostics' higher values indicate regions where the offset will be less accurate.

MULTIPATH TEMPLATE APPLICATIONS

In addition to ionospheric monitoring, the multipath template technique can also be used to improve the accuracy in the geodesy and navigation applications. Although many position solution algorithms rely mainly on the carrier phase observations, accurate pseudorange observations are important to a variety of applications.

Differential GPS (DGPS) reference station accuracy could be improved through using the multipath template technique. In DGPS the reference station is located over a known benchmark, thus the pseudorange measurements can be compared to the true satellite ranges to generate range corrections for broadcast to users. This range correction is composed of errors from the atmosphere, satellite orbits, Selective Availability [7], and multipath. Of these, only multipath is uncorrelated between the reference station and the user, thus acting as a limiting factor in DGPS accuracy.

As GPS technology evolves, the level of pseudorange noise in receivers will likely decrease, increasing the significance of multipath error in pseudorange measurement accuracy. Thus, as the GPS user can reduce the contribution of multipath error, more new pseudorange-based applications will become feasible.

For ionospheric monitoring applications, the significant improvement shown in Figure 2, compared to errors typical for real-time phase averaging [1], suggests that the multipath template technique could extend monitoring capability for ionospheric delay to much lower elevation angles, where multipath is typically large. Extending the elevation coverage down toward the horizon from 15 degrees (typical cutoff of a "tapered" antenna) could as much as double the radius of coverage at ionospheric altitudes [9]. This means a GPS-based ionospheric monitor could, in the limit, quadruple the area of the ionosphere monitored by use of the template technique. Further, capability to apply a template to remove multipath from the start of a satellite pass would allow observation of satellites that are just rising (which phase-averaging does not support). Similarly, the quantity of GPS satellites visible and the dilution of precision shows significant improvement as elevation coverage is extended toward the horizon.

CONCLUSIONS

Several important aspects of the multipath template technique have been investigated. The template has been shown to have an effective lifetime of at least several weeks (given an undisturbed antenna environment). This remains true despite our observation that only a fraction of a degree change in observed satellite path will significantly alter the template. A "spectral ratio" technique for quantifying the effectiveness of the multipath template technique in near real time has been developed. It has also been shown that template residual error may apparently be kept small for moderate multipath. Thus the template technique should significantly improve pseudorange accuracy and coverage for GPS ground stations.

ACKNOWLEDGEMENT

The authors wish to thank Mr. Min Shao for his diligent and exacting work in performing the processing and analysis of the entire Shemya data set.

REFERENCES

1. Bishop, G.J., and E. A. Holland, "Multipath Impact on Ground-Based Global Positioning System Range Measurements: Aspects of Measurement, Modeling and Mitigation", Proceedings of AGARD EPP 53rd Symposium, Oct 1993, Paper 29.

2. Bishop, G.J., J.A. Klobuchar, and P.H. Doherty, "Multipath effects on the determination of ionospheric time delay from GPS signals", Rad. Sci., 20(3), 388, 1985.

3. Coco, D.S., C.E. Coker, and G.J. Bishop, "A Real-Time GPS Ionospheric Monitor", Procedings of the Ionospheric Effects Symposium", Alexandria, VA, May, 1993.

4. Braasch, M.S., and F. van Graas, "Mitigation of Multipath in DGPS Ground Ref. Stations", Proceedings of ION National Technical Meeting, San Diego, CA, Jan., 1992.

5. van Nee, D.J.R., "Multipath Effects on GPS Code Phase Measurements", Proceedings of ION GPS-91, The Institute of Navigation, Albuquerque, NM, Sep., 1991.

6. Bishop, G.J., D.S. Coco, C. Coker, E.J. Fremouw, J.A. Secan, R.L. Greenspan, and D.O. Eyring, "GPS Application to Global Ionospheric Monitoring: Requirements for a Ground-Based System", Proceedings of ION GPS-92, The Institute of Navigation, Washington, D.C., Sept. 1992.

7. ICD-GPS-200, GPS Joint Program Office, AF Space and Missile Systems Center, Los Angeles, CA.

8. Andreasen, C.A., E.A. Holland, J.A. Secan. and J. M. Lansinger, "Comparative Investigation of High-Latitude Ionospheric Structure and Effects Near Solar Maximum", PL-TR-93-2088, 31 March 1993.

9. Bishop, G.J., "Specification of Trans-Ionospheric Effects for Space Surveillance", Proceedings of the 1992 Space Surveillance Workshop, Lincoln Laboratory Project Report STK-193, Vol. 1, Contract F19628-90-C-0002, Apr., 1992.

10. Bishop, G. J., I. K. Walker, C. D. Russell, and L. Kersley, "Total Electron Content and Scintillation Over Northern Europe", *in* "Proceeedings of the 1993 Ionospheric Effects Symposium", Alexandria, VA, May, 1993.

Analysis of the Temporal Stability of GPS and GLONASS Group Delay Terms Seen in Various Sets of Ionospheric Delay Data

G.J. Bishop, D. Walsh, P. Daly, A.J. Mazzella, E.A. Holland
from Proceedings of ION GPS-94, September, 1994

BIOGRAPHIES

Gregory Bishop is a Project Engineer in the Ionospheric Effects Division of the USAF Phillips Laboratory (PL). His work areas include monitoring and mitigation of ionospheric effects on AF systems.

David Walsh is a research fellow at the CAA Institute of Satellite Navigation at the University of Leeds, UK. PhD, Nottingham University 1994, he has worked at the FAF University in Munich and the Center of European Nuclear Research, Geneva. His research interests are precise kinematic positioning using GPS and GLONASS.

Peter Daly is Professor of Electronic Engineering and Director of the CAA Institute of Satellite Navigation at the University of Leeds. His research interests include GPS, GLONASS and integrated GPS/GLONASS systems.

Andrew Mazzella is a Senior Physics Analyst with RDP Inc., a small research and engineering firm performing mathematical analyses and physical modeling. He is involved in development and evaluation of parametric representations of physical systems and phenomena.

Elizabeth Holland is a Research Engineer with Northwest Research Associates, a small research and development firm that specializes in geophysical fluid dynamics. She studies ionospheric morphology and model performance for application to error correction for AF systems.

ABSTRACT

High accuracy application of the Global Positioning System (GPS) or GLONASS satellites in navigation, geodesy, or ionospheric monitoring requires close attention to the major error sources in GPS range measurement. These include: ionospheric delay, multipath from the receive antenna environment, the differential group delay correction term, T_{GD}, the difference in transmit time between the code on the two frequencies. Although comparatively small, difficulties in measuring T_{GD} have made it a major problem for receiver calibration and ionospheric monitors. This paper introduces a new algorithm for T_{GD}/receiver calibration. To perform this calibration, the algorithm only requires data from a single station on a single day. We apply this algorithm to GPS data from two sites, spanning several months. We also introduce a new method for representing the T_{GD} values, that will facilitate comparison of measurements at different sites. Initial results support the conclusion that GPS T_{GD}'s are quite stable over periods of months. We also apply this new technique to a first investigation of GLONASS data from the University of Leeds. Although GLONASS calibration is much more challenging, initial results are promising and show the technique to be very robust.

INTRODUCTION

Ionospheric delay, typically the greatest error source in GPS ranging, can be fully corrected by a two-frequency GPS measurement, or partially corrected via a model, [1]. Severe multipath from receive antenna environments can at times exceed the ionospheric delay, but can often be mitigated [2]. A third important error source is the differential group delay correction term, T_{GD}, the difference in transmit time between the code on the two frequencies. T_{GD} is broadcast as a clock correction for the single-frequency GPS user, [3]. However, any error in the broadcast T_{GD} appears as an error in the ionospheric delay correction (and thus in GPS range) for the two-frequency user. An error in T_{GD} could be within specification of the GPS-ICD and still be greater than the ionospheric delay, in many cases. Although comparatively small, T_{GD} can be comparable to nighttime ionospheric delay during low solar activity. T_{GD} is different for each satellite, has been difficult to measure, and has been believed to exhibit significant temporal variation. Recent results suggest that both short and long-

term stability of T_{GD} is better than previous work indicated, and adequate for ionospheric monitoring, [2, 5].

T_{GD} MEASUREMENTS

Some of the earliest efforts to measure T_{GD} reported the values to be relatively stable [4], within the scope of limited observations. Subsequent work studying temporal stability of the T_{GD} values produced conflicting results, and existence of significant temporal variation was claimed, [4, 8, 9]. But since the observers could not agree, it was felt that there could not be any certainty of the size or the *existence* of the claimed variations. Somewhat more recent reports, while still disclaiming capability to make measurements of accuracy/stability of T_{GD} to any better degree than approximately 3 ns, nevertheless presented data that showed that the *difference* between T_{GD} values of satellites 17 and 23 was stable to a level much better than that, *over a full year*. (This was demonstrated by the observation that temporal variation in the different ionospheric regions observed in looking at these two satellites was shown to match the variations predicted by a climatological model to an accuracy closer to 1 ns, [10]). Recent work shows better accuracy and more agreement, [5, 6].

PHILLIPS LAB MEASUREMENTS OF T_{GD}

Phillips Laboratory (PL) and NorthWest Research Associates (NWRA) have obtained a large data base of two-frequency GPS measurements of ionospheric delay, (or total electron content [TEC]), using a TI-4100 receiver for one year at the Shetland Islands UK, 1991-92, and subsequently at Shemya, Alaska, 1992-93. These TEC data sets were processed to remove the combined effects of receiver offset and satellite biases, using an earlier version of the iterative technique developed below. The analysis of each data set also yielded relative corrections for T_{GD}, which were compared by a differencing process. This is shown in Figure 1 (from [2]) where each T_{GD} value is differenced against that for satellite PRN 19, and then differenced against the same (T_{GD} PRN x - T_{GD} PRN 19) measure from pre-launch T_{GD} data. Therefore what is plotted is the *change* from the pre-launch differences seen in the PL Shetland data, and again in the PL Shemya data. The largest T_{GD} change shown in this data is *less than 2 ns* for each satellite. Since that 2 ns is the maximum change over 2 years for the *difference* between two T_{GD} values, this would imply that the typical T_{GD} change for one of these satellites over this period was closer to 1 ns, [2].

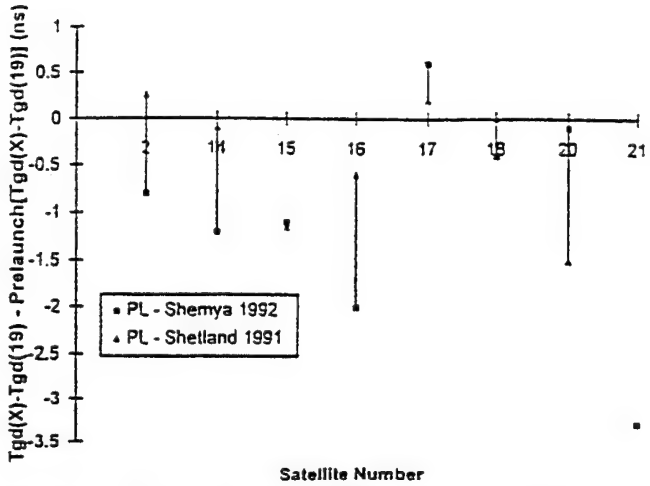

Figure 1. Comparison of GPS group delay correction terms, T_{GD}, derived from two large data sets: T_{GD} for PRN x is differenced vs PRN 19, then is differenced vs pre-launch data, from [2].

DISPLAY OF GPS TEC DATA

Ideal monitoring of ionospheric TEC (measured in "TEC units" where 1 TECu = 1×10^{16} electrons per meter^2 cross section integrated along a column over the entire signal path to the satellite, 2.85 TECu corresponds to 1 ns of differential pseudorange error) would be to measure TEC variation from a given site looking directly overhead (vertical) throughout a day. Such a measurement should show a relatively smooth diurnal cycle, which has a peak about 1400 LT, decays to a low constant before midnight, and begins to ramp up rapidly at dawn. However, except for observation of geostationary satellites from the equator, such an observing mode is not possible. GPS observing geometry is constantly changing in elevation, and the signal passes through a longer distance in the ionosphere at lower elevation angles resulting in larger TEC values than would be seen looking *directly up* through the ionosphere at the ionospheric penetration point (IPP). This "slant" TEC value is usually geometrically scaled to an "equivalent vertical" TEC value, for study. When this geometrical translation is made, the results are usually discontinuous between satellites and hardly resemble the smooth diurnal behavior described above. This is due to the fact that the observation point is moving to different parts of the sky where different time zones (local time of day in the ionosphere) and ionospheric regions may be seen, [11].

It is possible to address such discontinuities in GPS TEC data by a "windowing and translation" process (illustrated in [12]). Windowing is accomplished by plotting only those data where the IPP passes within a narrow band of latitude, such as $\pm 1°$, about the observing station. Secondly, to eliminate the effect of looking into different

time zones, data is translated so the abscissa plots local time at the IPP.

Applied to the PL Shetland data [12], this display technique made it possible to demonstrate that both the T_{GD} values and the receiver were stable enough to allow extraction and analysis of effects of magnetic storms and ionospheric disturbances. In addition, nearly a complete year of TEC data was processed using constant T_{GD} values and displayed [12]. Annual and storm-caused variations in TEC behavior were clearly evident, and no part of the data set was biased high or low as would be the case if a T_{GD} value changed by a large amount during the year.

Several check processes were developed to validate the TEC data using the display technique. These included: multi-day overplots to show trends, sequences of single-day profiles to show artifacts in the diurnal TEC behavior, contrasting single-day plots months apart to look for T_{GD} drift, and artificial introduction of T_{GD} errors to estimate sensitivity to errors. Some of these techniques are illustrated in [12]. We believe this process was sensitive to errors as small as 2 TECu.

ALGORITHM FOR T_{GD}/RECEIVER CALIBRATION

The concepts introduced above, (namely: analyzing a narrow window in latitude, displaying the data in terms of IPP local time, and requiring data agreement at near conjunctions), have been combined into an algorithm that will automatically calibrate a set of 24 (or more) hours of GPS TEC data. The algorithm is applicable to mid-latitude stations, where reasonably consistent diurnal TEC behavior can be expected. However, the algorithm does *not* assume any model ionosphere. A correction number is produced for each satellite which is the sum of the receiver offset and the T_{GD} for that satellite. To separate these two parameters it is proposed that GPS users adopt a *new standard procedure for comparing measured T_{GD} values, that is: normalize the set of T_{GD} values to zero mean first, and compare sets consisting of exactly the same group of satellites*. This procedure should eliminate errors due to inaccurate receiver calibration. We use this approach below to compare PL data to International GPS Service for Geodynamics (IGS) network data.

The technique of bias determination described above has been incorporated into a computational algorithm, with provisions for alternative generalized modes of operation. The fundamental objective is to minimize the difference in equivalent vertical TEC derived from observations of two satellites for the same Ionospheric Penetration Point (IPP) latitude and local time, by adjustment of the assigned bias values for each satellite. By imposing this consistency between multiple pairs of satellites for many observations, not only is a consistent set of bias values derived, but a reasonable representation of the diurnal vertical TEC profile is also obtained.

The mathematical quantity chosen to describe the equivalent vertical TEC difference for multiple observations is:

$$E = \frac{1}{2}\sum_{\alpha}\sum_{i=1}^{I_\alpha}\sum_{\beta\neq\alpha}\sum_{j=1}^{J_\beta} W_{\alpha i,\beta j}\times(T_{\alpha i}-T_{\beta j})^2$$

for αi = PRN α sample i

$W_{\alpha i,\beta j}$ = weighting factor between samples αi and βj

$T_{\gamma k}$ = calculated equivalent vertical TEC for sample γk, using the appropriate local zenith angle and satellite bias:

$$T_{\gamma k} = (S_{\gamma k}-B_\gamma)\times\cos(\arcsin(\mu\ \cos\epsilon_{\gamma k}))$$

for $S_{\gamma k}$ = slant TEC for the data sample

B_γ = combined receiver/satellite bias for PRN γ, in TEC units

$\epsilon_{\gamma k}$ = elevation angle for satellite sample, at observing site

μ = altitude scale factor for conversion to IPP zenith angle: $\mu = R_e / (R_e+H_{IPP})$

A Gaussian function of Local Time and Latitude differences was selected as an appropriate weighting factor, although other forms are possible:

$$W_{ij} = \exp\left(-\frac{1}{2}\left(\frac{\theta_i-\theta_j}{\theta_0}\right)^2-\frac{1}{2}\left(\frac{\lambda_i-\lambda_j}{\lambda_0}\right)^2\right)$$

for θ_k = LAT for sample k (degrees)

λ_k = combined MJD and LT for sample k (day and fraction of day, λ = MJD + LT/24)

θ_0 = reference latitude difference, for scaling (degrees)

λ_0 = reference local time difference, for scaling (days)

This algorithm has been implemented in conjunction with current GPS data processing efforts, utilizing routines presented in [13] to perform the minimization of the quantity E for the selected set of observations.

The current procedure utilizes data selection criteria and weighting parameter definitions which allow a close emulation of the original technique. Thus, the latitude scale parameter, θ_0, is defined to be much larger (15°) than the range of IPP latitudes selected (receiver site latitude ± 1.5°), while the local time scale parameter, λ_0, was defined to correspond to a smaller spatial domain (λ_0 = 0.0125 day = 18 minutes, or the equivalent of 4.5° in longitude) than the latitude scale parameter, but comparable to the latitude selection range. A change from the original technique is to use only a sparse subset of the sequence of observations (currently, every tenth data sample) to perform the calculation, to keep the computational duration reasonable.

Resulting diurnal TEC data are displayed in Figure 2, together with a representation of the IPP locations in latitude and local time. The criterion, set by Bishop and Holland, that the vertical TEC values derived from different satellite observations should match at latitude and local time "conjunction" occurrences, is seen to be satisfied for this case. Note that this is a sufficient condition for validation of the results, but not a necessary condition, because intrinsic temporal variations could occur in the ionosphere between the pair of events for the apparent "conjunction". An additional weighting term, dependent on Universal Time, could be incorporated into the algorithm, but the apparent stability of the diurnal TEC profile has not thusfar required consideration of this extension. For contrast, Figure 3 displays a day more than six months after the Figure 2 data, taken at the same station. The change in profile is consistent with known ionospheric seasonal variation.

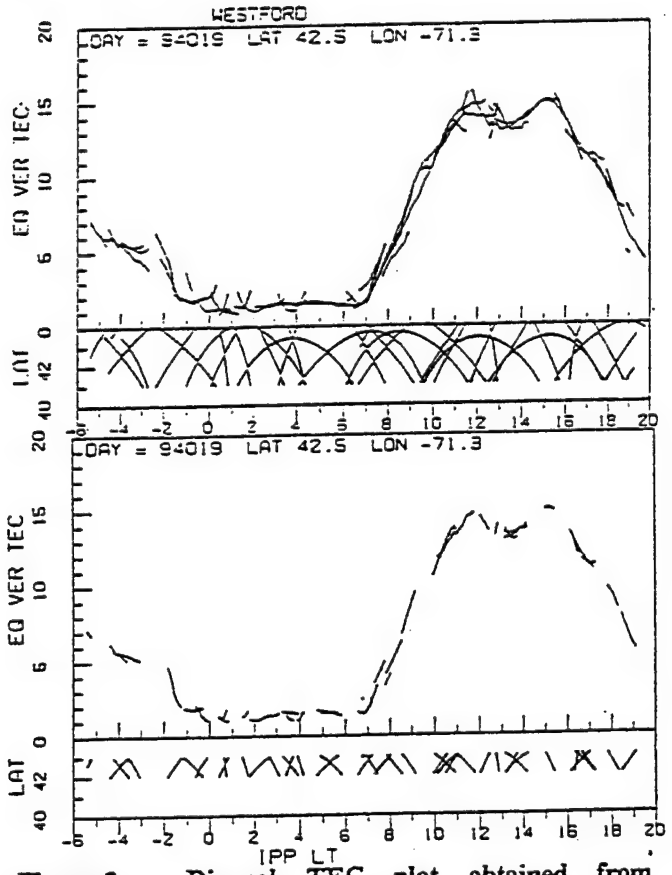

Figure 2. Diurnal TEC plot obtained from algorithm, 3° (top) and 1° latitude bands, day 19, Westford.

Figure 4 displays the successive improvements in the total TEC difference (E), in squared TEC units, versus the number of evaluations of this quantity. It must be noted that not all evaluated values of the total TEC difference are displayed, but only the ones indicating improved convergence to a minimum value. As described in [13], many intermediate evaluations are performed to insure that the minimum value is indeed in a domain bounded by limits of the bias value for each satellite.

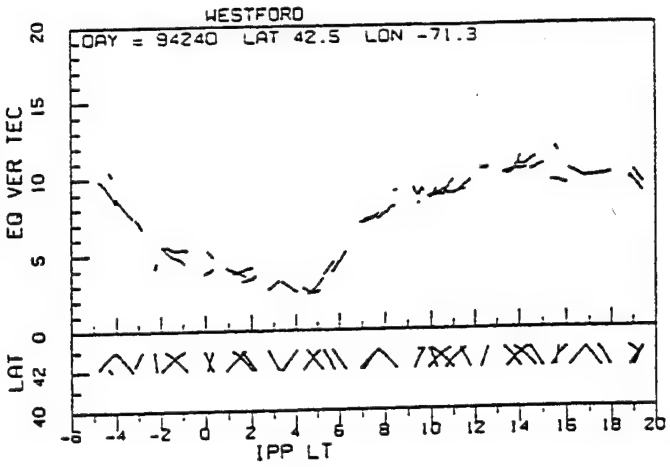

Figure 3. Diurnal TEC plot obtained from algorithm, 1° latitude band, Westford, more than 6 months after Fig. 1.

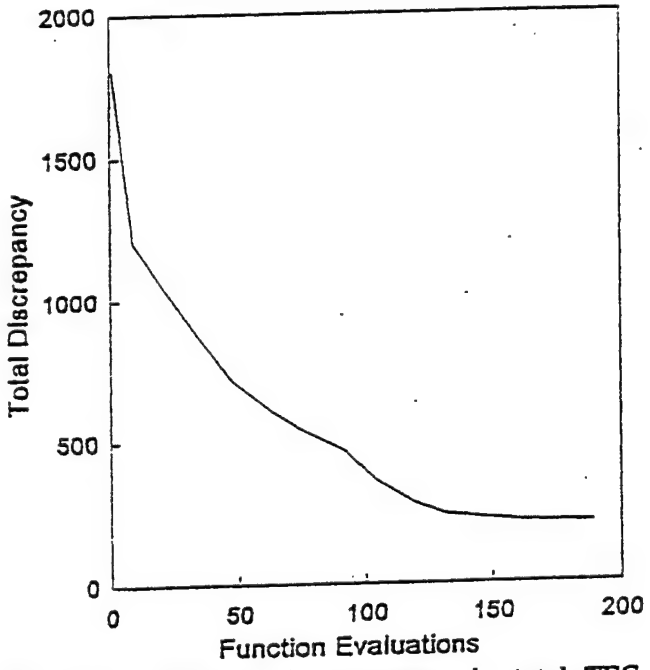

Figure 4. Successive improvements in total TEC difference, in squared TEC units, vs the number of evaluations.

Although there is no fundamental limitation for the time period over which a single bias determination can be performed, there is a practical limitation imposed by computational time requirements. The number of TEC comparisons incorporated in the evaluation of the total TEC difference varies as the square of the typical number of samples used for any individual satellite. Thus, longer

periods become substantially more difficult to process. (Typically, a one-day duration requires a few hours to process on a Pentium PC.)

TESTS OF CALIBRATION ALGORITHM ON VARIOUS GPS DATA SETS

Tests of the algorithm were made on eleven sets of data, one day each, from an Ashtech Z-12 receiver at Hanscom AFB (PL). and from the JPL Westford site. There were specific important differences in these sets, summarized in Table 1, below.

Table 1. Data sets used in algorithm tests, (PL is Hanscom AFB and W is Westford, about 25 miles away).

SET	SITE	DAY	CHARACTERISTIC
1	W	19	A-S OFF
2	PL	77	Micropulse antenna
3	PL	114	AOA antenna
4	PL	115	AOA antenna
5	PL	117	AOA antenna
6	PL	117	AOA antenna
7	PL	159	Ashtech antenna
8	W	77	A-S ON, compare to 1 & 2
9	W	114	A-S ON, compare to 3
10	W	159	A-S ON, compare to 7
11	W	240	A-S ON, 6 months after 1

Plots of the diurnal results from these data sets appear in Figures 2, 3, 5 and 6. It may be seen that there is an accurate and physically reasonable diurnal TEC profile produced in every case. (Day 77 was missing half of the day from one site, so both sets were limited to common satellites). The zero-referenced T_{GD} (ZRT) values were calculated for progressively smaller sets of satellites to compare progressively larger sets of days. (The more days you have, the harder to have satellites in common.) These ZRT values are given in Tables 2 & 3, and plotted with mean and standard deviation values in Figures 7 & 8. Day 159, PL, has less coverage than its counterpart at Westford, which may contribute to some of the day 159 T_{GD} values showing less agreement with other days. The top line in Tables 2 & 3 shows the mean correction (that was removed to get the ZRT values) which tracks receiver offset drift, if any. We can see, comparing PL 77 vs 114-117 that the receiver system offset changed about 25 TECu with the antenna change (see Table 1) and may have changed again with the third antenna on day 159. Also the Westford data may show a slow downward receiver offset drift. Westford day 19 (Figure 2) has a mean correction of -9.36 TECu which may be compared with a value of -10.9 TECu for the same group of satellites from Westford, day 159. This suggests that the turn-on of A-S did not affect the receiver offset for that location. From Tables 2 & 3, we see that the mean standard deviation of all the ZRT values is 0.95 TEC units or less, an encouraging result.

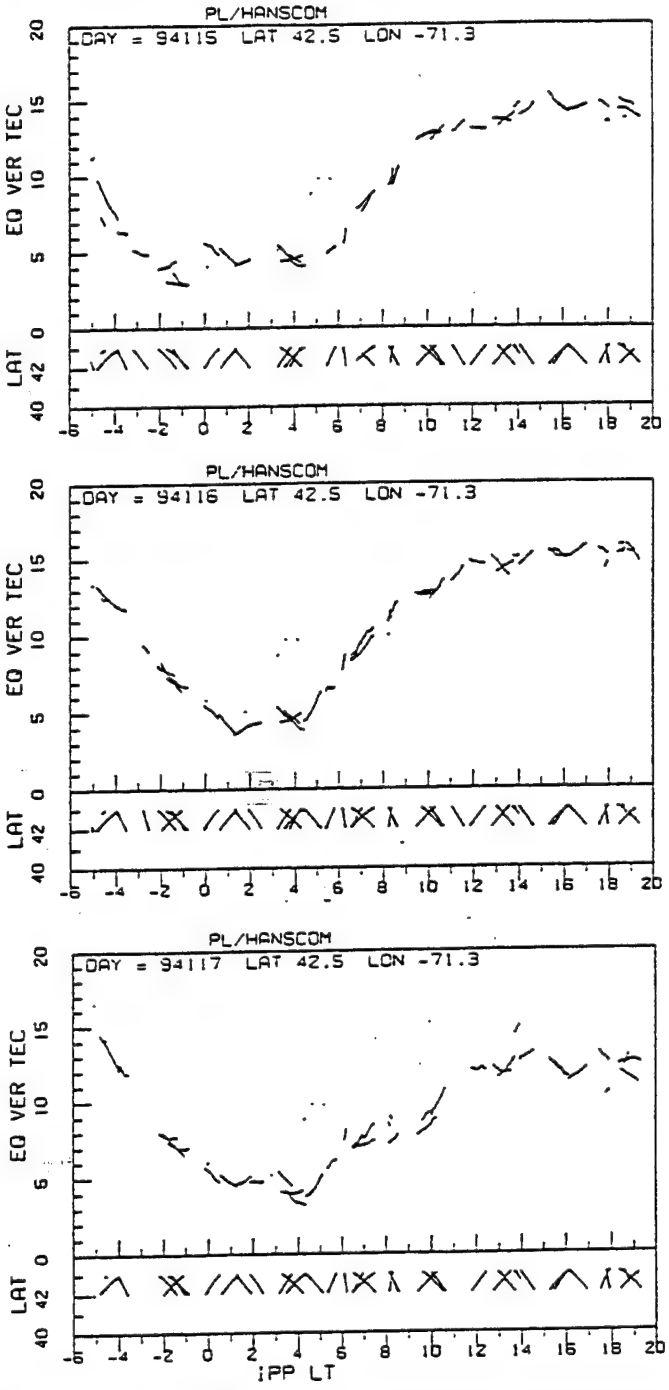

Figure 5. Diurnal TEC observations, Hanscom, days 115-117, 1° latitude band.

TESTS ON GLONASS DATA

The PL algorithm should, in principle, be applicable to calibrating GLONASS data with equal facility as GPS.

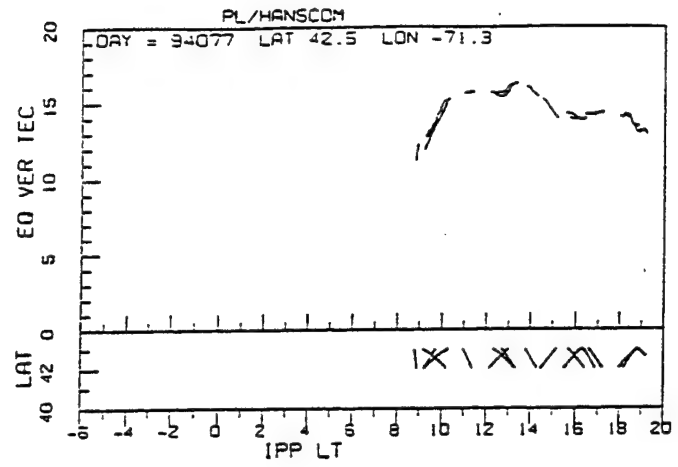

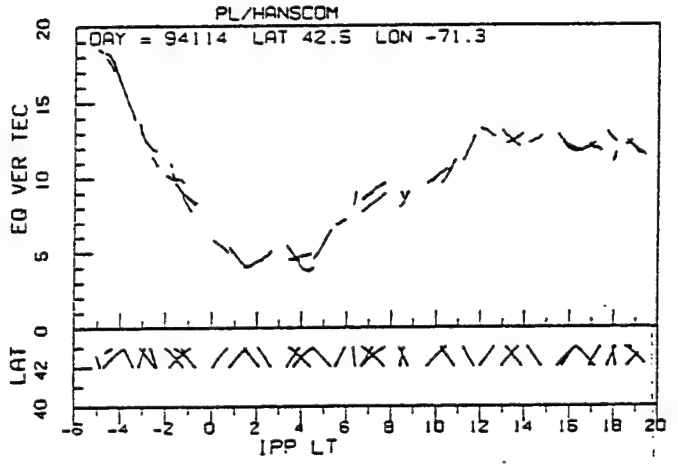

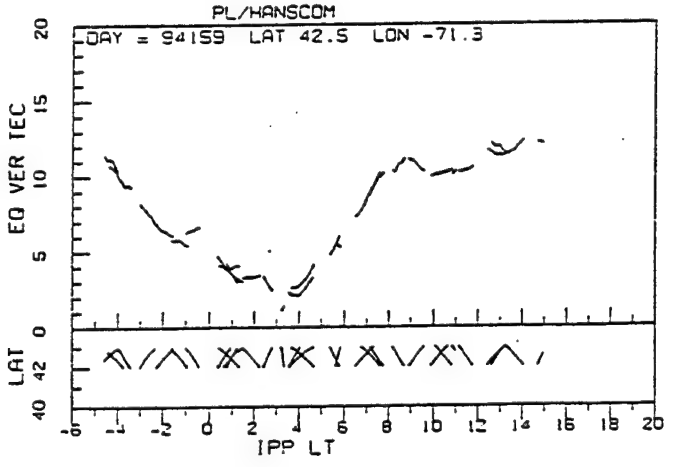

Figure 6a. Diurnal TEC observations, Hanscom, days 77, 114, & 159, 1° latitude band.

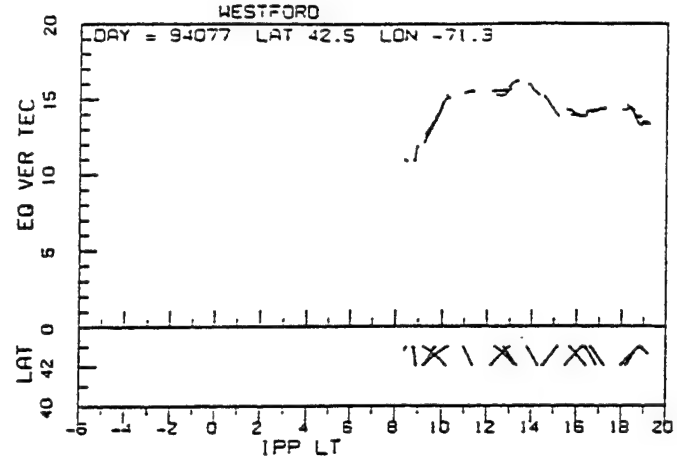

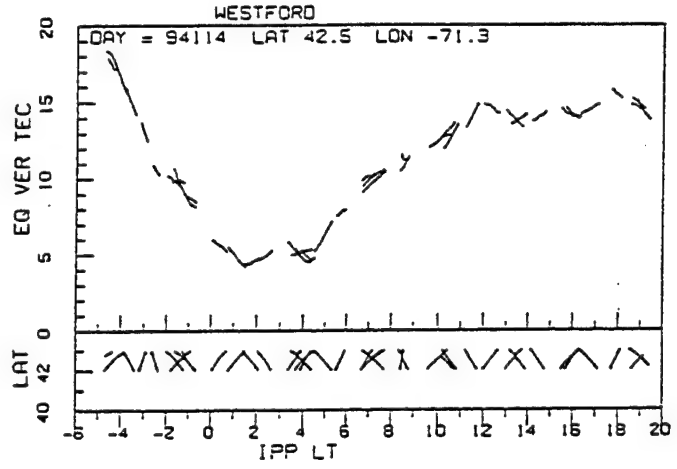

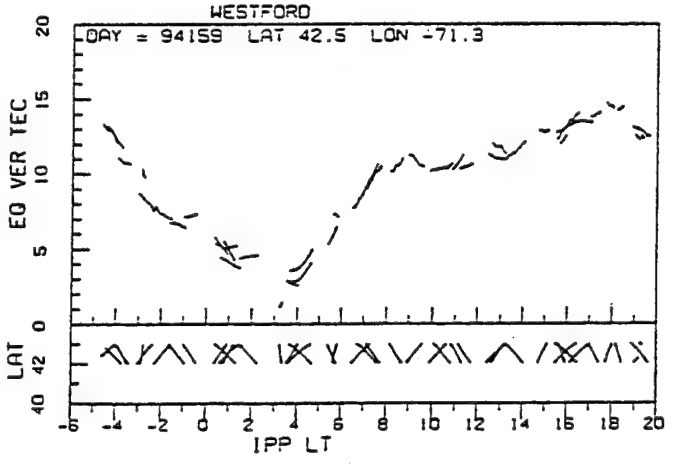

Figure 6b. Diurnal TEC observations, Westford, days 77, 114, & 159, 1° latitude band.

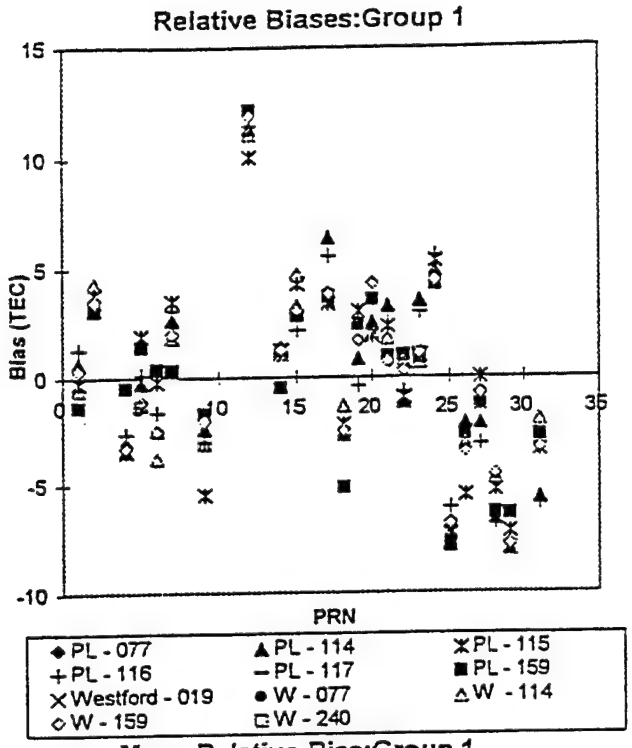

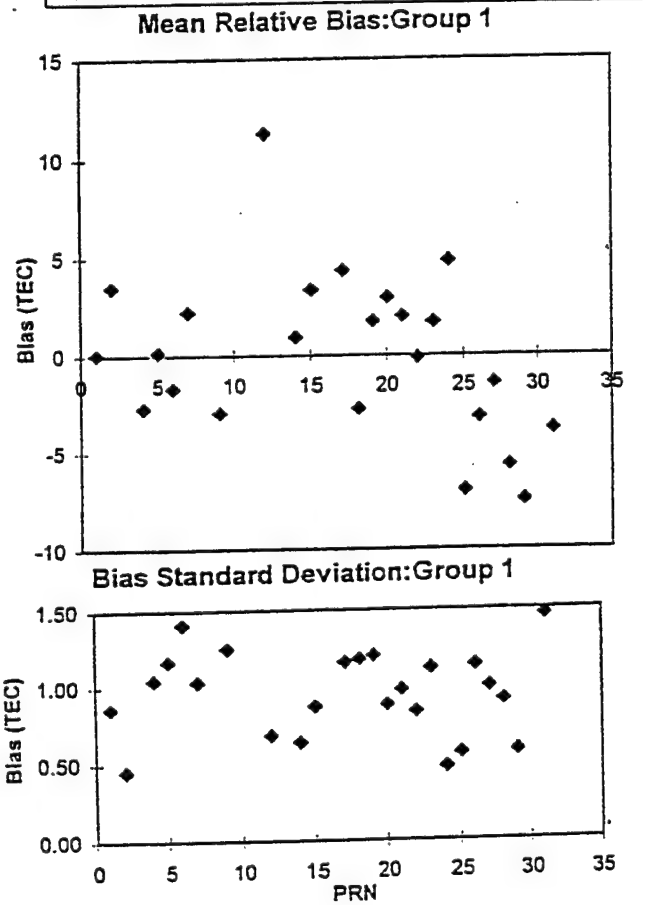

Figure 7. Plots of biases, their means and deviations for Group 1 - most satellites.

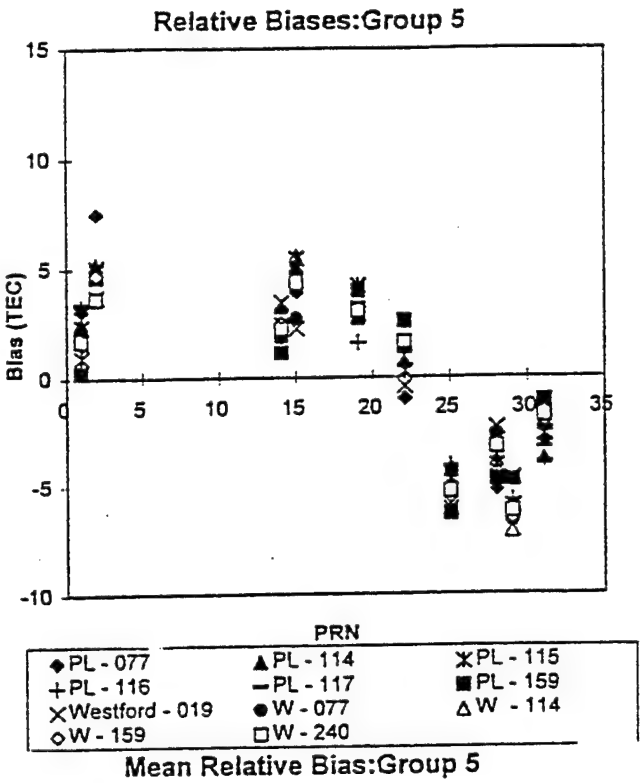

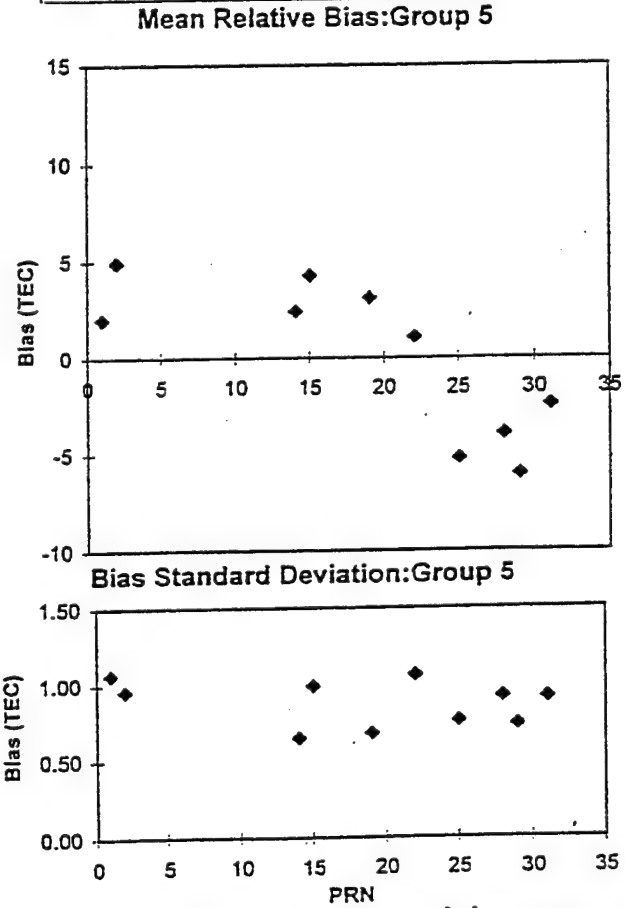

Figure 8. Plots of biases, their means and deviations for Group 5 - most days.

5i													
Average includes only PRNs 1, 2, 14, 15, 19, 22, 25, 28, 29, and 31													
Ave	37.38	14.22	17.03	15.81	17.72	20.26	-11.01	-13.16	-14.01	-12.92	-11.41		
Differences relative to daily averages													
PRN	PL - 077	PL - 114	PL - 115	PL - 116	PL - 117	PL - 159	Westford - 019	W - 077	W - 114	W - 159	W - 240	Sat Mean	Std Dev
1	3.08	2.57	0.96	3.28	3.40	0.24	2.38	2.18	0.36	1.57	1.70	1.97	1.06
2	7.48	5.04	5.04	5.18	4.52	4.64	3.75	4.84	5.19	4.70	3.63	4.91	0.96
14	2.29	3.26	2.44	3.09	2.39	1.12	3.45	1.82	1.95	2.48	2.22	2.41	0.64
15	3.90	5.13	5.44	4.12	4.73	4.40	2.26	2.70	5.58	4.27	4.33	4.26	0.99
19	3.04	2.73	4.21	1.59	2.86	3.98	2.90	3.06	3.74	2.89	3.04	3.09	0.67
22	-1.00	0.74	0.26	1.28	1.12	2.57	-0.42	2.50	1.55	1.53	1.62	1.07	1.06
25	-4.23	-4.92	-6.10	-4.10	-4.60	-6.30	-4.68	-5.42	-6.32	-5.55	-5.29	-5.23	0.76
28	-5.24	-4.70	-4.08	-4.82	-4.58	-4.74	-2.33	-2.65	-3.85	-3.31	-3.23	-3.96	0.92
29	-6.37	-6.10	-5.97	-5.71	-6.57	-4.79	-4.66	-6.68	-7.14	-6.54	-6.22	-6.07	0.73
31	-2.95	-3.75	-2.19	-3.90	-3.26	-1.11	-2.64	-2.35	-1.07	-2.05	-1.79	-2.46	0.91
													0.87

Table 2. Average corrections, biases and statistics for Group 5 - most days.

frequencies, (whereas GPS satellites share a common frequency) T_{GD} values (even zero-mean) will be contaminated with any frequency-dependence of the receiver offset. Thus algorithm products should be valid to calibrate a single site, but seldom transferrable to another site. Valid ZRT values for GLONASS will be producible only if bench measurements can calibrate the frequency dependence of the offset value on different satellite channels.

1i								
Average includes only PRNs 1, 2, 4 - 7, 9, 12, 14, 15, 17 - 29, and 31								
Ave	16.12	18.24	17.79	21.86	-13.14	-11.67		
Differences relative to daily averages								
PRN	PL - 114	PL - 115	PL - 116	PL - 159	W - 114	W - 159	Sat Mean	Std Dev
1	0.67	-0.25	1.30	-1.36	-0.51	0.33	0.03	0.86
2	3.14	3.82	3.20	3.04	4.32	3.45	3.50	0.45
4	-3.42	-3.51	-2.61	-0.49	-2.99	-3.30	-2.72	1.04
5	-0.24	1.90	0.12	1.36	-1.22	-1.12	0.13	1.17
6	-2.45	-0.22	-1.59	0.36	-3.76	-2.51	-1.70	1.41
7	2.65	3.45	3.07	0.29	1.83	1.97	2.21	1.03
9	-2.38	-5.50	-3.00	-1.58	-3.05	-2.00	-2.94	1.25
12	11.32	9.99	11.41	12.10	11.05	11.88	11.29	0.68
14	1.36	1.22	1.11	-0.47	1.08	1.24	0.92	0.63
15	3.23	4.22	2.14	2.80	4.71	3.02	3.35	0.86
17	6.33	3.31	5.52	3.65	3.43	3.80	4.34	1.16
18	-2.59	-2.18	-2.73	-5.16	-1.30	-2.47	-2.75	1.18
19	0.83	2.99	-0.39	2.38	2.87	1.65	1.72	1.20
20	2.51	1.87	3.48	3.54	1.99	4.24	2.94	0.87
21	3.24	2.29	3.04	0.92	1.76	0.68	1.99	0.97
22	-1.15	-0.95	-0.70	0.97	0.58	0.28	-0.14	0.83
23	3.50	0.99	2.96	0.87	0.69	1.08	1.68	1.11
24	4.87	5.29	5.53	4.20	4.60	4.41	4.82	0.47
25	-6.82	-7.32	-6.08	-7.90	-7.19	-6.80	-7.02	0.56
26	-2.12	-5.51	-2.30	-2.58	-3.09	-3.47	-3.20	1.13
27	-2.14	-0.02	-3.13	-1.31	-1.25	-0.74	-1.43	0.99
28	-6.60	-5.30	-6.80	-6.34	-4.71	-4.55	-5.72	0.90
29	-8.00	-7.19	-7.69	-6.39	-6.01	-7.79	-7.51	0.57
31	-5.65	-3.40	-5.88	-2.71	-1.94	-3.29	-3.81	1.46
								0.95

Table 3. Average corrections, biases and statistics for Group 1 - most satellites.

The University of Leeds [14] provided a data set which was tested against the PL algorithm. Despite the limited GLONASS working constellation at the time and the reduced receiver coverage during dual frequency operation, the algorithm was able to bring the resulting data into an apparently reasonable range, Figure 9. Unfortunately, residual calibration errors, and the variation of the receiver delay with temperature, meant that some different sections of data from the same satellite appeared to have a different offset. (Improved calibration procedures to resolve this are currently being investigated at Leeds). The algorithm was modified to treat each piece as a separate satellite to produce Figure 9.

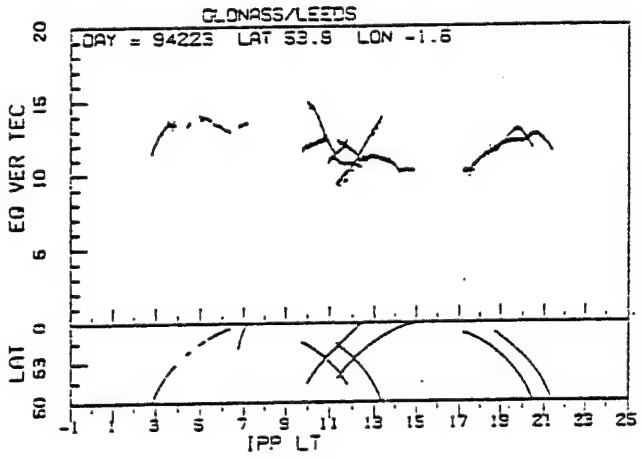

Figure 9. Diurnal TEC product from algorithm application to GLONASS data from the University of Leeds, UK.

In Figure 9, due to loss-of-lock, the residual calibration errors, and the lack of overlap in coverage the algorithm couldn't connect large disjoint segments. Data from a UK JPL net GPS station is plotted in Figure 10 for comparison. It may be seen that there is good agreement between the algorithm result of Figure 9 and the GPS data where the GLONASS data is abundant enough to have several conjunctions (1030-1230 LT). The algorithm brought the other two sections of the GLONASS data "into the ballpark" (some values started with offsets of many tens of TECu's) but the data segments were apparently too sparse and short to do better. We expect that with results this good from such a limited set of

GLONASS data, the algorithm will yield results comparable to GPS from subsequent larger, better-calibrated GLONASS data sets.

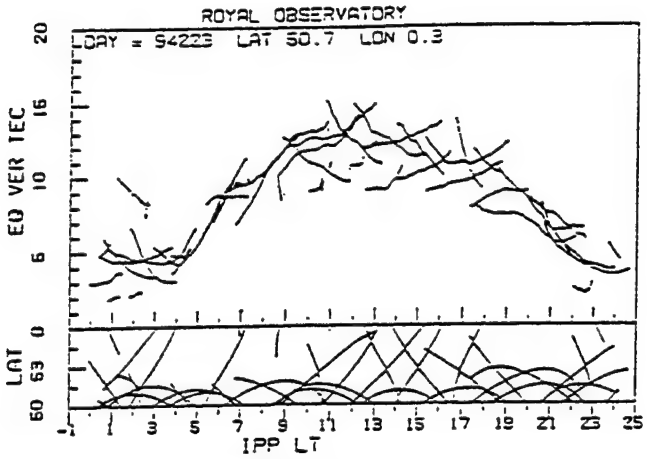

Figure 10. Diurnal TEC product from algorithm application to GPS data from UK JPL network station, same day as Fig. 9.

CONCLUSIONS

PL and NWRA, in earlier work with two large GPS data sets, produced results indicating that both the short and long-term stability of T_{GD} is adequate for ionospheric monitoring and better than previous work had suggested. The results suggests that the typical change to be expected in T_{GD} for a given satellite over one to two years would be about 1 ns, or less. The PL effort has produced a new algorithm for T_{GD}/receiver calibration, which requires data from a single station on a single day. Results from a small data set from two sites, spanning several months give an average standard deviation of T_{GD} values of less than one TEC unit. (The algorithm was also able to detect offset changes due to swapping antennas and apparent receiver drift.) To facilitate further such comparisons, PL has proposed that GPS users adopt a new standard procedure for comparing measured T_{GD} values, namely: to normalize the set of T_{GD} values to zero mean first, and compare sets consisting of exactly the same group of satellites. The current results further support the conclusion that GPS T_{GD}'s are quite stable over periods of months. The PL algorithm was also applied to a first investigation of GLONASS data from the University of Leeds. Although GLONASS calibration is much more challenging, reasonable results were obtained from the limited set of GLONASS data available. We believe the algorithm should yield results comparable to GPS from subsequent larger, better-calibrated GLONASS data sets.

ACKNOWLEDGEMENT

The authors wish to thank SSgt Carlton Curtis for performing all the measurements at Hanscom AFB. Access to data from the IGS Network was provided by the Jet Propulsion Laboratory.

REFERENCES

1. Klobuchar, J.A., and P.H. Doherty, "The Statistics of Ionospheric Time Delay for GPS Ranging on L1", Proceedings of ION GPS-90, The Institute of Navigation, Washington, DC, Sep. 1990.

2. Bishop, G.J., D.S. Coco, P.H. Kappler, and E.A. Holland, "Studies and Performance of a New Technique for Mitigation of Multipath Effects in GPS Ground Stations", Proceedings of 1994 National Technical Meeting, The Institute of Navigation, Washington, D.C., Jan. 1994.

3. ICD-GPS-200, GPS Joint Program Office, AF Space and Missile Systems Center, Los Angeles, CA.

4. Wilson, B.D., A.J. Mannucci, C.D. Edwards, and T. Roth, "Global Ionospheric Maps Using a Global Network of GPS Receivers", *in* Proceedings of International Beacon Satellite Symposium, Plasma Fusion Center, Massachusetts Institute of Technology, July, 1992.

5. Wilson, B.D., and A. J. Mannucci, "Instrumental Biases in Ionospheric Measurements Derived from GPS Data", *in* "Proceedings of ION GPS-93", The Institute of Navigation, Washington, DC, September, 1993.

6. Sardon, E., A. Ruis, and N. Zarraoa, "Estimation of the transmitter and receiver differential biases and the ionospheric total electron content from Global Positioning System Observations", Rad. Sci., Vol 29, No. 3, 577-586, May-June 1994.

7. Coco, D.S., C. Coker, S.R. Dalke, and G.T. Davidson, "Variability of the GPS Satellite Differential Group Delay Biases", IEEE Trans. Aerosp. Electron. Sys., Vol. 27, No. 6, 99 71-78, 1991.

8. Goposchkin, E.M., and A.J. Coster, "GPS L1-L2 Bias Determination", *in* Proceedings of International Beacon Satellite Symposium, Plasma Fusion Center, Massachusetts Institute of Technology, July, 1992.

9. Doherty, P.D., and J.A. Klobuchar, "The Effects of Transmitter Offsets on Absolute TEC Obtained from the GPS Satellites", *in* Proceedings of International Beacon

Satellite Symposium, Plasma Fusion Center, Massachusetts Institute of Technology, July, 1992.

10. Klobuchar, J.A., and P.H. Doherty, "Potential Ionospheric Limitations on Making Absolute Ionospheric Measurements Using Dual-Frequency Radio Waves from GPS Satellites", *in* "Proceedings of the 1993 Ionospheric Effects Symposium", Alexandria, VA, May, 1993.

11. Bishop, G.J., D.S. Coco, and C. Coker, "Variations in Ionospheric Range Error with GPS Look Direction", *in* "Proceedings of ION GPS-91", The Institute of Navigation, Washington, DC, September, 1991.

12. Bishop, G. J., L K. Walker, C. D. Russell, and L. Kersley, "Total Electron Content and Scintillation Over Northern Europe", *in* "Proceedings of the 1993 Ionospheric Effects Symposium", Alexandria, VA, May, 1993.

13. Press, W.H., B.P. Flannery, S.A. Teukolsky. and W.T. Vetterling, Numerical Recipes, The Art of Scientific Computing (FORTRAN Version), Cambridge University Press, 1989.

14. Riley, S., and P. Daly, "Performance of the GLONASS P-Code at L1 and L2 Frequencies", Proceedings of ION GPS-93, The Institute of Navigation, Washington, DC, September, 1993.

GPS Measurements of L-Band Scintillation and TEC in the Northern Polar Cap Ionosphere at Solar Maximum

G. J. Bishop[1], T. W. Bullett[1] and E. A. Holland[2]
[1]Phillips Laboratory - Geophysics, Hanscom AFB, MA, 01731-3010 USA
FAX +1 617 377 3550, e-mail: bishop@zircon.plh.af.mil
[2]NorthWest Research Associates, Bellevue, WA USA

INTRODUCTION

Absolute total electron content (TEC) and L-band scintillation were first measured in the northern polar cap ionosphere in early 1984 using GPS signals. These near-solar-minimum observations made by Phillips Laboratory (PL) at Thule, Greenland, revealed the existence of a UT variation in TEC, with large TEC/scintillation enhancements occurring preferentially in the 1200-2400 UT period, and often more than doubling background TEC values in less than ten minutes, (Klobuchar et al., 1984). Simultaneous observations using an ionospheric sounder and an all-sky imaging system at 6300 Å, showed a direct link between the TEC variations, scintillation and passage of the raypath through large-scale 'F-layer ionization patches', with scale sizes up to 1000 km and drift velocities of 100 to 1000 m/s, (Buchau et al., 1988). PL observations from October 1987 through March 1988 show frequent occurrence of large TEC variations similar to 1984. TEC variations observed in the October 1988 - March 1989 polar winter, when monthly SSN varied from 125 to 150, were three times larger than in 1984, (Bishop et al., 1990). Both the UT variation and enhancements of TEC and scintillation persisted through the peak of the recent solar maximum, 1989-1990. Background TEC values were still seen to be more than doubled in less than ten minutes during these greater enhancements, implying that significantly greater spatial TEC gradients occur at solar maximum.

1989-1990 SOLAR MAXIMUM OBSERVATIONS

Seasonal occurrence and magnitude of 1989 TEC disturbances and scintillation varied from high during October to quite low in July, as illustrated in Figure 1, left, (gaps are due to lack of satellite coverage). July is fairly typical of observations in the May - August period, while the October - November was the time of highest disturbances. TEC profiles for October (SSN 159) show very high TEC values, very large patches, significant UT variation, and TEC variations of 30-50 TEC units on a background of 20-30 units. These variations are more than three times greater than those seen in the 1984 measurements. Variations observed in February 1990 - same month as the 1984 data - show almost exactly a three-fold increase in size over 1984. Both October 1989 and February 1990 often show TEC variations more than doubling background values in less than 10 minutes. October 1989 scintillation shows both high S4 values and UT variation - with higher values at 1200-2400 UT. Higher scintillation levels are generally associated with TEC enhancements, and the highest S4 values are concurrent with the largest TEC patches, which occurred 1200-2100 UT. In contrast, TEC profiles for July 1989 (SSN 158) show neither large UT variation nor large patch structures, while July 1228 MHz scintillation reveals consistent low values, with occasional small increases, and no UT variation. In the right half of Figure 1 we examine TEC and scintillation for one day from July 1989 and three from October. Day 284 (Kp ≈ 2) shows fairly typical October high scintillation - varying TEC behavior, while day 203 (Kp ≈ 1+) similarly represents the low level - low variation conditions of July. Days 286 ($K_p \approx 0$) and 293 ($K_p \approx 7$) contrast extremely quiet vs storm conditions during the most disturbed month. On day 286 the TEC shows UT variation, very high TEC values, and few large patch-type enhancements. The scintillation, however, shows some moderate scintillation and a few very high levels, associated with TEC enhancements, despite the low Kp condition. Day 293 (magnetic storm onset at ≈1000 UT), shows UT variation with extremely large TEC enhancements, linked with sustained high scintillation. In contrast, day 274 (Kp ≈ 2.5, not shown) exhibited no UT variation in TEC or scintillation, no large TEC enhancements, and much lower scintillation, thus Kp is not the only driver. Although the strong association of scintillation levels and TEC enhancements for increasing sizes of TEC enhancements is supportive of the validity of the large TEC values, confirming data from independent sensors is also needed.

A simple analytical model of a patch (peak density 9.6×10^5 electrons/cm^3) has been used to simulate GPS TEC (Bishop et al., 1990), yielding a maximum vertical TEC variation of about 16 units, *supporting the*

smaller TEC patches in the 1989 data. Figure 2 shows: Thule GPS TEC, Qaanaaq sounder foF2 data, Sondrestrom incoherent scatter radar (ISR) electron density profiles, and single profile reconstructions for estimating TEC, from day 302, 1989. Similarity in the overall TEC and foF2 profiles may be noted, particularly in the 1200-2400 UT period. The ISR patch profile at 2250 UT has a peak density of 10.5×10^5 electrons/cm^3, one of the higher values seen in the 2100-2400 UT period, and yields an estimated TEC of 35 units. The peak of the ISR profile at 2206 UT has one of the lower values, 6.0×10^5 electrons/cm^3, and yields an estimated TEC of 20 units. These results agree fairly well with the 2200-2400 UT GPS TEC observations, *supporting validation of the mid-range 1989 TEC data.* It should be noted that the drift carries the patches from the Thule region toward Sondrestrom, and some decay in patch densities is to be expected by the time the patch is seen by the ISR. Also, these two sensors are not likely to have observed the same portion of the patch structures. Thus close correspondence is unlikely, but range of variation over a few hours should correspond. Figure 3 compares TEC within 300 km of Qaanaaq, foF2, bottomside density profile data, and profile reconstructions, from day 326, 1989 (World Day). A TEC depletion at 1320 UT shows 2.0×10^5 electrons/cm^3, and 8 units. The low value of measured GPS TEC in the depletion limits the likely contribution from the plasmasphere in this case, which was estimated here at 1 unit, vs larger values suggested by previous work (Doherty et al. 1992). A large patch at 1525 UT has a peak density of 19.0×10^5 electrons/cm^3 and an estimated TEC of 72 units (*which agrees well with GPS and supports 1989 high TEC values*). Scintillation associated with this patch peaked on the trailing edge although leading/trailing gradients looked symmetric. After correction using digisonde drift data, the trailing edge TEC gradient was indeed greater. The highest TEC values (day 293) have been seen at storm times, and may be associated with "storm-enhanced densities" (Foster, 1993). Similar high values were seen on that day by the PL GPS instrument at the Shetland islands, and comparable levels appear during storms as late as February 1992 (Bishop et al. 1993).

CONCLUSIONS

GPS measurements of L-band scintillation and TEC in the northern polar cap at solar maximum have shown very high TEC values and scintillation levels associated with patch-type features. TEC values up through 70 TEC units appear to have good initial validation from simultaneous digisonde and incoherent scatter radar data, while higher values may be storm-related. Dramatic day-to-day changes in behavior were observed that cannot be solely attributed to magnetic activity. These data will be examined further to address: diurnal and seasonal statistics of L-band scintillation, specification of polar cap circulation, and modeling of polar cap patch generation.

ACKNOWLEDGEMENT

The authors wish to thank the Danish Commission for Scientific Research in Greenland for permission to conduct experiments at Thule AB, Greenland.

REFERENCES

Bishop, G.J., J.A. Klobuchar, Sa. Basu, J.R. Clynch, D.S. Coco, and C. Coker, Measurements of trans-ionospheric effects using signals from GPS, Proc. 1990 Ionospheric Effects Symp., J.M. Goodman, ed.

Bishop, G.J., I.K.Walker, C.D.Russell, and L. Kersley, Total electron content and scintillation over northern europe", Proc. 1993 Ionospheric Effects Symp., J.M. Goodman, ed.

Buchau, J., B.W. Reinisch, D.N. Anderson, E.J. weber, and C. Dozois, Polar cap plasma convection measurements and their relevance to the modeling of the high latitude ionosphere, Rad. Sci., 23, 521 (1988).

Doherty, P.H., J.A. Klobuchar, G.J. Bailey, Balan, N., and M.W. Fox, Determinations of protonospheric electron content from TEC measurements from GPS and faraday rotation and comparisons against the Sheffield plasmasphere model, Proc. International Beacon Satellite Symp., MIT, Cambridge, MA, July 1992.

Foster, J.C., Storm time plasma transport at middle and high latitudes, JGR, 98, 1675-1698, Feb. 1, 1993.

Klobuchar, J.A., G.J. Bishop, and P.H. Doherty, Total electron content and L-band amplitude and phase scintillation measurements in the polar cap ionosphere, Paper 2-2, NATO AGARD Conf. Proc., 382, 1985.

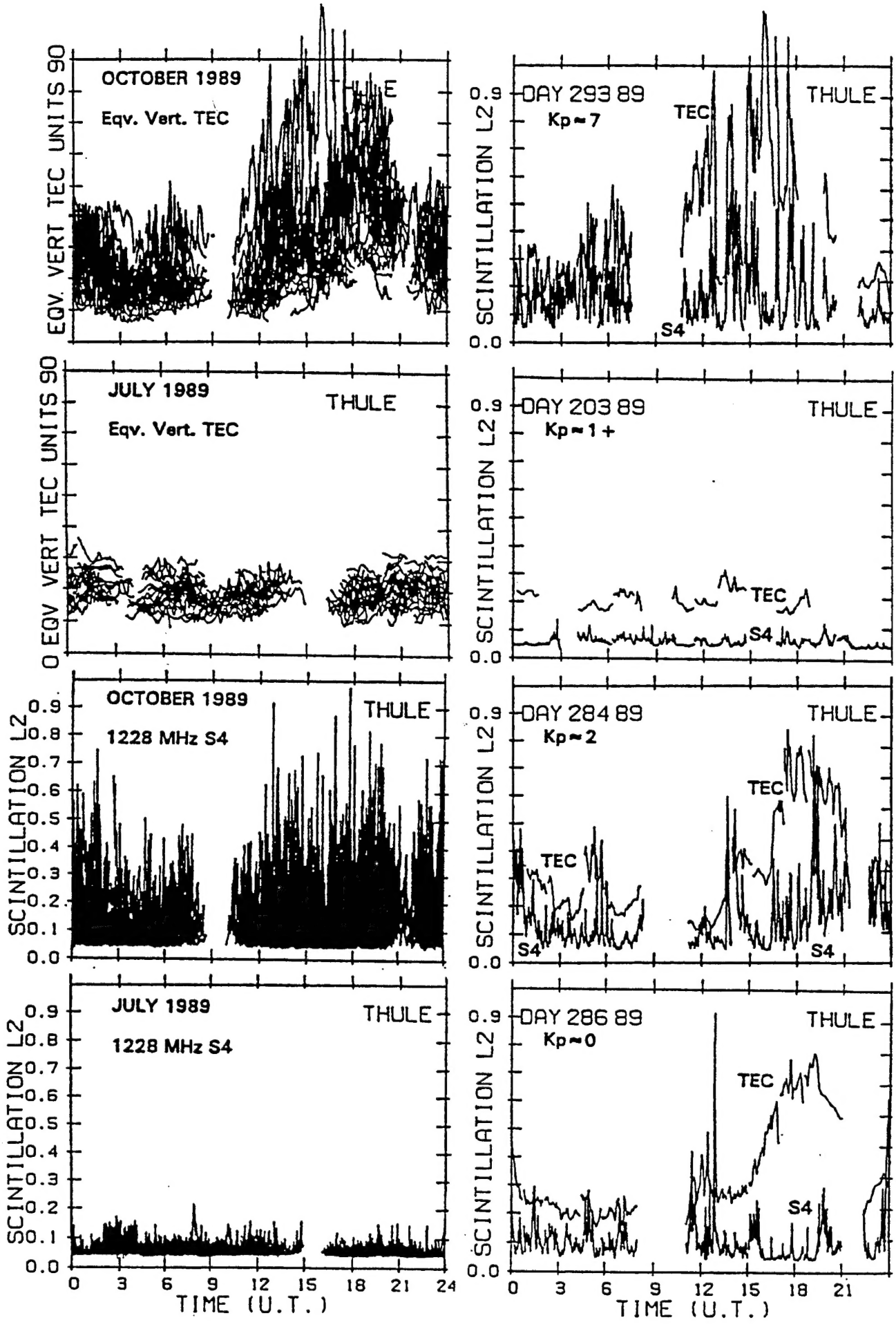

Figure 1. Solar maximum GPS observations of TEC and scintillation from Thule, Greenland, contrasting m active vs most quiet months and high vs low Kp days.

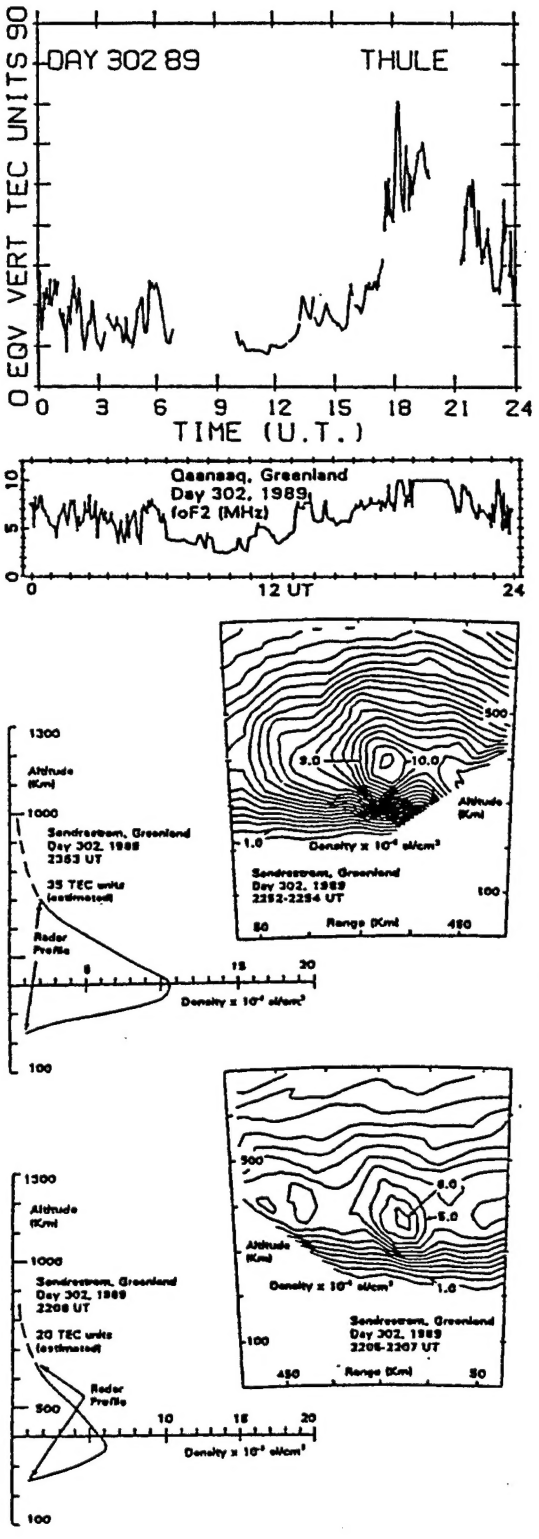

Figure 2. GPS TEC, digisonde foF2, radar profiles and TEC estimates for day 302, 1989, Greenland.

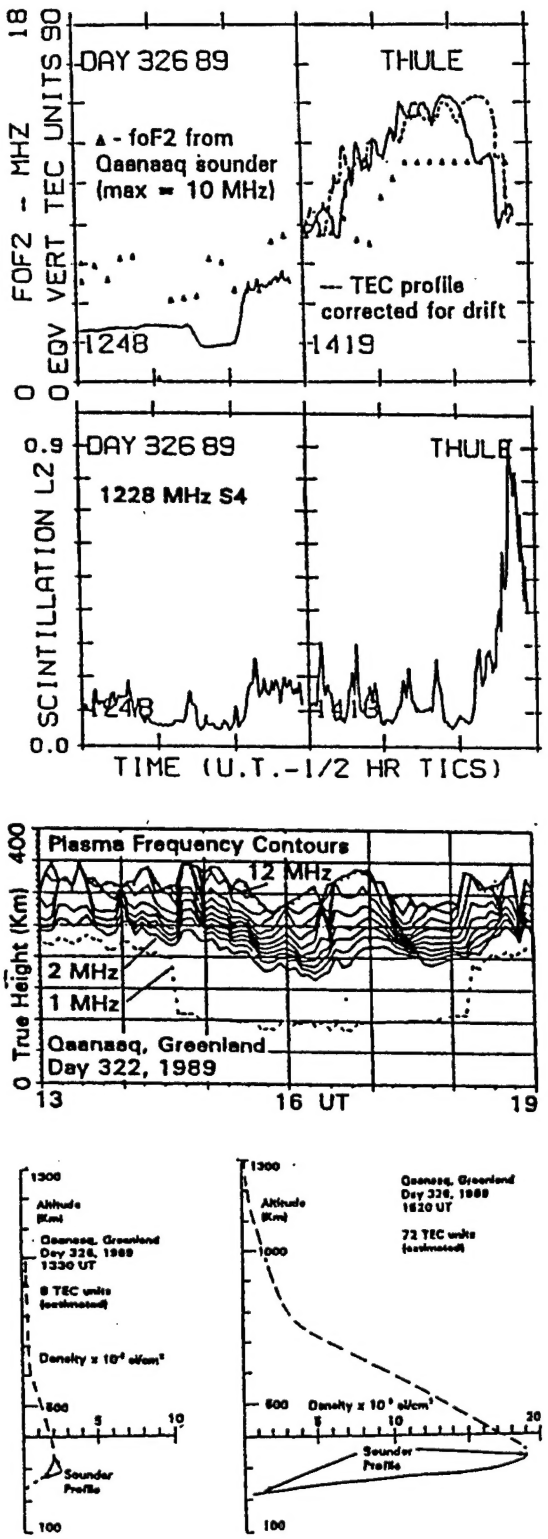

Figure 3. GPS TEC & scintillation, digisonde 256 foF2 & plasma frequency contours, and TEC estimates, day 326, 1989, Greenland.